# NTNU

Norwegian University of
Science and Technology

# Encapsulation of Human Mesenchymal Stem Cells in Phosphate Mineralized Alginate Beads

Marita Westhrin

Chemical Engineering and Biotechnology
Submission date: June 2011
Supervisor: Gudmund Skjåk-Bræk, IBT
Co-supervisor: Berit Løkensgard Strand, IBT

Norwegian University of Science and Technology
Department of Biotechnology

## Declaration

I hereby declare that this master thesis was written independently and in agreement with "Reglement for sivilarkitekt- og sivilingeniøreksamen" at the Norwegian University of Science and Technology.

Trondheim, June 14 2011

Marita Westhrin

# Preface

This master thesis is a part of the master degree program "Industrial Chemistry and Biotechnology" in the faculty of Natural Science and Technology at the Norwegian University of Science and Technology. The work was carried out at the Department of Biotechnology (IBT) and at the Department of Cancer Research and Molecular Medicine (IKM).

I would like to thank my supervisors Berit Løkensgard Strand, Therese Standal, Minlie Xie, Magnus Ø. Olderøy and Pawel Sikorski for their invaluable help and guidance for the duration of my master work. In addition I would like to thank Minli for running SEM analysis.

Furthermore, I would like to thank all the co-workers at IKM for guidance in the laboratory whenever I was lost.

Last, but not least, a big thanks to all of my friends for getting my mind off work whenever I needed. You know who you are.

# Abstract

Alginate scaffolds show good promise for bone tissue engineering using stem cells. This is due to the fact that alginate is biocompatible, non-immunogenic, and in addition may direct differentiation of stem cells into a given phenotype. Finally, due to their ability to gel at physiological conditions, living and functional tissue are easily encapsulated into alginate beads.

Alginate beads can be modified in a range of ways, not only to enhance the matrix stiffness and stability, but also to promote cell adhesion and direct differentiation towards a given phenotype. A method currently used to encourage bone growth is to mineralize the alginate beads, thus mimicking the structure of bone *in vivo*. Recently, Xie et al. (2011) demonstrated that enzymatic mineralization of alginate beads serves as a potent method for mineralizing beads as lower concentrations of $CaCl_2$ is needed, which is beneficial for cell viability. In addition, the enzymatic method produces alginate beads with a uniformly distribution of calcium phosphate (CP) and stiffer mechanical properties.

Mesenchymal Stem cells (MSCs) have the potential to differentiate into a variety of tissues, including cartilage, adipose, muscle and bone. MSCs extracted from bone marrow seem to possess the greatest potential for bone tissue engineering, as they are more easily differentiated into osteogenic phenotypes when compared with MSCs from e.g. adipose tissue.

The main objective in the present study was to encapsulate MSCs into alginate beads mineralized with alkaline phosphatase (ALP) and study cell survival, as well as their potential to differentiate into mature osteoblasts inside the beads. To mineralize beads (ALP) was added to the alginate solution, whilst the precursors were added to the growth medium. The mineralization medium was changed every 3 hours (12 hours over night) for the first 2 days post encapsulation.

Cell viability was surveyed by live/dead assay and imaging by Confocal Laser Scanning Microscopy (CLSM), and metabolic activity by Alamar Blue (AB) and colorimetric techniques. Examination of cell morphology was accomplished by phalloidin/DRAQ5 staining. Moreover, to investigate cell differentiation, PCR analysis on selected RNA candidates was performed. Quantification of mineral content was accomplished by running Alizarin Red-S (ARS-S) assay. ALP activity was determined using ALP assay. Finally, further investigation of cell- and alginate matrix structure was accomplished using scanning electron microscopy (SEM).

To study capsule properties and cell survival, osteosarcoma cells were utilized as model cells. The main objective was to study bead stability, and how the beads and the cells within were affected by the enzymatic mineralization method. Alginate beads proved to be unstable and needed addition of $CaCl_2$ for stabilization purposes. Furthermore, in order to recover cells, citrate was added to the cell/bead suspension. Initially, results were unsatisfactory, as little, or no, RNA was recovered. After optimizing the citrate treatment it was discovered that a *sequential* method needed to be utilized. Results demonstrated a successful recovery of cells, and RNA of excellent quality.

Enzymatic mineralization of alginate beads was found to be a cell friendly way of mineralizing alginate beads. Mineralization of beads was observed in the light microscope, by visual inspection, as well as by SEM. Cell viability remained high when using a concentration of 0.25mg/ml ALP. The osteosarcoma cells proved to be good for optimizing the enzymatic mineralization method, but behaved differently compared with mesenchymal stem cells in terms of viability, and mineralization

activity. Furthermore, mineralization of beads by addition of 0.25 mg/mL ALP compared with 0.5mg/mL appeared to be beneficial as image acquisition on CLSM was facilitated and slightly higher viability of cells was observed.

In the second part of the present study, human MSCs were encapsulated into alginate beads. After initial experiments the optimal condition for cell survival, and bead stability was determined. Consequently, in the final experiment 16 million MSCs were encapsulated in beads containing 0.25mg/mL ALP, together with a sample without addition of ALP. At day 2 post encapsulation both samples were divided into two batches, one cultured in regular medium, and one in differentiation medium. All samples were stabilized with 7.5 mM of $CaCl_2$.

Observations in both light microscope and CLSM revealed that only beads given ALP were mineralized before reaching day 21. At day 21 the sample receiving no ALP, cultured in differentiation medium also appeared mineralized.

Mesenchymal stem cells receiving differentiation medium were observed to differentiate into mature osteoblasts in the beads. This was verified by gene expression analysis, cell morphology studies, the presence of collagen in beads seen by SEM and analysis of ALP activity. Metabolic activity measurements confirmed little cell proliferation, nor cell death. However, an increased metabolic activity was observed for encapsulated cells cultured in regular medium relative to cells in differentiation medium. Cell morphology in differentiated samples was recognized by showing elongated actin filaments, compared with the ones cultured in regular medium, which appeared round in shape. The elongated filaments suggest that the cells are able to interact with the alginate matrix and/or minerals. The occurrence of collagen fibers in SEM images further confirmed presence of mature osteoblasts.

Samples cultured in regular medium with or without added ALP both showed an increase in osterix expression until day 21 when the study was ended. This was surprising, as it inferred that the alginate matrix itself might influence differentiation of MSCs into osteoblasts, and that the minerals have little effect on differentiation. Runx2 expression was detected in all samples, including unencapsulated hMSCs. The expression of runx2 was at its maximum on day 21, when the study was ended.

Encapsulating mesenchymal stem cells into alginate beads mineralized by the enzymatic method is cell friendly, and allows the cells to differentiate into mature osteoblasts when cultured in differentiation medium. Alginate without minerals seems to influence differentiation to a certain extent, suggesting that minerals are not needed for differentiation to occur. The minerals do, nonetheless, speed up the continuing mineralization process.

# Abbreviations

| | |
|---|---|
| AB | Alamar Blue |
| ALP | Alkaline Phosphatase |
| ARS-S | Alizarin Red-S |
| BSA | Bovine Serum Albumin |
| bsp | Bone Sialoprotein |
| cDNA | Complementary DNA |
| CLSM | Confocal Laser Scanning Microscopy |
| CP | Calcium Phosphate |
| CPC | Cetylpuridinium Chloride |
| CPC | Calcium Phosphate Cement |
| $C_t$ | Cycle Threshold |
| DNA | Deoxyribonucleic Acid |
| ELF | Enzyme Labeled Fluorescence |
| Eth-1 | Ethidium Homodimer-1 |
| FAH | Formaldehyde |
| FBS | Fetal Bovine Serum |
| FCS | Fetal Calf Serum |
| gapdh | Glyceraldehydes-3-phosphate Dehydrogenase |
| G-block | Blocks of solely guluronic acid monomers in an alginate chain |
| HA | Hydroxyapatite |
| HBSS | Hanks Buffered Salt Solution |
| hMSC | Human Mesenchymal Stem Cell |
| hUCMSC | Human Umbilical Cord Mesenchymal Stem Cell |
| M-block | Blocks of solely mannuronic acid monomers in an alginate chain |
| MG-block | Blocks of alternating guluronic and mannuronic acids in an alginate chain |
| mMSC | Mouse Mesenchymal Stem Cell |
| MSCBM | Mesenchymal Stem Cell Basal Medium |
| MSCDM | Mesenchymal Stem Cell Differentiation Medium |
| MSCGM | Mesenchymal Stem Cell Growth Medium |

| MSCMM | Mesenchymal Stem Cell Mineralization Medium |
|-------|---------------------------------------------|
| MTT | 3-[4,5-dimethylthiazol-2-yl]-2,5-diphenyl Tetrazolium Bromide |
| Ocn | Osteocalcin |
| opn | Osteopontin |
| OSGM | Osteosarcoma Growth Medium |
| OSMM | Osteosarcoma Mineralization Medium |
| osx | Osterix |
| PBS | Phosphate Buffered Saline |
| PCR | Polymerase Chain Reaction |
| RNA | Ribonucleic Acid |
| RT | Reverse Transcriptase |
| RT | Room Temperature |
| runx2 | Runt-related Transcription Factor 2 |
| SIV | Sterile, Ion-free Water |
| SEM | Scanning Electron Microscope |
| sMSC | Swine Mesenchymal Stem cell |
| TEM | Transmission Electron Microscope |

# Contents

# 1. Introduction

## 1.1 Background

Alginate scaffolds show good promise for bone tissue engineering using stem cells. This is due to the fact that alginate is biocompatible, non-immunogenic, and may direct differentiation of stem cells into a given phenotype. By encapsulating cells in alginate beads for transplantation purposes the bead will create a protective atmosphere and prevent cellular interaction. Cells can also be more meticulously studied as they consistently achieve a longer lifespan in culture compared with non-encapsulated cells. In addition one cell line can be more easily co-cultured with another without them interacting directly with each other (Ghidoni, 2008).

Encapsulation of cells in gel beads serves as a potent method for both tissue engineering scaffolds and bone graft substitutes. These injectable scaffolds will reduce the need for invasive surgery as they can be injected directly into the bone defect site (Roeder, 2008). This has been demonstrated using different polymers, including collagen (Tsuchida, 2003) and alginate (Wang, 2003). Stem cells capable of differentiating into bone cells are especially interesting as they may address the pathological insufficiencies in an array of bone disorders, often affecting bone metabolism (Jethva, 2009).

Alginate beads can be modified in a range of ways, not only to enhance the matrix stiffness and stability, but also to promote cell adhesion and direct differentiation towards a given phenotype. One commonly used method is to attach peptides to the monomers creating an ECM-mimicking environment for the cells. Another method currently used to encourage bone growth is to mineralize the alginate beads, thus mimicking the structure of bone *in vivo*.

Previously, mineralization of alginate beads has been achieved by an in situ one-step method. This means that sodium phosphates are added to the alginate solution prior to encapsulation of cells, whereupon calcium ions both cross-link alginate and precipitates with phosphate ions to form hydroxyapatite (Xie, 2010). An alternative to the one-step method is the enzymatic method. Here, alkaline phosphatase (ALP) is added to the alginate solution, whilst the precursors are added to the growth medium. Many advantages emerge with the enzymatic method. First and foremost one can direct the mineralization process more thoroughly by controlling the amount of enzyme and precursors to be added. Secondly, mineralization can be achieved using a lower ionic strength, yet creating beads with stiffer mechanical properties compared with the in-situ method. Finally, it has been demonstrated that minerals are more evenly distributed in alginate beads compared with the minerals formed by the one-step method (Xie, 2011).

The latter article forms the basis for this thesis, with the main objective being to study how the enzymatic method influences mesenchymal stem cell` viability and differentiation inside mineralized alginate beads. Cell viability will be surveyed by live/dead assay and imaging by Confocal Laser Scanning Microscopy (CLSM), and metabolic activity by Alamar Blue (AB) and colorimetric techniques. Examination of cell morphology will be accomplished by phalloidin/DRAQ5 staining. Moreover, to investigate cell differentiation, PCR analysis on selected RNA candidates will be performed. Quantification of mineral content will be accomplished by running Alizarin Red-S (ARS-S) assay. Finally, ALP activity will be determined using ALP assay.

## 1.2 Alginate – Structure, properties and applications

Alginate is a polysaccharide produced by some brown algae and by certain bacteria species, such as *Azotobacter vineladii* and *Pseudomonas aeruginosa*. Alginate extracted from seaweed has a variety of different applications. Today, alginates are used primarily as a thickening agent, for example in paint and food. Other applications include the production of many chemicals such as ethanol, ammonia, hydrocarbons and interferons (Smidsrod and Skjak-Braek, 1990).

### 1.2.1 Structure

Alginates are built up by two uronic acids, β-D-mannuronic acid (M) and α-L-guluronic acid (G). These monomers are linked through (1→4) glycosidic linkages as shown in figure 1. The M monomers exist in a $^4C_1$ conformation, and the linkages between two Ms are consequently diequatorial. The G monomers exist in a $^1C_4$ conformation, and the linkages between these monomers are diaxial (Smidsrød and Andresen, 1979).
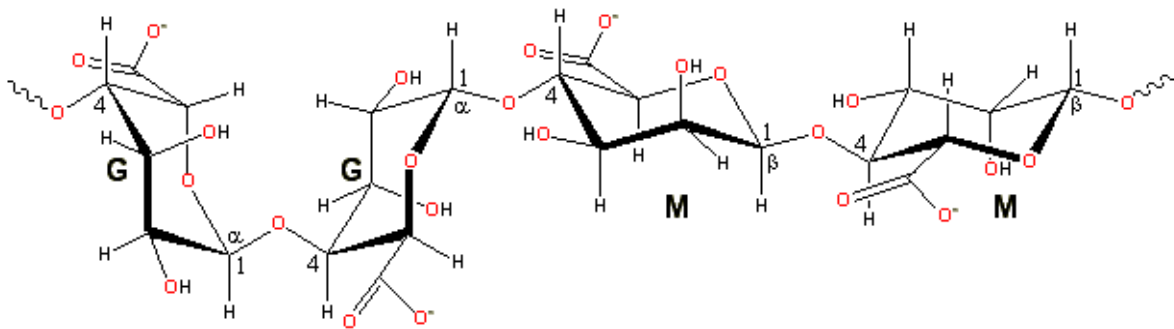


**Figure 1 Alginate chain. The figure illustrates the different possible linkages between different monomers (Chaplin, 2010). The linkage between two G monomers is diaxial, whereas the linkage between two M monomers is diequatorial.**

### 1.2.2 Gelling, alginate beads and encapsulation of cells

The properties of the alginate vary greatly according to its composition. Chains of sequential G monomers (G-blocks) lead to the formation of a gel in the presence of divalent cations (Haug, 1961). Recently it has been demonstrated that, in addition, sequences with alternating M and G monomers (MG-blocks) may form gels (Donati, 2005). The selectivity towards G-blocks can be explained by the egg-box model as presented in figure 2.
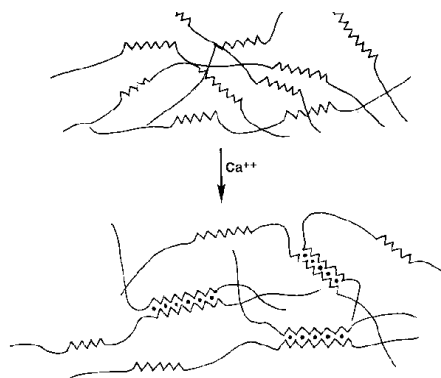


**Figure 2 The egg-box model. G-blocks are built up by diaxial linkages between the G-monomers creating a zig-zag structure. When calcium ions are bound between these monomers they create the structure known as the egg-box model (McHugh, 2003).**

The calcium ion, $Ca^{2+}$, is the most commonly used cation for cross binding of alginate, although it is not the ion with the highest affinity for alginate (Smidsrod, 1974). This is due to the fact that $Ca^{2+}$-ions are non-toxic at low concentrations, which makes them a popular choice for cell immobilization purposes. As $Ca^{2+}$-ions do not possess the highest affinity for alginate, the beads are not as rigid compared with using other ions, such as $Ba^{2+}$ and $Sr^{2+}$ (Smidsrod and Skjak-Braek, 1990). The stability of beads can be improved, for example through addition of small concentrations of $Ca^{2+}$-ions to the culture medium. The addition of $Ca^{2+}$-ions are thought to counterbalance the exchange of $Ca^{2+}$ with $Na^+$ and the subsequent swelling due to osmotic pressure (Martinsen et al., 1989).

Several techniques exist to encapsulating live cells in gel beads, including numerous dripping methods for creating small beads with a narrow size distribution. Briefly, an alginate solution (~2%) containing cells is dripped into a calcium chloride solution, creating gel beads instantaneously, as illustrated in figure 3. The set up of the bead generator apparatus (needle size, voltage and flow) determines the size of the droplets, and hence the bead size. The properties of the gels depend also on other factors, including the composition and properties of the alginate. Gel beads made from alginate containing more than 70% guluronic acid and an average length of G-blocks longer than 15 monomers have been demonstrated to possess the highest mechanical strength, the lowest syneresis and the highest porosity (Martinsen et al., 1989).
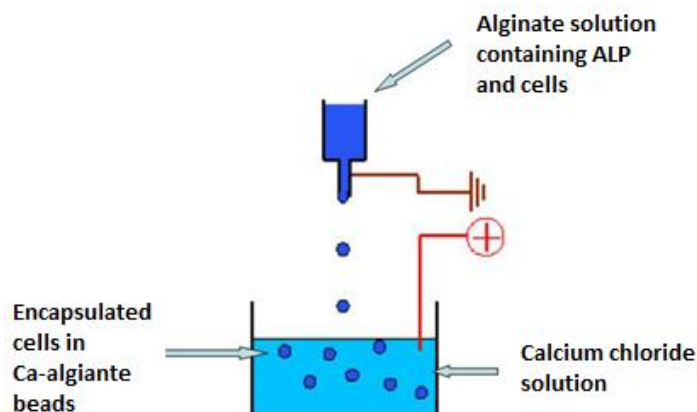


**Figure 3 Encapsulation of cells using the dripping method and an electrostatic bead generator. An alginate solution is mixed with cells inside a syringe, and dripped into a beaker containing a calcium chloride solution. The size of the beads can be predetermined by adjusting the settings of the bead generator apparatus, and by using alginate with a given composition. Modified from (Sundrønning, 2010).**

By encapsulating living cells, for instance for transplantation purposes, the alginate beads create a protective atmosphere from the immune system of the host (Mørch, 2009). There are several advantages of using alginate gels, including their biocompatibility, thermostability, simplicity of production and the possibility of tailoring stability, porosity and mechanical strength trough selection of alginate, gelling ions and formation of inhomogeneous beads. Finally, and most importantly, due to their ability to gel at physiological conditions, living and functional tissue are easily encapsulated.

There are, nevertheless, drawbacks including low stability and swelling of the gel (Skjåk-Bræk, 1991). The low stability becomes more predominant as cells are encapsulated within (Hwang, 2009b). This might be explained by the mechanical properties of the polymer being affected by the surrounding culture medium (Petrenko, 2011). That is, all calcium chelators will reduce the mechanical strength of the alginate, and some of these chelators are commonly found in the growth/ differentiation medium of the cells in question. These include phosphates, monovalent ions and non cross linking divalent ions (Berger, 1988).

As the concentration of calcium needed to stabilize the beads is dependent on alginate origin, alginate composition, cross-linking density, and the calcium concentration already present in the medium, there is no given concentration that will stabilize any given bead (Kuo, 2008, Mørch, 2006). In addition, cellular growth will affect the stability, as different cell lines have been shown to destabilize beads, probably due to their different growth patterns (Rokstad, 2006).

More recently studies have focused on how the cells are affected by the alginate gels. One factor affecting cells is the bead size which may influence cell survival, as smaller beads provides a shorter route for nutrient delivery (Grellier, 2009). Additionally, if cells die inside the beads they may affect the remaining living cells more strongly than *in vivo*. This might be explained by accumulation of waste products that are both toxic to the living cells, and obstruct the diffusion of nutrients and oxygen (Rokstad, 2002). In culture flasks cells are in a 2D environment. The use of beads will create a 3D environment, resembling the *in vivo* extracellular matrix. This has been shown to increase osteogenic differentiation, probably due to the more suitable environment (Abbah, 2008). It seems that survival and proliferation is similar in 2D and 3D. However, differentiation into osteogenic phenotypes seem to be accelerated in 3D environments (Juhásová, 2011).

Additionally, alginates and their building blocks have been shown to influence crystallization of calcium carbonate and calcium phosphate (Olderøy, 2009, Olderøy, 2011, Xie, 2010). In the latter study no mineral particles in the nano-scale were found using crystallization procedures without alginate. Furthermore, it has been demonstrated that the mineral phase after the crystallization process in alginate was similar to the mineral phase in bone (Xie, 2010).

## 1.3 Mesenchymal stem cells

Mesenchymal stem cells (MSCs) are stem cells capable of differentiating into a variety of connective tissues such as cartilage, bone, adipose and muscle as presented in figure 4 (Caplan, 1991). MSCs can be extracted from both adipose tissue and bone marrow. In bone marrow they exist in relatively low concentrations (Hwang, 2009a). *In vitro*, conversely, they can be easily expanded whilst preserving their differentiation ability (Docheva, 2008). On the downside, it usually takes weeks to yield the desired cell number (Panetta, 2009). MSCs from bone marrow seem to possess the greatest potential for bone tissue engineering, as they are more easily differentiated into osteogenic phenotypes when compared with MSCs from adipose tissue (Shafiee, 2011).

Furthermore, MSCs are immunosuppressive, meaning that they create a regenerative microenvironment by secreting bioactive molecules, thus suppressing graft versus host disease. Due to this ability, allogenic MSCs have been delivered intravenously to patients suffering from various injuries/diseases (Caplan, 2007, Caplan, 2006). MSCs are even known to promote angiogenesis (Bidarra, 2010).
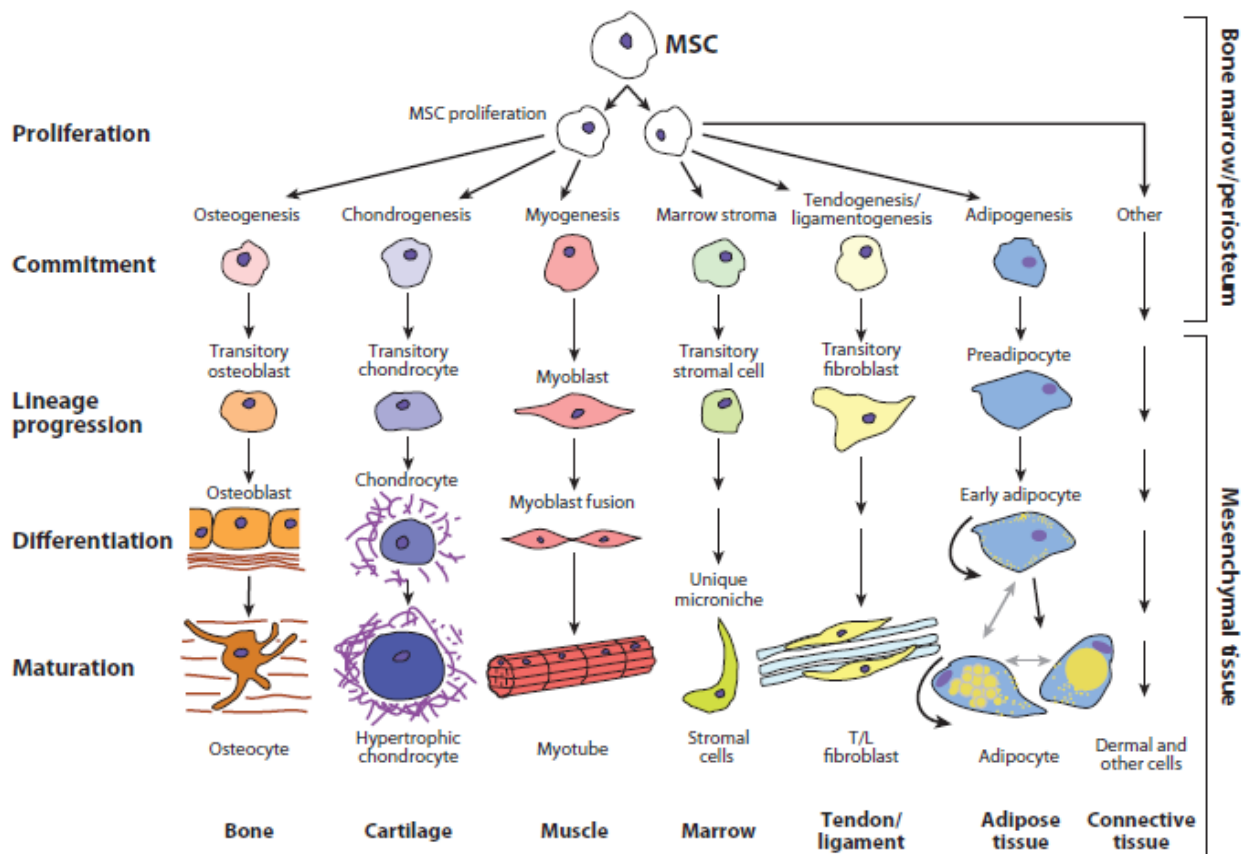


**Figure 4 Differentiation potential of human MSCs (Singer, 2011). The stem cells are capable of differentiating into a variety of connective tissues.**

The gene expression of MSCs changes as they differentiate into different phenotypes. Differentiation into osteoblasts can be monitored using methods for determining the gene expression of certain bone markers, specific for this lineage (Nakamura, 2007), or by simple enzyme activity detection (Christenson, 1997).

For osteoblast differentiation Runt-related transcription factor 2 (runx2), osterix (osx), alkaline phosphatase (alp), type I collagen (type I col), osteocalcin (ocn), osteopontin (opn) and bone sialoprotein (bsp) have been found to be important markers (Yao, 1994). Runx2 is a transcription factor that induces osteoblast differentiation early in the process, from stem cell to preosteoblast (Kassem, 2008). Osterix is important in later stages, where preosteoblasts differentiate into mature osteoblasts (Zhang, 2010). Alp and type I collagen are induced early in the differentiation and are important osteoblast phenotype markers. All of these genes can be detected at the RNA level using standard PCR technology. The expression of the runx2 and osterix at different stages during differentiation is given in figure 5.
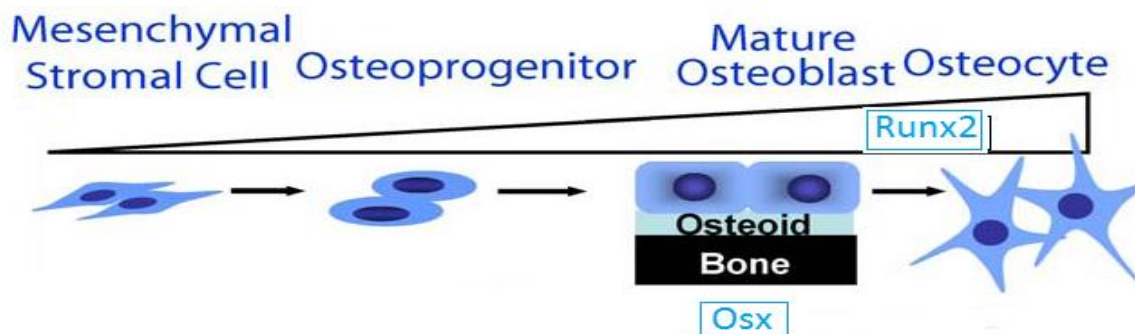


**Figure 5 Expression of runx2 and osterix during differentiation from stem cell to mature osteoblast. Modified from (Lian, 2006). Runx2 expression continues to increase throughout differentiation, whereas osterix is specific for mature osteoblasts.**

In addition, osteoblast differentiation can be detected by measuring ALP activity directly. This is accomplished by adding a fluorescence labeled substrate for the enzyme to the cell suspension, and consequently measuring the fluorescent intensity (Cox, 1999). *In vitro*, by induced differentiation of MSCs, a typical ALP activity is at its maximum at day 10, before decreasing with time (Shin, 2004).

Furthermore, some signaling molecules are known to promote the expression of the above mentioned genes. The most important are the BMPs, particularly BMP-2. This growth factor has been shown to induce bone formation through the promotion of osteoblastic lineages (Yilgor, 2010). Other growth factors that promote osteogenesis include VEGF, IGF-1 and FGF-2. Conversely, in excess, these latter growth factors will exhibit an inhibitory effect (Huang, 2010). When encapsulating MSCs in alginate beads the effect of growth factors on these cells may differ from the effect on cells in culture. This might be explained by hindered diffusion of the molecules into the encapsulated cells. This has been hypothesized in a previous study as it was observed that the diffusion of larger molecules decreased over time (Endres, 2010).

Recently, the importance of mechanical signals (as opposed to the biochemical signals described above) has been discussed. For example, the shape of the MSCs will in part be determined by the surrounding matrix, which in turn will, to a certain degree, determine which phenotype the cell will express (McBeath, 2004). Other mechanical factors shown to influence the route of differentiation include the local matrix stiffness, fluid flow outside the cells, tension and hydrostatic pressure (Kelly, 2010).

When it comes to encapsulation of MSCs into beads, studies have shown that the cells are more compelled to be directed towards an osteogenic phenotype inside the bead if high concentrations of hydroxyapatite (HA) is present (Kwei, 2010). This has been demonstrated in studies where inorganic HA crystallites are systematically attached to the scaffolds in use, and shown to promote osteoblast adhesion and protein adsorption, consequently leading to enhanced osteoblast function (Liu, 2004).

## 1.4 Biomineralization

Biomineralization is the process by which minerals are deposited in the extracellular or intracellular matrix, resulting in a material with both organic and inorganic constituents (Boskey, 1998). These materials are often strong due to the inorganic part and elastic due to the organic part.

An example of this process is the mineralization of bone in vertebrates which occurs in two steps. Initially, the accumulation of $Ca^{2+}$ and inorganic phosphate leads to the formation of HA in extracellular vesicles. These vesicles bud from the plasma membrane of all mineral forming cells and contain the necessary proteins for this purpose (Golub., 2009). The second step involves the elongation of the crystals, a process facilitated by the enzyme alkaline phosphatase (ALP). The exact mechanism of biomineralization by ALP on collagen was just recently discovered, although it has been hypothesized for some while that the enzyme acts on organic phosphate to release phosphate ions (Yamauchi, 2004, Tomomatsu, 2008). This was later proved after discovering that mineralization did not occur unless the organophosphate β-glycerophosphate was present (Spoerke, 2009). Finally, the crystals are deposited between collagen fibers (Orimo, 2010). The organization of HA between collagen fibers is illustrated in figure 6. As mentioned, much remains unknown regarding the exact mechanism of mineralization, but it seems that not only enzymes are involved in directing the mineralization, but also the extracellular matrix, i.e. collagen, at least in an *in vitro* system (Nudelman, 2010, Colfen, 2010).
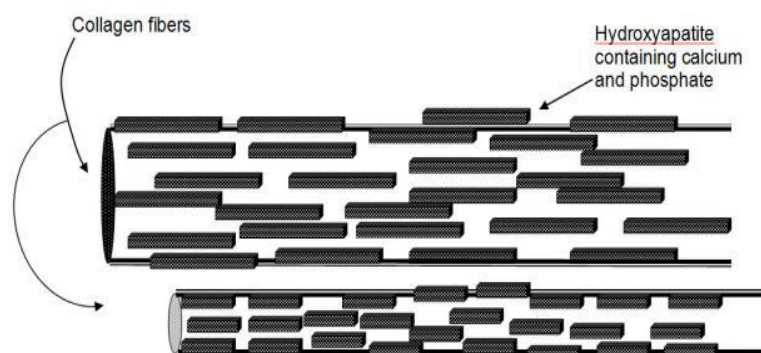


**Figure 6 Organization of hydroxyapatite between collagen fibers. In the last step of biomineralization of bone, hydroxyapatite is deposited between collagen fibers (Wildman, 2007).**

## 1.5 Enzymatic mineralization of alginate using alkaline phosphatase

Different strategies exist to mineralize hydrogels and scaffolds. These include the addition of inorganic phases, chemical modifications of the hydrogels to prevent inertia and biomimetic mineralization. The latter includes enzymatic mineralization where the above mentioned enzyme, ALP, is utilized (Gkioni, 2010). Additionally, it has been revealed that immobilized ALP in hydrogels made from fibrin enhance new bone formation (Osathanon, 2009). The use of ALP to make HA/Collagen composites has also been demonstrated in various studies (Unuma, 2007).

Recently, Xie et al. demonstrated that enzyme mineralization of alginate beads is favored over in situ mineralization for cell encapsulation, as lower concentrations of $CaCl_2$ is needed, which is beneficial for cell viability. In addition, the enzymatic method produces alginate beads with an uniformly distribution of calcium phosphate (CP) and stiffer mechanical properties (Xie, 2011). The former may be explained by the uniform distribution of ALP throughout the beads as given in figure 7A. Figure 7B and 7C give a comparison between the mineral distributions of beads mineralized with the enzymatic method, and the in situ method respectively. The stiffer mechanical properties of the beads might be explained by the mineral distribution, as a homogeneous distribution of mineral will lead to closer interactions between the polymer and the minerals.
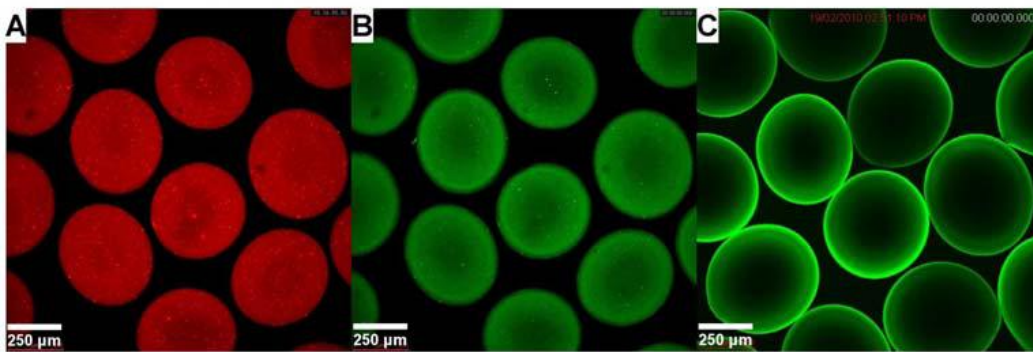


**Figure 7 CLSM images showing the distribution of ALP (figure A), minerals (B) in alginate beads mineralized by the enzymatic method using 0.1mg/mL ALP. Distribution of minerals in alginate beads mineralized with the in situ method (C) (Xie, 2011). The images are taken 24 hours post encapsulation, and show equatorial slices of the beads.**

Additionally, Xie et al. (2011) demonstrated that beads mineralized by the enzymatic method using 0.5mg/ml ALP contained an estimate of 27% of minerals in the total dry weight. About 13% of the weight was found to be hydroxyapatite. The reminder constituted of other calcination products including calcium deficient hydroxyapatite and/or amorphous calcium phosphate. The mineral composition was dependent on pH, time and enzyme concentration, as well as the concentrations of the precursors (β-glycerophosphate and calcium).

## 1.6 Encapsulation of MSCs in alginate beads

Encapsulation of hMSCs in *mineralized* alginate beads has previously been attempted (Sundrønning, 2010). In this study the alginate beads were mineralized using the *in situ* method. Sundrønning encapsulated 1 million hMSCs/mL alginate solution, and mineralized the beads using 100mM of phosphate and 300mM of $CaCl_2$. Post encapsulation (day 2) the viability was approximately 80% for all samples. A decrease in viability was observed in cells encapsulated in mineralized beads compared with unmineralized beads from day 11 (60% versus 80% live cells). Metabolic activity remained stable for both samples throughout the time of the study. Differentiation was examined using PCR technology. The purity of the isolated RNA was low, most probably due to DNA and/or alginate contamination. Genes indicating osteoblast differentiation were expressed in all samples (strong positive reaction), including samples neither mineralized nor given MSCDM.

In an expanded experiment using 6 million hMSCs, Sundrønning reported a stable and slowly increasing metabolic activity for all samples, as given in figure 8. Live/dead assays were also performed, and evaluation on the CLSM indicated a gradually decreasing viability for all samples. At day 23 (end point) 40% of cells were alive. To test degree of mineralization Alizarin Red-S staining was carried out. The mineralized samples showed an increase in mineral content compared to the unmineralized ones, regardless of differentiation. This was further confirmed by visual inspection as the mineralized samples were the only ones appearing white in the light microscope. Cell proliferation, measured by ^{3}H-thymidine incorporation, was observed to a small degree in all samples as demonstrated in figure 9.

RNA isolated from these cells was again of poor quality. runx2 was detected in all samples (positive reaction) at day 3 post encapsulation. At day 7 similar results were obtained. Also non encapsulated hMSCs were observed to exhibit osteoblast phenotype by expressing runx2 and osterix. For all other samples gapdh had a relatively low $C_t$ value[1], indicating that the cDNA concentration was low to begin with. Also, the high $C_t$ values of runx2 and osterix indicates that they are present in very small amounts. No osterix was detected in undifferentiated samples. $C_t$ values for every sample are given in table 1.

---

[1] $C_t$ values (cycle threshold) refer to the number of PCR cycles needed to accumulate enough cDNA for it to be detected above background noise. The $C_t$ value is inversely proportional to the concentration on cDNA in the sample. $C_t$ values ≤ 29 indicates a strong positive reaction of the target gene. Values from 30-37 indicates a positive reaction. Values above 38 indicate a negative reaction that can be explained by contamination or other factors.
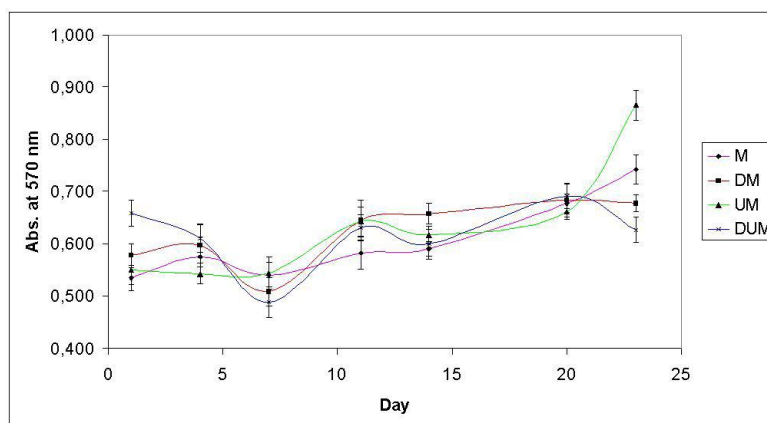
**Figure 8   Metabolic activity of hMSCs encapsulated in alginate beads (Sundrønning, 2010). Samples include undifferentiated mineralized (M), differentiated mineralized (DM), undifferentiated unmineralized (UM), and differentiated unmineralized (DUM) beads.**
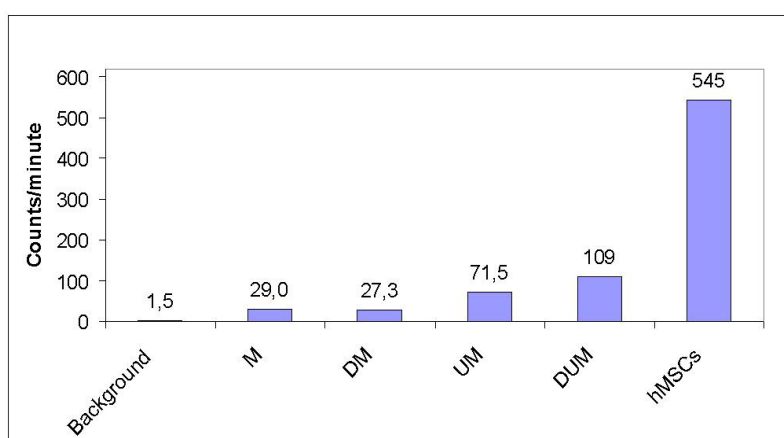


**Figure 9 Proliferation of encapsulated hMSCs in alginate beads measured by ^{3}H-thymidine incorporation. All samples show proliferation from day 16 to day 18 post encapsulation. Samples include undifferentiated mineralized (M), differentiated mineralized (DM), undifferentiated unmineralized (UM), and differentiated unmineralized (DUM) beads.**

**Table 1 $C_t$ values from PCR experiments with encapsulated in hMSCs in undifferentiated mineralized (M), differentiated mineralized (DM), undifferentiated unmineralized (UM), and differentiated unmineralized (DUM) alginate beads.**

| Sample Target | $C_t$ | Mean |
|---|---|---|
| M | gapdh | 30.23 |
| M | runx2 | 36.79 |
| M | osterix | - |
| DM | gapdh | 31.07 |
| DM | runx2 | 36.78 |
| DM | osterix | 35.07 |
| UM | gapdh | 24.88 |
| UM | runx2 | 23.50 |
| UM | osterix | -- |
| DUM | gapdh | 27.05 |
| DUM | runx2 | 32.64 |
| DUM | osterix | 33.72 |
| hMSC | runx2 | 20.19 |
| hMSC | gapdh | 14.85 |
| hMSC | osterix | 32.55 |

# 2. Materials and methods

## 2.1 Alginate solution

Ultrapure high-G alginate (UP MVG, batch: FP-505-01, $M_w$= 238.000 g/mol, $[\eta]$ = 1105 ml/g, $F_G$= 0.67, $F_{GG}$= 0.56, $N_{G\geq1}$= 13) purchased from NovaMatrix was used throughout this study.

All equipment was thoroughly washed with alcohol (70%), and all glassware, scissors etc. had been sterilized by autoclaving.

Experimental: The alginate powder was added to stirring sterile water to make a 4% alginate solution. NaCl (0.9 % w/v) was added to sterile water, and the two solutions were mixed and left on the stirrer for at least 5 hours to completely dissolve the alginate powder to a 2% solution. At this point the pH was adjusted to 7.2-7.4. The final solution was sterile filtered (0.2μm), and stored in a refrigerator until used.

## 2.2 Gelling solution

Experimental: Calcium chloride dihydrate ($CaCl_2$ * $2H_2O$ (50 mM)) was dissolved in sterile water. Following, NaCl (0.9 % w/v) and HEPES (10mM) were added. The pH of the solution was adjusted to the desired pH of 7.2-7.4. The solution was sterile filtered and stored in a sterile plastic bottle in a refrigerator until used.

## 2.3 Bead preparation

Experimental: Before encapsulation of cells in alginate beads, the enzyme ALP (12.5 or 25 μl) was mixed with the alginate solution (0.9mL) inside a syringe with an outer diameter of 0.35μm. After thorough mixing, cells in medium (0.1mL) were added, and the solution was yet again mixed. The syringe was mounted to an infusion pump, and attached to a needle by a plastic tube. The needle was set up about 2cm above the gelling solution, which was continuously stirred by a magnet stirrer. The electrostatic potetial was set to 7 kV and the infusion rate was 8 mL/h. The cell/alginate/enzyme solution was subsequently dripped into the gelling solution. After encapsulation the beads were left in the gelling solution for approximately 10 minutes, prior to a thorough washing in Hanks Buffered Salt Solution (HBSS).

Roughly 200 mL gelling solution was used for every 1 ml of alginate/cell solution.

For the last experiment (M4) a multihead with four syringes was set up to prevent the cells from being exposed to the gelling solution for a long period of time.

Encapsulated cells were incubated at 37°C and 5% $CO_2$.

## 2.4 Alamar Blue assay

Principle: The Alamar Blue (AB) assay is performed to evaluate cellular health by measuring metabolic activity. The principle is based on the living cell´s natural reducing power as described in figure 2.1. The Alamar Blue dye is non toxic and very stable, and has proven to be superior to similar assays, such as the 3-[4,5-dimethylthiazol-2-yl]-2,5-diphenyl tetrazolium bromide (MTT) assay (Hamid, 2004). When Alamar Blue is added to a cell suspension the dye enters the cells and becomes reduced by electron donors such as $FADH_2$ and NADH. This reaction results in a shift of color that can be correlated to the health of the cells. As the redox reaction is dependent on the metabolic state of the cells it cannot give an accurate measure of cell viability (Al-Nasiry, 2007).
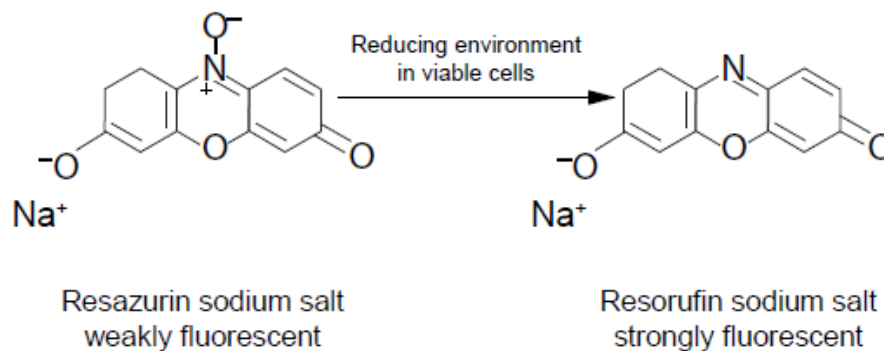


**Figure 2.1 Alamar Blue assay principle. When resazurin is reduced to resorufin it produces a bright red fluorescent signal which in turn can be detected spectrophotometrically (Markaki, 2009).**

Experimental: An estimate of 5000 cells in beads was transferred to a 96 well plate. Medium from the culture flasks was added to the bead/cell suspension to make up a total of 180μl. Five parallels were prepared for each sample. As a control medium from each culture flask without beads were used. Alamar Blue (18μl) was added to each well, and the plate was incubated for 4 hours before measuring fluorescence on a multilabel counter (Victor, Perkin Elener). The readings from the control were subtracted from the sample measurements.

## 2.5 RNA isolation, cDNA synthesis and PCR

Principle: The gene expression of a cell can be studied by extracting its RNA, synthesize the RNA into complementary DNA (cDNA) and subsequently running the Polymerase chain reaction (PCR). Quantification can be done either absolutely or relatively. For studying the difference in gene expression for a given gene, the relative quantification method is adequate. In the real time-PCR (RT-PCR) the gene is studied as it is amplified. The stronger the expression of the gene, the faster it will be detected. These results will be given as a cycle threshold ($C_t$) values. The smaller the $C_t$ values, the greater the amount of target gene is present in the sample[2]. Using a household gene as a control, one can calculate the relative expression of the target gene. For this reason, RT-PCR are commonly used for studying the effect of a given target gene compared to an untreated sample (Livak, 2001).

---

[2] $C_t$ values ≤ 29 indicates a strong positive reaction of the target gene. Values from 30-37 indicates a positive reaction. Values above 38 indicate a negative reaction that can be explained by contamination or other factors.

Experimental: Approximately 1 000 000 cells were transferred to a 50 mL centrifuge tube. Citrate (50mM, approximately 5mL- appendix A for details) was added to the cell suspension and gently vortexed. After dissolving the beads, the sample was centrifuged for 3 minutes at 1000 rpm and the supernatant removed. At this point, the solution was washed with Phosphate buffered saline (PBS), before a second round of centrifugation and supernatant removal. The sample was resuspended in PBS (200µl) before the RNA isolation step. For RNA isolation the ROCHE High Pure Isolation Kit was used. The isolation was performed according to the manufactures procedure. Briefly, a lysis buffer (400µl) was added to the cell suspension and vortexed. The sample was transferred to a "collecting tube" and centrifuged. A mixture of DNAse buffer (90µl) and DNAse (10µl) was added to the tube, the sample was centrifuged, and the supernatant removed. The sample was at this point incubated in room temperature for 15 minutes. Three rounds of washing were performed, before the RNA was eluated with an eluating buffer (60µl). A part of the sample (6µl) was taken out for OD determination. The rest of the sample was frozen at -80°C.

For determination of RNA concentration and RNA quality the NanoDrop Spectrophotometer (ND-1000 Spectrophotometer, NanoDrop Technologies Inc.) was employed. Each sample was run in three parallels, and the mean concentration was utilized hereinafter.

For cDNA synthesis the High Capacity RNA-to-cDNA Kit (Applied Biosystems) was utilized. In brief, the isolated RNA, sterile ion free water (SIV) and a mixture of reverse transcriptase (RT) buffer and enzyme mix was added to an eppendorf tube and vortexed shortly. A control without RT buffer was also prepared. All samples were incubated at 37°C for 60 minutes before the reaction was stopped by increasing the temperature to 95°C for 5 minutes. The samples were put on ice and vortexed abruptly, before they were frozen in -20°C until used.

RT-PCR analysis was performed using TaqMan Gene Expression Array (Applied Biosystems). Briefly, cDNA was diluted to the same concentration for all samples. Master Mix, probes and cDNA dilutions were mixed thoroughly and added to a 96 well plate in three parallels for each sample. The probes for detection of osteogenic phenotype were runx2 (Hs00231692_m1, lot 959159) and osterix (Hs00541729_m1, lot 961822). The housekeeping gene glyceraldehydes-3-phosphate dehydrogenase (gapdh, Hs99999905_m1, lot 853053) was used as an endogenous control. Furthermore, RT negative samples were prepared for each of the probes. The Applied Step One Software 2.1 was used to analyze the samples.

## 2.6 Live/dead assay and imaging by Confocal Laser Scanning Microscope

Principle: Determination of cell viability can be performed by investigating certain biologic properties specific for either live or dead cells. In the live/dead assay two dyes are used for visualization of these properties, Calcein-AM and Ethidium homodimer-1 (Eth-1). Calcein-AM enters the live cells and is converted by esterases to calcein that produces an intense green signal, which can be detected by Confocal Laser Scanning Microscope (CLSM). Eth-1 will cross the membrane of dead cells only and bind to nucleic acids. This can be visualized by a red signal (Invitrogen, 2005). Figure 2.2 depict mesenchymal stem cells stained with live/dead dyes. Table 2.1 gives an overview over the settings of the CLSM.

Experimental: A live/dead Viability Kit was purchased from Invitrogen. The stock solutions were left on the bench to warm to room temperature. A working solution was prepared by adding Eth-1 (8 µl) and Calcein AM (10 µl) to PBS (5 mL). The solution was vortexed to ensure thorough mixing. The solution was kept in a refrigerator and stored for no more than one week. Beads and medium (~0.2 mL) were transferred to an eppendorf tube, and washed with PBS. The working solution containing the two dyes was added to the tube in a 50:50 relationship to the bead/PBS solution. The mixture was transferred to a sterile plastic petri dish, and incubated for a few minutes before imaging by CLSM.
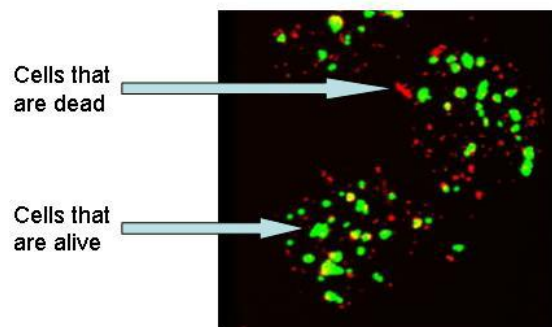


**Figure 2.2 Mesenchymal stem cells encapsulated in alginate beads mineralized by the in situ method stained with calcein-AM (green) and eth-1 (red). Modified from (Sundrønning, 2010).**

**Table 2.1 Settings of the CLSM for live/dead assay.**

| | |
|---|---|
| Scan Mode; | Plane, original data, multi track, 8 bit |
| Objective; | C-Apochromat 10x/0.45W |
| Beamsplitters; | MBS-1: HTF UV/488/543/633 |
| | DBS1-1: Mirror |
| | DBS1-2: Mirror |
| | NDD MBS1-1: None |
| | MBS-2: HTF UV/488/543/633 |
| | DBS1-2: Mirror |
| | DBS2-2: NFT 545 |
| | NDD MBS1-2: None |
| | MBS-3: HTF UV/488/543/633 |
| | NDD MBS: None |
| Lasers; | Argon (488nm) |
| | HeNe (543nm) |
| Filters; | BP 505-530 |
| | LP 650 |
| Pinholes; | 199µm |

## 2.7 Actin filament and nucleus staining using Phalloidin and DRAQ5

Principle: Visualization of cell morphology can be performed by staining the cytoskeleton and the nucleus. Phalloidin bind to actin filaments in the cytoskeleton (Wulf, 1979). DRAQ5 has a high capacity to permeate the cell membrane, and bind to DNA with high affinity and selectivity (Smith, 2004). Figure 2.3 depict a comparison between the morphology of an osteoblast with elongated actin filaments (left), and an osteoblast without elongation (right). Table 2.2 gives an overview over the settings on the CLSM.

Experimental: One part bead/medium suspension was added to an eppendorf tube. The beads were allowed to segregate and the remaining medium was pipetted off. The beads were washed with 0.1% PBS/ Bovine serum albumin (BSA). Following, the cells were fixed by adding 2 parts 0.1% PBS/BSA with 3.7% FAH, and incubated for 15 minutes. Subsequently, the excess fixation medium was removed by washing with 0.1% PBS/BSA 3 times. One part Saponin in 0.1% PBS/BSA was added and the sample was incubated for 10 minutes in RT. Ultimately, the two dyes, Phalloidin (1 part) and cyto5 (1 µl) were added. After about 10 minutes the samples were washed with 0.1% PBS/BSA before imaging by CLSM.
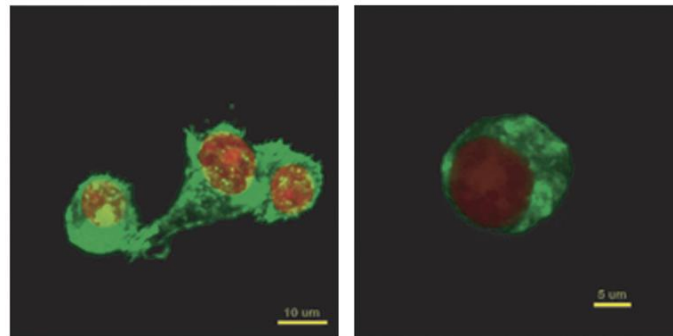


**Figure 2.3 A mouse osteoblast (MC3T3-E1) stained by propidium iodide (red) and Phalloidin (green) inside alginate beads with RGD (right) and without (left). The left image shows a cell with elongated actin filaments, whereas the right image shows a cell without elongation. Images are taken at day 21 post encapsulation. Modified from (Evangelista, 2007).**

**Table 2.2 Settings of the CLSM for cell morphology imaging.**

| | |
|---|---|
| Scan Mode; | Plane, original data, multi track, 8 bit |
| Objective; | C-Apochromat 10x/0.45W, C-Apochromat 40x/1.2W, C-Apochromat 63x/1.2 W |
| Beamsplitters; | MBS-1: HTF UV/488/543/633 |
| | DBS1-1: Mirror |
| | DBS1-2: NFT 610 |
| | NDD MBS1-1: None |
| | MBS-2: HTF UV/488/543/633 |
| | DBS1-2: Mirror |
| | DBS2-2: NFT 610 |
| | NDD MBS1-2: None |
| | MBS-3: HTF UV/488/543/633 |
| | NDD MBS: None |
| Lasers; | Argon (488nm) |
| | HeNe (633nm) |
| Filters; | BP 505-530 |
| | LP 650 |
| Pinholes; | 166µm, 212µm |

## 2.8 ALP activity measurements

Principle: ALP activity serves as a potent endogenous marker for distinguishing osteoblast phenotype from MSCs (Wang, 2008). Briefly, the substrate ELF-97 will fluoresce brightly upon cleavage by the ALP enzyme, and the enzymatic activity can thus be measured spectrophotometrically (Telford, 2001, Telford, 1999).

Experimental: Approximately 10 beads were transferred to an eppendorf tube, and exposed to citrate (50 mM) to dissolve the beads. At this point the cells were fixated in FAH (~3.5%, 100 µl) for ten minutes, and subsequently centrifuged (5min, 800g, RT). Next, the cells were permeabilized by adding 200 µl Tween 20 in PBS (0.2%), and left in RT for 15 minutes, before another round in the centrifuge. At this point the cells were washed once with saline water (1 mL), incubated for 10 minutes and centrifuged (5 min, 800g, RT). Following, the substrate (ELF-97), diluted 1:20 in the substrate buffer, was added to every sample (50 µl in each well). After incubation for 5 minutes the samples were read on a Victor plate reader, program ELF 97.

## 2.9 Scanning electron microscopy

Principle: Scanning electron microscope (SEM) is used to image cross sections of beads under greater magnifications then what is possible in the light microscope. For that reason the structure of the mineral composites can be further studied. SEM is also used to study cell morphology (Gargioni, 2006). One major drawback is that preparations of sections involve steps that may collapse/shrink the samples. This is especially evident when using alginate, due to its high content of water (97%) (Bevan, 1995).

Experimental: At the end of the study (experiment M4, day 21) samples were taken out of the culture flask and mixed with Tissue Tek (Qiagen). Following, the beads were frozen using acetone precooled with liquid nitrogen. The frozen beads were sectioned with a microtome (Leica CM 3050 S). To prepare the sections for imaging they were dried in a critical point dryer (Emitech K850 Critical Point Dryer). Following, the dried beads were coated with platinum (80%) and palladium (20%). Characterization of the sections was accomplished using a scanning electron microscope.
Sample preparation and SEM analysis were carried out by M. Xie (post doc candidate).

## 2.10 Cells and cell culturing

In initial experiments the cell line U2OS was utilized. This is a line of osteosarcoma cells derived from the bone tissue (tibia) of a 15 year old female who suffered from the disease.  In the main part of this study human Mesenchymal stem cells (hMSCs) purchased from Lonza Inc (PT 2501) were utilized. These cells were donated from healthy, consenting individuals. In each experiment a concentration of 2 million cells per 0.1 mL medium/mL alginate solution was used. U2OS cells were quantified using trypan blue and a coulter counter, and hMSCs were counted manually in Burker cell chambers.

The U2OS were cultivated in cell culture flasks ($75cm^2$) receiving RPMI 1640 medium with added Fetal Calf Serum (FCS, 50 mL), glutamine (2 mL) and garamycin (250 µl) making a total of 500 mL. This medium will henceforth be referred to as OSGM (osteosarcoma growth medium). U2OS cells encapsulated in alginate beads received OSGM with added $CaCl_2$ and β-glycerophosphate during the mineralization process, and this medium will be referred to as OSMM (osteosarcoma mineralization medium). After the mineralization period the encapsulated cells received OSGM with supplementary $CaCl_2$.

The MSCs were also cultivated in cell culture flasks of 75cm$^2$ receiving Mesenchymal Stem cell Growth Medium (MSCGM, Lonza Inc, Walkerswille, MD, USA) which constitutes of Mesenchymal Stem Cell Basal Medium (MSCBM) with added Mesenchymal Cell Growth Supplement, glutamine and gentamycin. The Mesenchymal Stem cells were reseeded as few times as possible as they differentiation potential decreases after recurrent trypsine treatments. However, they were reseeded as soon as they obtained about 80 % confluence. As a rule of thumb, the MSCs for differentiation study purposes should not be trypsinized more than 7 times. Similar to the U2OS cells the MSCs received mineralization medium containing $CaCl_2$ and β-glycerophosphate the first 48 hours after encapsulation (henceforth referred to as MSCMM (MSC mineralization medium)), and subsequently MSCGM containing $CaCl_2$.

In experiment M4, the samples containing cells were split in two at day 2 post encapsulation. One of the batches received MSCGM containing $CaCl_2$, and the other received MSCDM (MSC differentiation media). This includes BMP-2 (300 ng/mL, R&D Systems, Minneapolis, MN, USA), ascorbic acid (50 mg/mL), dexamethasone (5 µl 10$^{-4}$ M) and glycerophosphate (500 µl, 1M) for every 50 mL of medium. Furthermore, the culture flasks were changed as soon as MSCs were observed growing outside of the beads.

All solutions were sterile filtered and stored in a refrigerator for a maximum of one week.

## 2.11 Experiment setup

In all experiments cells were encapsulated, and the beads were mineralized for 48 hours. Following mineralization the batches were given different media depending on the experiment at hand. An overview over the process is given in figure 2.4. Table 2.3 gives as overview over the different concentrations/ component utilized in each experiment.
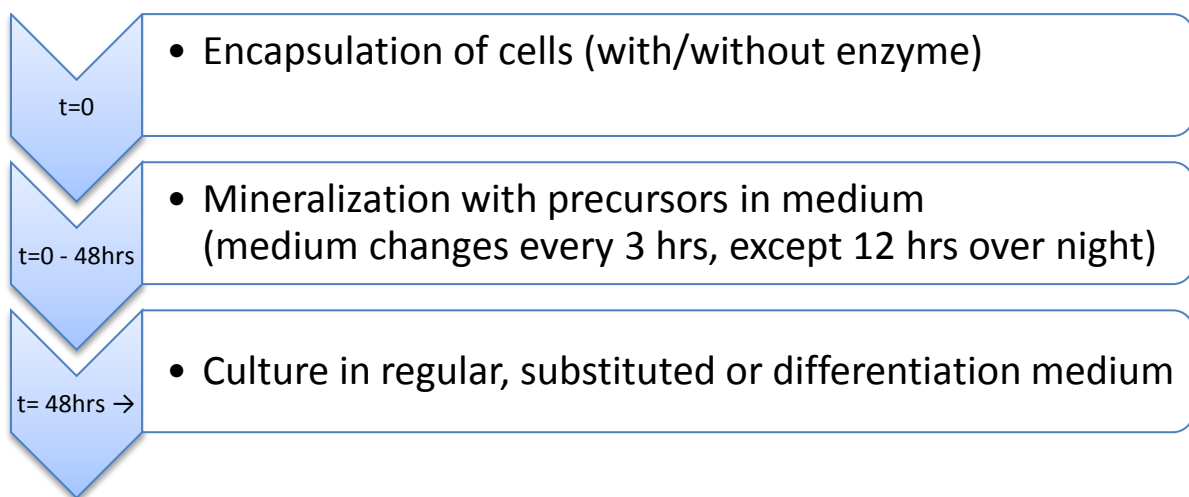
| t=0 | • Encapsulation of cells (with/without enzyme) |
|---|---|
| t=0 - 48hrs | • Mineralization with precursors in medium (medium changes every 3 hrs, except 12 hrs over night) |
| t= 48hrs → | • Culture in regular, substituted or differentiation medium |

**Figure 2.4 Flow sheet for experiment set up. All samples were prepared as described in the figure.**

Table 2.3 Experiment setup. All experiments were conducted as described above. U-experiments refers to experiments with the cell line U2OS, whereas M-experiments refers to experiments with hMSC-10 (experiments M1-3) or MSC-9 (M4). These are cell lines from two different individuals. The first 48 hours after encapsulation the medium was changed every 3 hours (12 hours over night).

| Experiment number | Cell line | Medium (day 2 →) | CaCl$_2$ conc. for stabilization (mM) | Enzyme concentration |
|---|---|---|---|---|
| U1 | U2OS | OSGM | 0 | 0.5mg/mL |
| U2 | U2OS | OSGM | 15 | 0.5mg/mL |
| U3a | U2OS | **1** OSGM | 0 | 0.5mg/mL |
|  |  | **2** OSGM | 7.5 |  |
|  |  | **3** OSGM | 15 |  |
| U3b | U2OS | **1** OSGM | 0 | 0.25mg/mL |
|  |  | **2** OSGM | 7.5 |  |
|  |  | **3** OSGM | 15 |  |
| U4 | U2OS | **2** OSGM | 7.5 | 0.25mg/mL |
|  |  | **3** OSGM | 15 |  |
| M1 | hMSC-10 | **1** MSGM | 7.5 | 0.25mg/mL |
|  |  | **2** MSGM | 15 |  |
| M2 | hMSC-10 | MSGM | 7.5 | 0.25mg/mL |
| M3 | hMSC-10 | MSGM | 7.5 | 0.5mg/mL |
| M4-1 | None | MSGM | 7.5 | None |
| M4-2 | None | MSGM | 7.5 | 0.25mg/mL |
| M4-3 | hMSC-9 | **3b** MSCGM | 7.5 | None |
|  |  | **3a** MSCDM | 7.5 |  |
| M4-4 | hMSC-9 | **4b** MSCGM | 7.5 | 0.25mg/mL |
|  |  | **4a** MSCDM | 7.5 |  |

## 2.12 Additional methods

Recovering cells from alginate beads was attempted several times. A description of the procedures and results are given in appendix A. Quantification of mineral content using Alizarin red –S was also attempted. Description of the experimental set up is given in appendix B.

## 2.13 Statistical analysis

A two tail Student t-test assuming equal variances was performed for assessment of statistical significance. A $p$ value less than 0.05 was considered as significant.

# 3. Results

## 3.1 Initial experiments with osteosarcoma cells

To study capsule properties and cell survival, osteosarcoma cells were utilized as model cells. The main object was to study bead stability, and how the beads and the cells within were affected by the enzymatic mineralization method. The following section describes the results found during these initial experiments.

### 3.1.1 Examination of bead stability and cell survival

To test cell survival and capsule properties (experiment U1) cells from the cell line U20S were encapsulated in mineralized alginate beads as described in section *2 (Materials and methods)*. At day 5 the beads were investigated in a light microscope and the result is given in figure 3.1. The beads appeared dark indicating mineralization. This was further confirmed as beads appeared white by visual inspection. However, many of the beads were cracked or ruptured completely.

As bead stability proved to be poor, a new experiment (experiment U2) was arranged. To stabilize the beads 15mM of $CaCl_2$ was added to the growth medium at day 2 post encapsulation and the culture flask was incubated for three days. The mineralization at day 0, day 2 and day 5 is demonstrated in figure 3.2. Again, mineralization was confirmed as the beads appeared dark in the light microscope and white by visual inspection. The mineralization process seemed to continue on even after the first 48 hours when cells were no longer given OSMM, as the beads continued to get darker in the light microscope. Furthermore, addition of $CaCl_2$ stabilized the beads as they were all intact.

At day 2 and 5 the number of intact beads was estimated by counting 100 beads. An evaluation of cell viability was performed by using live/dead assay and CLSM. The results are presented in table 3.1. Images from CLSM are presented in figure 3.3. Most cells survived the encapsulation process, seen at day 0, and the following mineralization, seen at day 2 post encapsulation. However, as the mineralization process progressed, viability decreased. Additionally, the heavily mineralized beads made CLSM image acquisition difficult. This might be explained by the density of minerals in the core of the bead. At day 5 only the cells in the outer part of the beads were visible, making it hard to estimate the viability correctly.

To test RNA quality the beads were dissolved in citrate, washed with PBS and the cells were counted. At this point almost all cells were gone. As an explanation for the great cell loss was not found, further studies were performed in order to optimize the citrate treatment. All results from the citrate treatment optimizing process are given in appendix A.
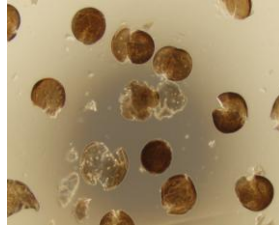
**Figure 3.1 Osteosarcoma cells encapsulated in alginate beads given 0.5mg/mL ALP (experiment U1) at day 5 post encapsulation. About 80 % of the beads are broken and/or completely dissolved.**
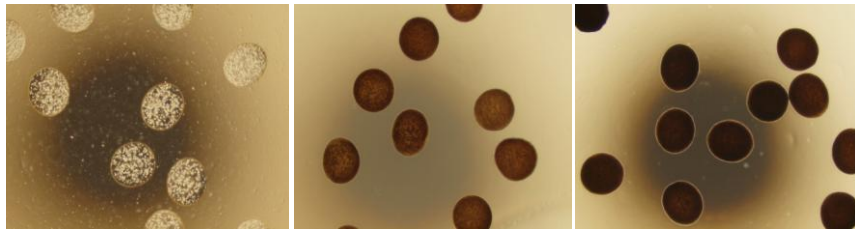


**Figure 3.2 Osteosarcoma cells encapsulated in alginate beads given 0.5 mg/mL ALP (experiment U2) at day 0, day 2 and day 5 post encapsulation, respectively. 15mM of CaCl$_2$ was added to the culture medium to stabilize the beads at day 2 post encapsulation.**

**Table 3.1 Viability and number of intact beads at day 0, 2 and 5 post encapsulation. The beads were given 0.5 mg/mL ALP. The beads were stabilized by adding 15mM of CaCl$_2$ to the culture medium.**

| Day (post encapsulation) | Viability (%) | Intact beads (%) |
|---|---|---|
| 0 | 97 | 100 |
| 2 | 75 | 98 |
| 5 | 55 | 98 |

## Alginate beads given 0.5mg/mL ALP



**Day 2**



**Day 5**
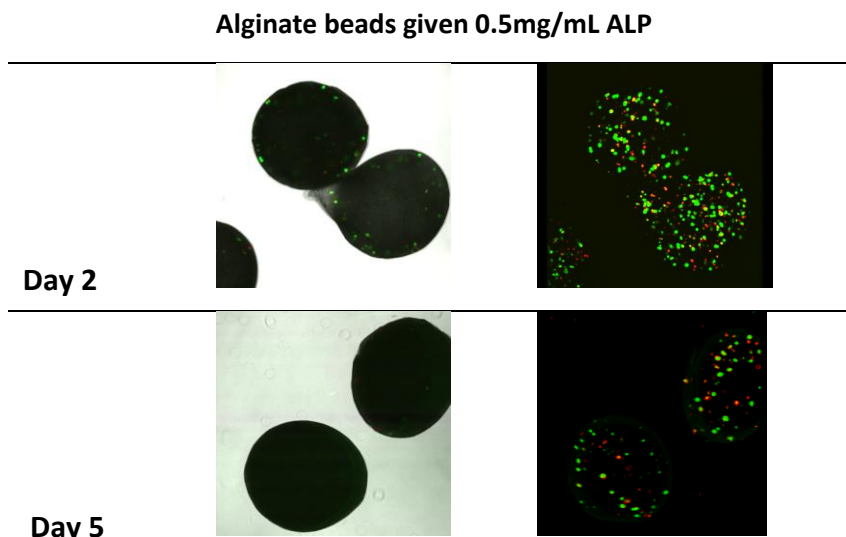
**Figure 3.3 CLSM pictures of U2OS cells encapsulated in alginate beads given 0.5 mg/mL ALP. Beads were stabilized by adding 15mM CaCl$_2$ to the culture medium. Left picture: CLSM cross section. Right picture: CLSM Z stacks 3D projection of the same beads. Live cells are indicated by a green color, whereas red cells are dead. Magnification: 100X.**

### 3.1.2 Extended experiment of osteosarcoma cells in mineralized beads

It was hypothesized that the beads became brittle from the fast mineralization process. This was likely caused by continuous production of phosphate ions by ALP, which precipitated with $Ca^{2+}$-ions in the gel, thereby destabilizing the alginate cross-links. For that reason a new experiment (experiment U3) was set up with the goal of comparing bead stability and cell survival in beads given different ALP concentrations. Seeing that addition of 15mM $CaCl_2$ improved bead stability this was repeated in the experiment at hand. However, as high concentration of $CaCl_2$ may affect cell viability, the sample was split in three at day 2. One batch was given no $CaCl_2$, one 7.5mM $CaCl_2$ and one 15mM $CaCl_2$ to uncover at what concentration viability was favored.

The beads from the two batches with different enzyme concentrations were monitored, and light microscope pictures were taken during the mineralization process. The results are given in figure 3.4. All beads were mineralized at day 2 post encapsulation, regardless of enzyme concentration. The beads given 0.5mg/mL ALP appeared darker compared with the beads given 0.25mg/mL, suggesting that they were more mineralized. The images are all from batches stabilized with 15mM $CaCl_2$. All beads remained intact in these batches. This was not the case for batches with less, or no addition of $CaCl_2$.

For that reason, bead stability was examined by counting 100 beads. Figure 3.5 compares how the stability of the different beads was influenced by different calcium concentrations. It seemed that bead stability was superior in beads stabilized with 7.5 or 15mM $CaCl_2$ as most of the beads remained intact reaching day 8 post encapsulation. At this point beads in batches without addition of $CaCl_2$ were all gone. Comparing the two batches of beads added different concentrations of $CaCl_2$, addition of 15mM seemed to give a slightly increased stability. Furthermore, enzyme concentration seemed to affect stability as well. Stability of beads given 0.25mg/mL ALP was superior compared to those given 0.5mg/mL ALP.
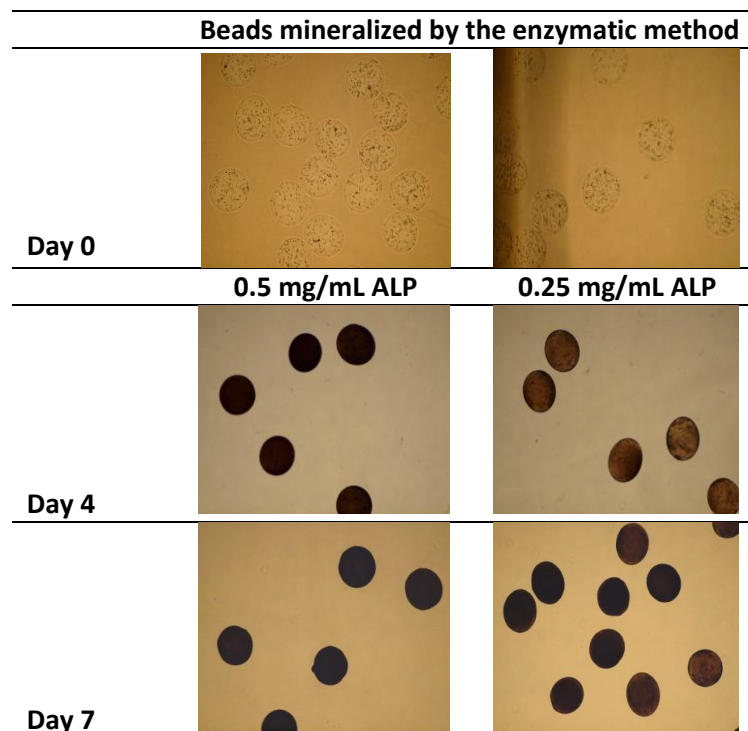


**Figure 3.4 Light microscope pictures at day 0, 4 and 7 post encapsulation from beads given 0.25mg/mL and 0.5mg/mL ALP. Beads were stabilized with 15mM $CaCl_2$. Image magnification: 40X.**
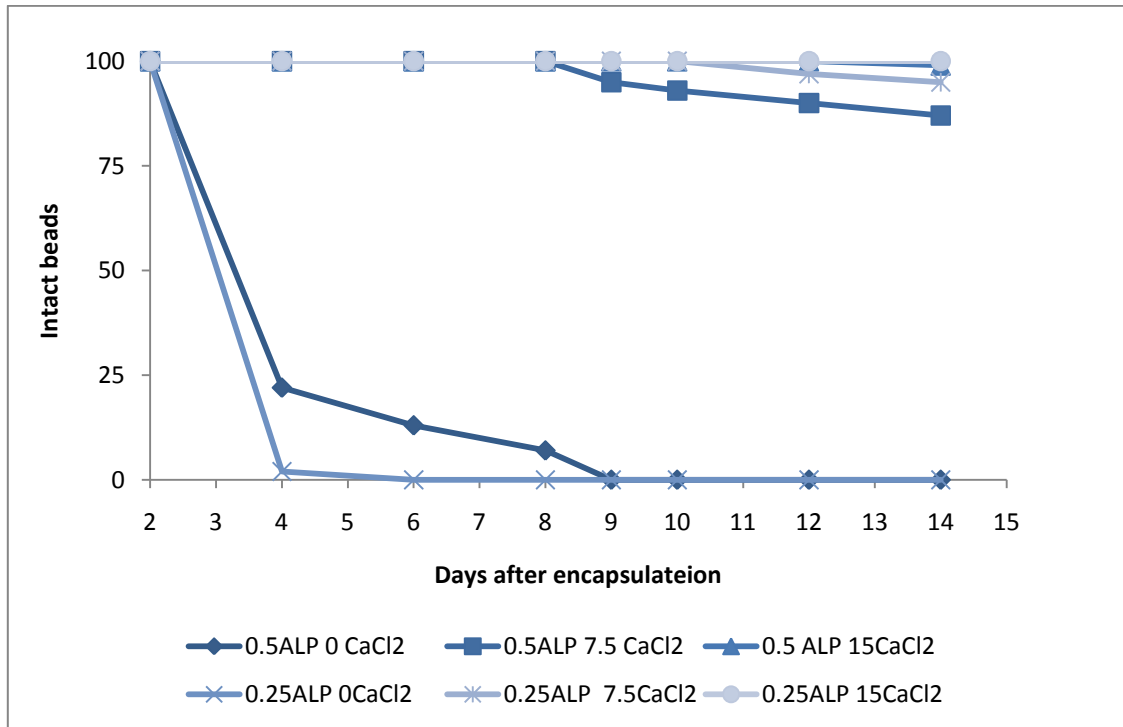
**Figure 3.5 A comparison of bead stability in beads given 0.25mg/mL, and 0.5mg/mL ALP respectively, and between the two batches given different calcium concentrations in the culture medium (0, 7.5 and 15mM, respectively).**

CLSM images from the experiment are given in figure 3.6 and 3.7. As no, or only 22%, of the beads remained intact at day 4 post encapsulation in medium without addition of $CaCl_2$, no further live/dead assays were performed on these samples.

It appeared to be a slight tendency to augmented cell survival in beads given 7.5mM $CaCl_2$ for stability over the ones given 15mM. Cell survival in beads mineralized with different concentrations of ALP appeared to be fairly equivalent, although the survival seemed to be higher in beads given 0.25 mg/mL ALP until reaching day 9 post encapsulation.

As beads became increasingly mineralized, difficulties arose regarding image acquisition. The viability estimates after day 2 post encapsulation are consequently uncertain, particularly in beads given 0.5 mg/mL ALP.
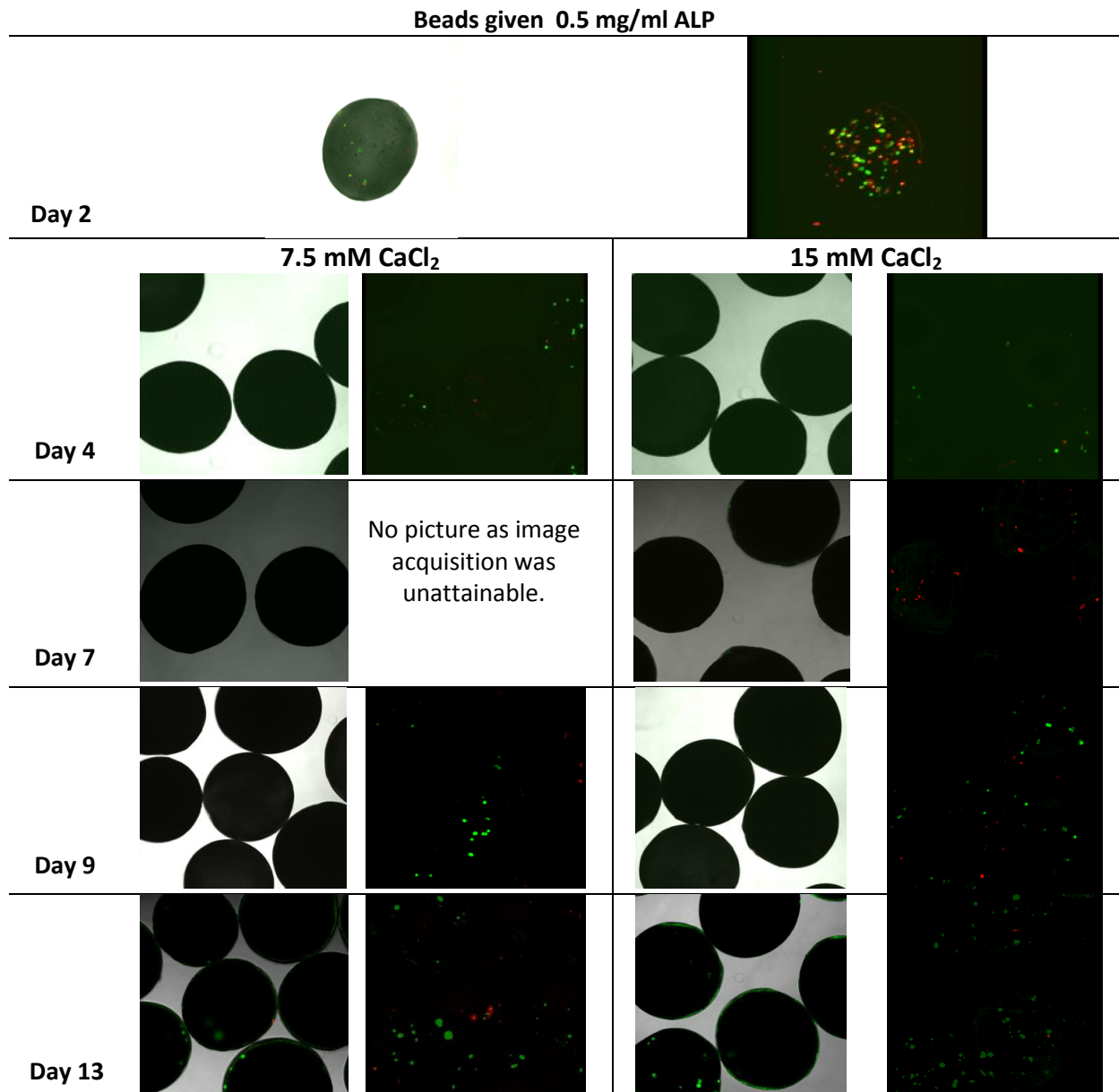
**Beads given  0.5 mg/ml ALP**



**Figure 3.6 CLSM images of U2OS cells encapsulated in alginate beads given 0.5 mg/mL ALP. Samples were cultured in 7.5 and 15 mM CaCl$_2$ from day 2 to day 13 post encapsulation. Right picture: CLSM Z stacks 3D projection of the same beads. Live cells appear green, whereas dead cells appear red. All images were magnified 100X.**
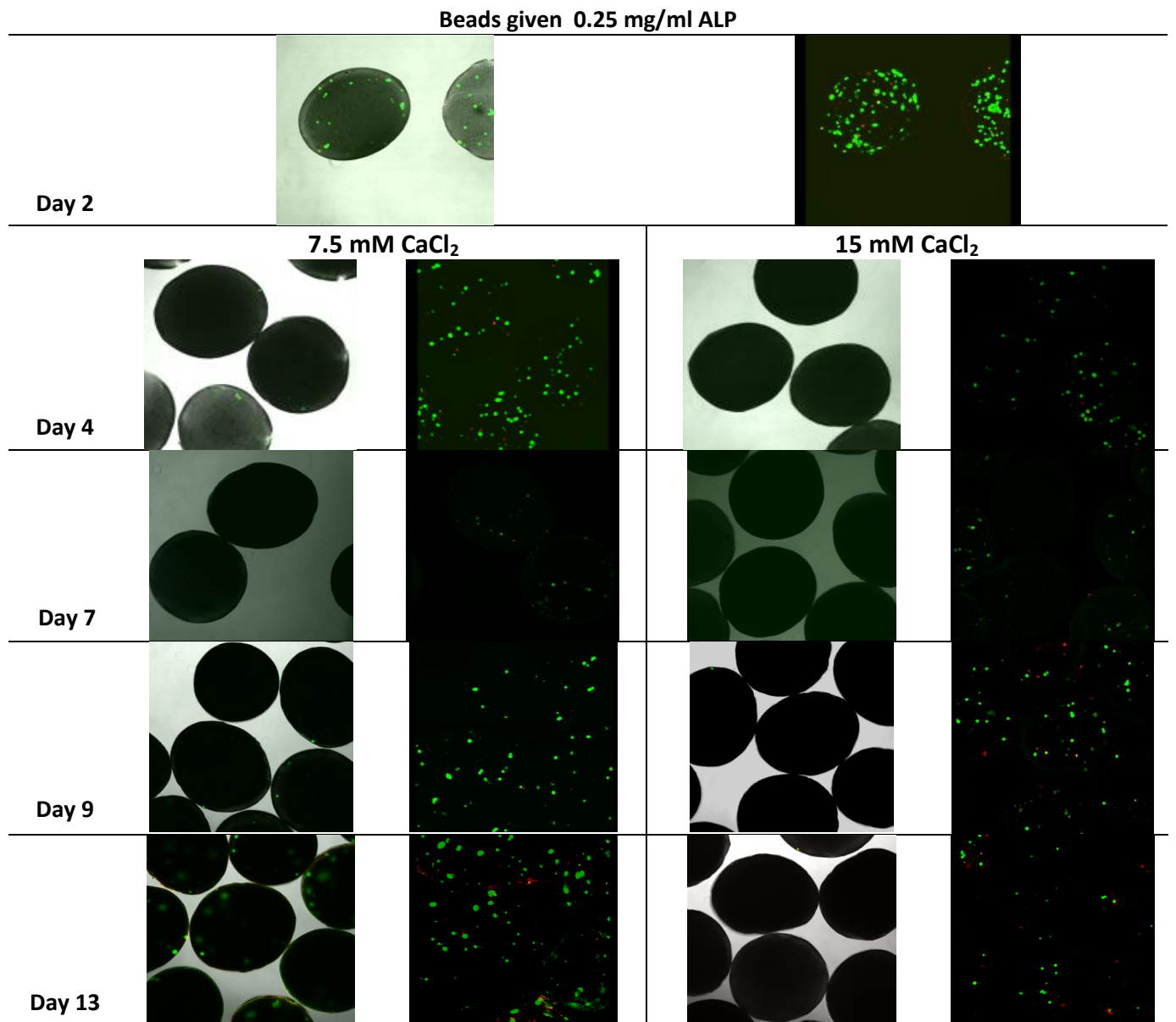
**Beads given  0.25 mg/ml ALP**

| | 7.5 mM CaCl$_2$ | 15 mM CaCl$_2$ |
|---|---|---|

**Day 2**

**7.5 mM CaCl$_2$**   **15 mM CaCl$_2$**

**Day 4**

**Day 7**

**Day 9**

**Day 13**



**Figure 3.7 CLSM images of U2OS cells encapsulated in alginate beads mineralized using 0.25 mg/mL ALP.  Samples were cultured in 7.5 and 15 mM CaCl$_2$ from day 2 to day 13 post encapsulation. Right picture: CLSM Z stacks 3D projection of the same beads. Live cells appear green, whereas dead cells appear red. All images were magnified 100X.**

## 3.2 Initial experiments with mesenchymal stem cells

Before initializing an extensive experiment, preliminary experiments were carried out in order to determine whether the MSCs would behave in a similar fashion as the osteosarcoma cells inside the mineralized alginate beads. The following sections describe results obtained during these initial experiments.

### 3.2.1 Mineralization with 0.25mg/mL ALP

From initial experiments with osteosarcoma cells it appeared that addition of $CaCl_2$ to the basal medium after day 2 post encapsulation helped stabilizing the beads. Furthermore, mineralization of beads by addition of 0.25 mg/mL ALP compared with 0.5mg/mL appeared to be beneficial as image acquisition on CLSM was facilitated and slightly higher viability of cells was observed.

Consequently, MSCs were encapsulated in beads given 0.25mg/mL ALP (experiment M1). At day two the MSCMM was changed to MSCGM with 7.5mM/15mM of added $CaCl_2$. Figure 3.8 gives light microscope pictures of the beads at different time points during the mineralization and culture. From the figure it is apparent that the MSCs cluster inside the beads. This is a known tendency for MSCs and may influence the result of the present study. From a cell survival point of view, the clustering may be beneficial, as cells may support each other. The clustering may, however, camouflage the effect of the matrix material efficiency of supporting the cells inside the matrix.

The mineralization process in beads with MSCs also seemed to differ somewhat from the mineralization process in beads with U20S. In beads with MSCs it seemed that the mineralization starts in the core of the bead rather than in the outskirts, as was observed in experiments with osteosarcoma cells. Also, the degree of mineralization is rather low compared to the experiments with osteosarcoma cells.
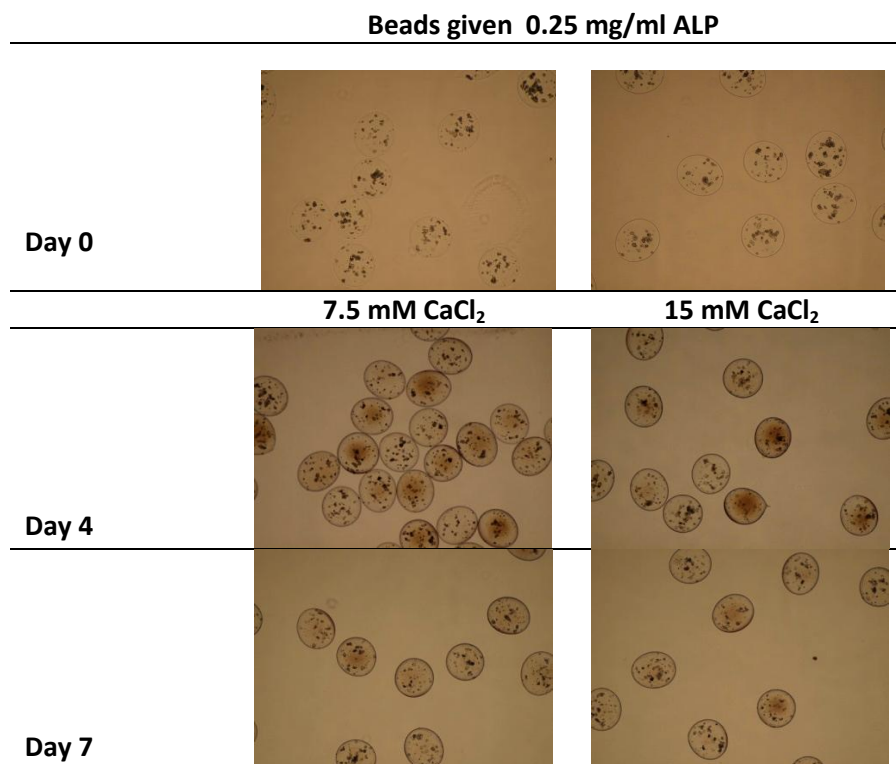


**Figure 3.8 Light microscope pictures of encapsulated MSCs in beads mineralized with 0.25 mg/mL ALP. At day 2 post encapsulation the sample was split in two, and given different CaCl$_2$ concentrations. Images are magnified 40X.**

At day 2, 4 and 7 post encapsulation live/dead assays were performed. The results are given in figure 3.9. Cell viability remained high throughout the experiment.
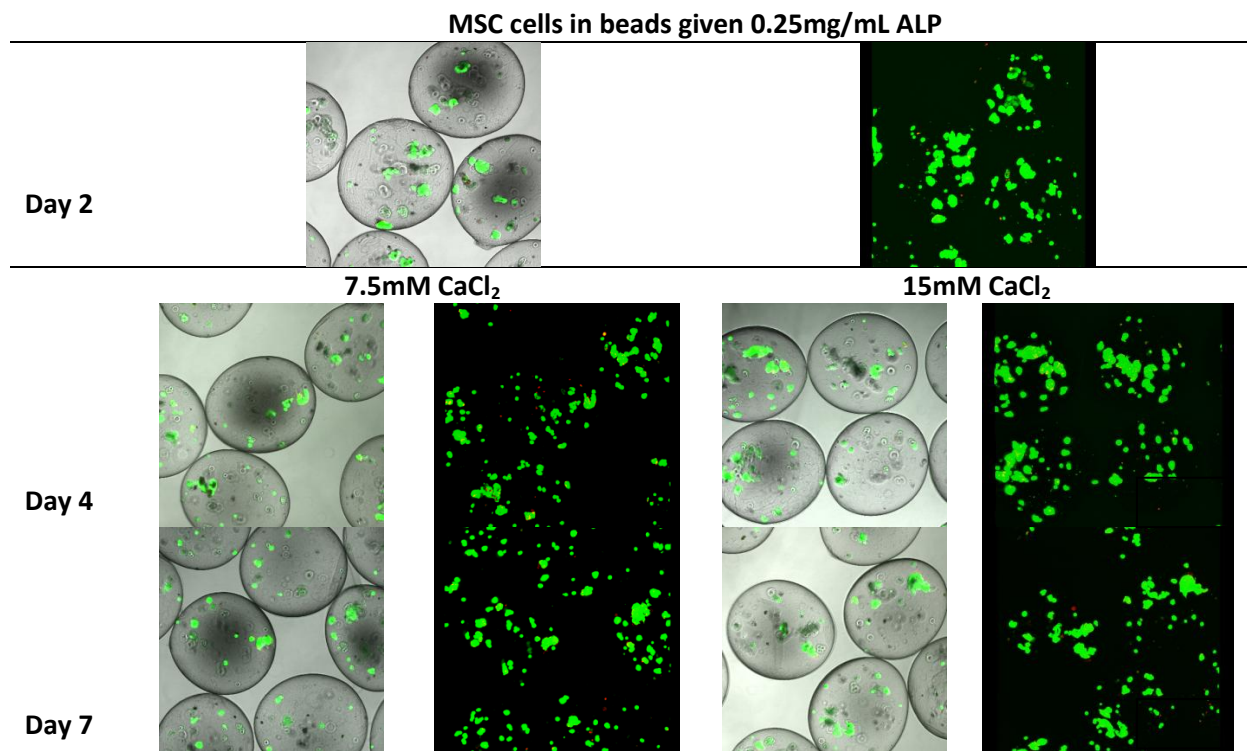
**MSC cells in beads given 0.25mg/mL ALP**



Figure 3.9 CLSM pictures of MSCs encapsulated in alginate beads given 0.25 mg/mL ALP. At day two the sample was split in two and added CaCl$_2$ in different concentrations. Left picture: CLSM cross section. Right picture: CLSM Z stacks 3D projection of the same beads. Live cells appear green, whereas dead cells appear red. All images were magnified 100X.

At day 7 post encapsulation the cells were attempted recovered by dissolving the beads with citrate, and RNA isolation analysis was subsequently performed (see Appendix A.5 for details).

As the beads were mineralized to a smaller extent compared with experiments with osteosarcoma cells, a new experiment (M2) was set up where a freshly made enzyme was utilized. Images from the mineralization process are given in figure 3.10.
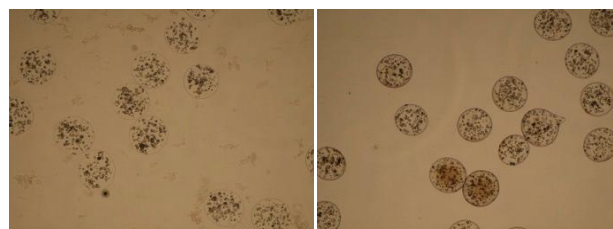


Figure 3.10 MSCs encapsulated in alginate beads mineralized with 0.25mg/mL ALP at day 0 and day 2 post encapsulation, respectively. The beads were stabilized by adding 7.5mM CaCl$_2$ to the culture medium. Images are magnified 40X.

### 3.2.2 Mineralization with 0.5mg/mL ALP

Considering that addition of 0.25mg/mL ALP did not mineralize the beads as much as expected, the enzyme concentration was increased again (experiment M3). Images from the mineralization process with the elevated enzyme concentration are given in figure 3.11. Again, the minerals appeared to be centered in the core of the bead. As for the experiments with osteosarcoma cells, the beads seem to be further mineralized even after day 2 post encapsulation. Increasing the concentration of ALP appeared to increase the mineralization process as the beads appear darker than in the experiments where 0.25mg/mL ALP was utilized.

At day 8 post encapsulation the morphology of cells inside beads was investigated by staining the actin filaments and the nucleus. Images from CLSM are given in figure 3.12. From the picture to the right the cells appear to interact with each other as their actin filaments seem to elongate toward each other. Again image acquisition was difficult as the beads were heavily mineralized, making the cells in the core of the bead invisible in the microscope.

At day 2 and 5 post encapsulation the viability of the cells were investigated using live/dead assay and CLSM. The images are given in figure 3.13. It seems that the MSCs were as viable inside beads given 0.5mg/mL ALP compared to the ones prepared with 0.25mg/mL ALP showing high viability throughout the 8 days of culture. Conversely, image acquisition by CLSM was more intricate. As a result, it is hard to say if cells in the core of the bead are alive or dead.
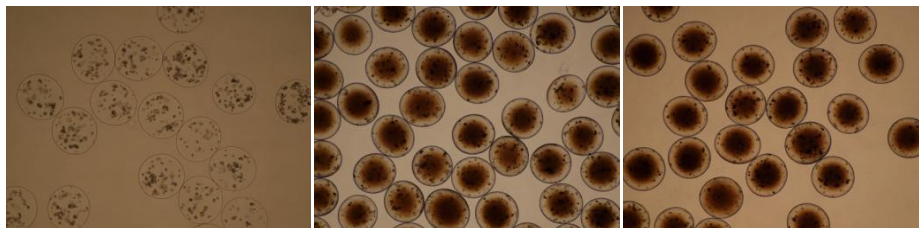


**Figure 3.11 MSCs encapsulated in alginate beads mineralized with 0.5mg/mL ALP at day 0, day 2 and day 5 post encapsulation, respectively. The images are magnified 40X.**
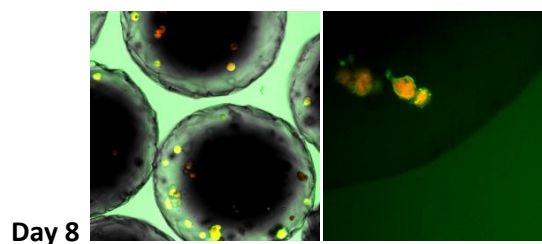


**Day 8**

**Figure 3.12 CLSM images of the morphology of cells inside beads mineralized with 0.5mg/mL ALP on day 8 post encapsulation. Left picture: CLSM cross section. Right picture: Cross section. The nucleus appears red, whereas the actin filaments appear green. Left image is magnified 100X, whereas the right image is magnified 400X.**
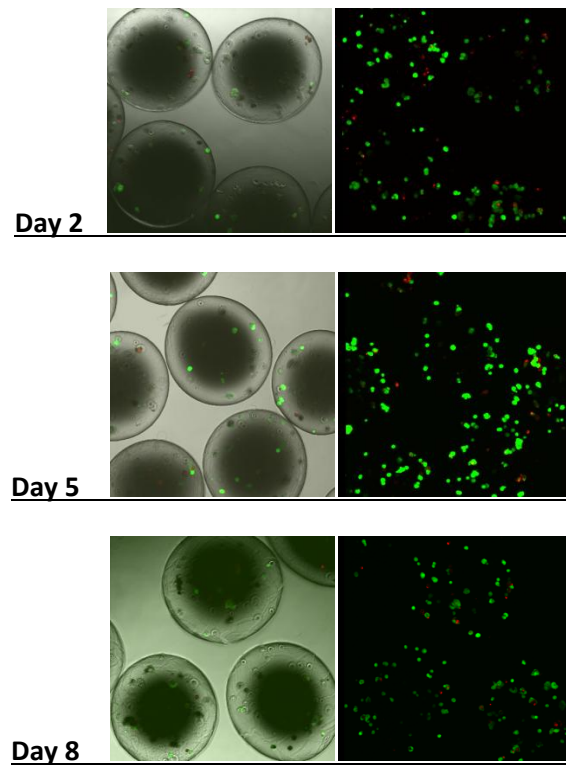
**Day 2**

**Day 5**

**Day 8**

**Figure 3.13 CLSM pictures of MSCs encapsulated in alginate beads mineralized with 0.5 mg/mL ALP. Left picture: CLSM cross section. Right picture: CLSM Z stacks 3D projection of the same beads. Live cells appear green, whereas dead cells appear red. The samples were magnified 100X.**

Finally, at day 9 post encapsulation, beads containing roughly 1 million cells were dissolved in citrate, and RNA was extracted from the cells. In table 3.2 the concentration and purity of the isolated RNA are listed. The purity of the RNA was good as the OD 260/280 > 2. After cDNA synthesis the expression of runx2, an osteoblast phenotype marker was quantified using RT PCR. The mean $C_t$ values and relative gene expression are given in table 3.3 and figure 3.14, respectively. gapdh was used as an endogenous control. The confirmed expression of runx2 suggests that the encapsulated MSCs had the potential to differentiate into preosteoblasts.

**Table 3.2 RNA isolation. The table gives information regarding amount of RNA isolated, and the purity of the RNA. OD260/280> 2, indicating that RNA quality is good.**

| Sample | Day (post enc.) | Concentration of RNA (ng/µl) | Amount of RNA | 260/280 |
|--------|-----------------|------------------------------|---------------|---------|
| 1 | 9 | 66.9 | 3.6 | 2.02 |

**Table 3.3 Mean $C_t$ values of samples from encapsulated MSCs in beads mineralized with 0.5mg/mL ALP. gapdh was used as a endogenous control, whereas runx2 is an osteoblast specific gene. Controls (samples without RT, or without cDNA) were both negative.**

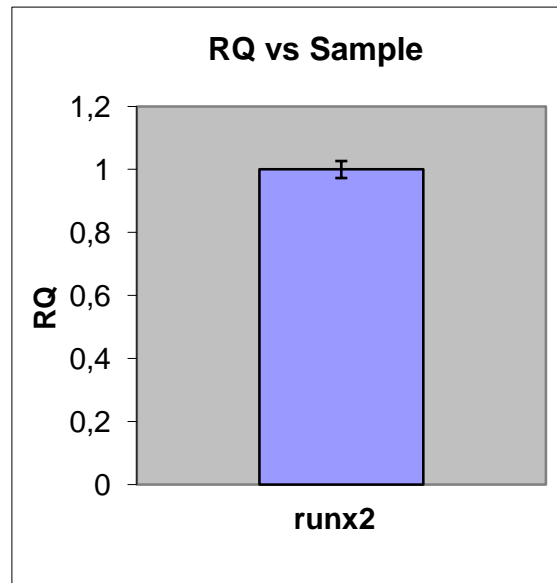| Sample | Mean $C_t$ |
|--------|------------|
| gapdh  | 23.5       |
| runx2  | 29.8       |



**Figure 3.14 Relative expression of runx2 in MSCs encapsulated in alginate beads mineralized with 0.25mg/mL ALP. Error bars are +/- 1 SD.**

## 3.3 Extended experiment using 0.25mg/mL ALP

As a final experiment 16 million MSCs were encapsulated in alginate beads, containing 0.25mg/ml ALP (samples 4a/b) and containing no ALP (samples 3a/b). Half of each batch was given differentiation medium (samples 3a/4a) starting at day 2 post encapsulation. Alginate beads without cells were also prepared, not containing ALP (sample 1), and containing ALP (sample 2), making the total of 6 batches. At day 2, 7, 9, 14 and 21 post encapsulation beads and cells were tested using an array of analysis as described in the following sections.

Before and after the mineralization process (day 0 to day 2 post encapsulation) light microscopy pictures were taken of the different samples. There were only four samples at this point as they had not been split for differentiation purposes up till now. The images are displayed in figure 3.15.

At day 0 post encapsulation all beads looked the same with no mineralization as expected, and appeared to be similar in size. Also, cells seemed to be homogeneously distributed between the beads. Inside the beads, some of the cells were clustered together.

At day 2 post encapsulation samples receiving ALP enzyme appeared to be slightly mineralized as they appeared darker in the light microscope. Visual inspection confirmed this, as the beads appeared white. The degree of mineralization seemed to differ somewhat between the beads, indicating that the enzyme, and/or phosphate/calcium-ions were not homogeneously distributed in the culture flask.

The mineralization seemed to continue after the initial 48hrs were the samples were given calcium phosphate precursors. This was observed in the light microscope as shown in figure 3.16. These images were collected at day 21 post encapsulation. At this point sample 3a (no ALP, but given differentiation medium) also appeared to be mineralized. Sample 3b was the only sample not mineralized, which was expected, as these cells were neither given differentiation, nor mineralization medium.

Furthermore, sample 4a was more mineralized than sample 4b even though both samples received the same concentrations of ALP.
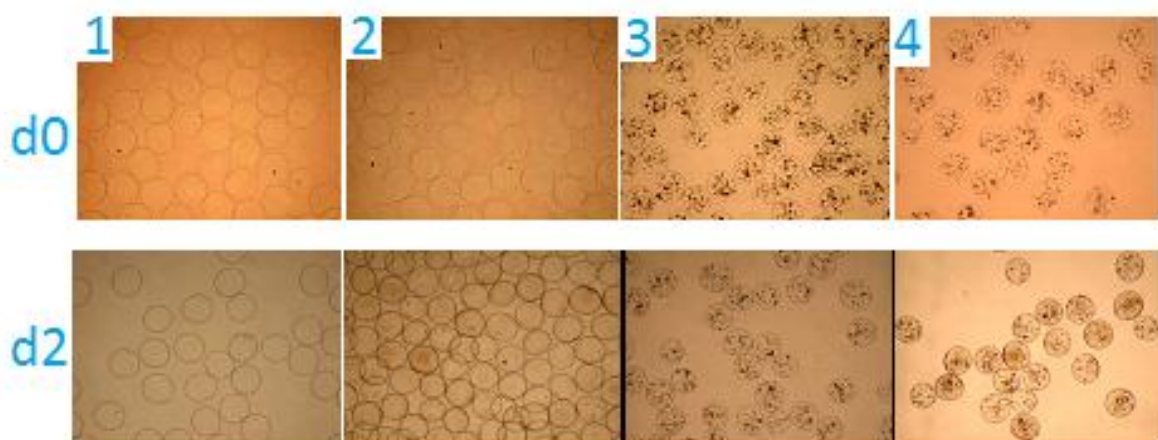


**Figure 3.15 Light microscope images of beads at day 0 and day 2, post encapsulation. Top: Beads at day 0. From the left; beads without enzyme and cells (Samples 1); beads with enzyme but without cells (sample 2); beads without enzyme but cells (sample 3); beads with enzyme and cells (Sample 4). Bottom: Beads at day 2. Images are magnified 40X.**
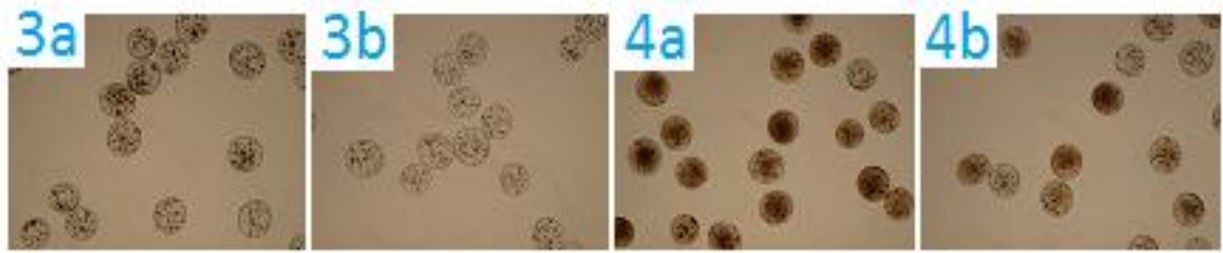
**Figure 3.16 Light microscope pictures from day 21 post encapsulation. Sample 3a is without enzyme but with added differentiation medium; sample 3b is with enzyme, but without differentiation medium; sample 4a is given both enzyme and differentiation medium, whereas sample 4b is without enzyme and differentiation medium. All images are magnified 40X.**

### 3.3.1 Live/dead and CLSM

At day 2, 7, 14 and 21 post encapsulation the survival of MSCs encapsulated in alginate beads was evaluated using live/dead assay and CLSM. The results are given in figure 3.17 and 3.18. It seemed that MSC survival was good inside the beads as viability remained <90%. No obvious difference between samples given differentiation medium (samples 3a/4a) and samples not given differentiation medium (3b/4b) was observed. Furthermore, the viability of cell seemed to be unaffected by the mineral content of the beads.

Cells inside beads seemed to have proliferated from day 7 to day 14 as cell clusters were more frequently observed at day 14 compared to day 7. This was especially evident in both unmineralized and mineralized beads not exposed to differentiation medium. The proliferation seemed to have stopped after day 14 as the clustering did not continue.

At day 21 beads not containing ALP but receiving differentiation medium seemed to be mineralized as they appeared darker in the microscope. This confirmed the observations made from the light microscope pictures.

**Live/dead of MSCs in beads not containing ALP**



**Day 2**

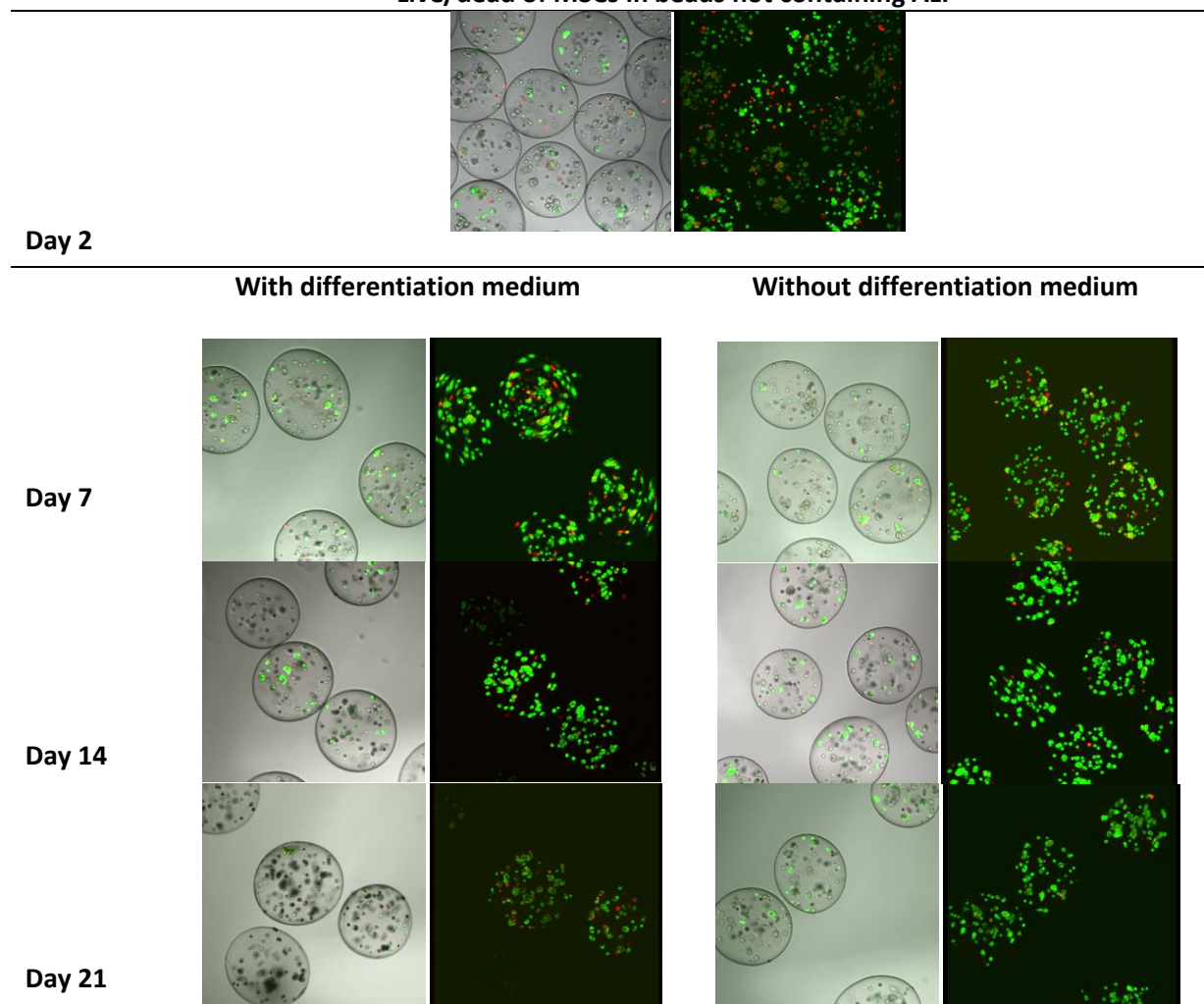|  | **With differentiation medium** | **Without differentiation medium** |
|---|---|---|
| **Day 7** | | |
| **Day 14** | | |
| **Day 21** | | |

Figure 3.17 CLSM pictures of MSCs encapsulated in alginate beads not containing ALP. Left picture: CLSM cross section. Right picture: CLSM Z stacks 3D projection of the same beads. Live cells appear green, whereas dead cells appear red. All samples are magnified 100X.

**Live/dead of MSCs in alginate beads containing 0.25mg/mL ALP**



**Day 2**

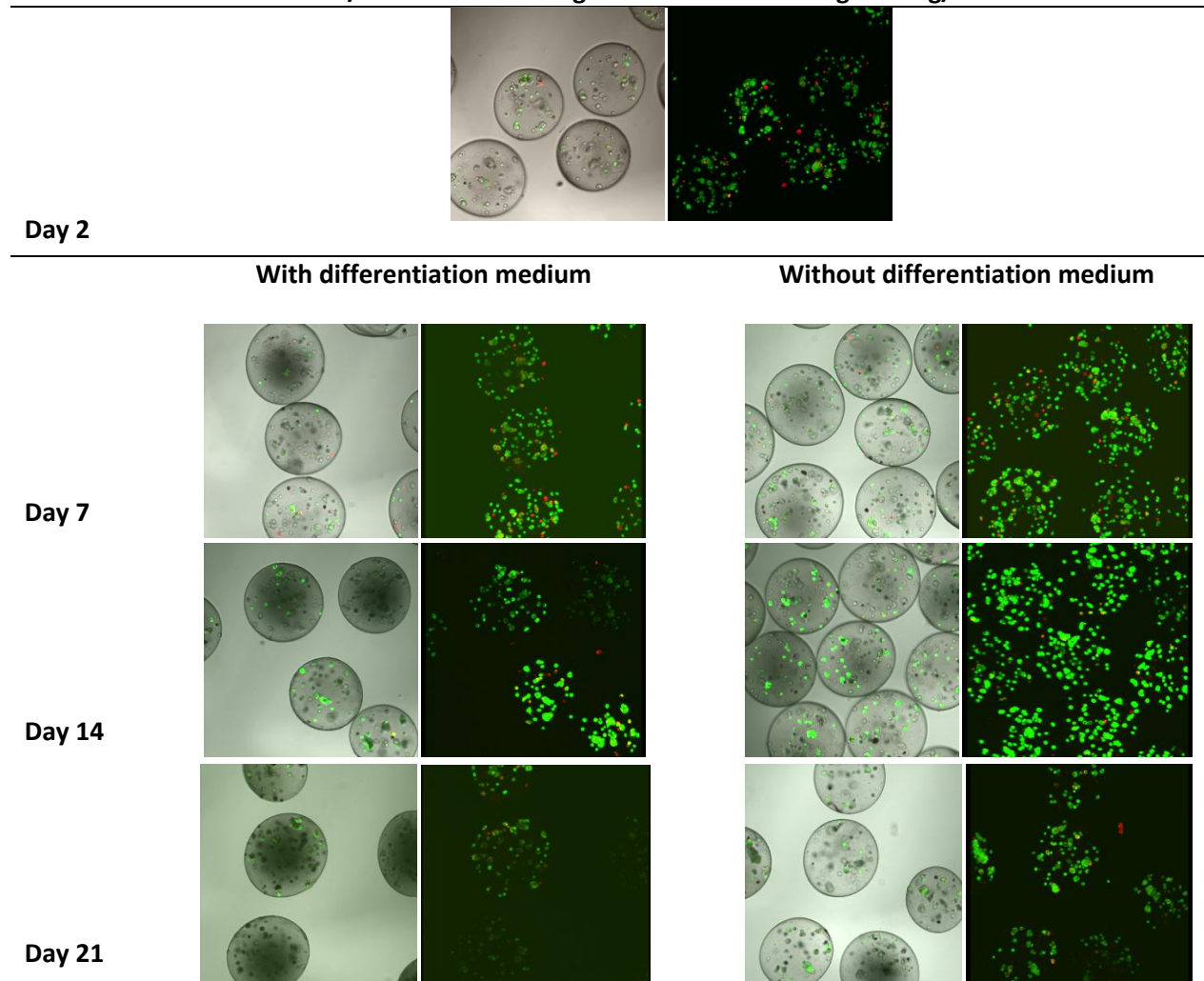| | With differentiation medium | Without differentiation medium |
|---|---|---|
| **Day 7** | | |
| **Day 14** | | |
| **Day 21** | | |



Figure 3.18 CLSM pictures of MSCs encapsulated in alginate beads containing 0.25 mg/mL ALP. Left picture: CLSM cross section. Right picture: CLSM Z stacks 3D projection of the same beads. Live cells appear green, whereas dead cells appear red. All samples were magnified 100X.

## 3.3.2 Alamar Blue

Alamar Blue analysis was completed to measure the cells metabolic activity. Measurements were performed at day 2, 7, 14 and 21 post encapsulation and the results are given in figure 3.19.

The metabolic activity increased over time for all four samples, which indicated good cell viability, and little occurrence of cell death. All samples showed an increase in metabolic activity between day 7 and 14 which was also reflected in the live/dead assay previously described. This might be explained by cell proliferation. The increase in samples receiving differentiation medium might be explained by them differentiating into osteoblasts.
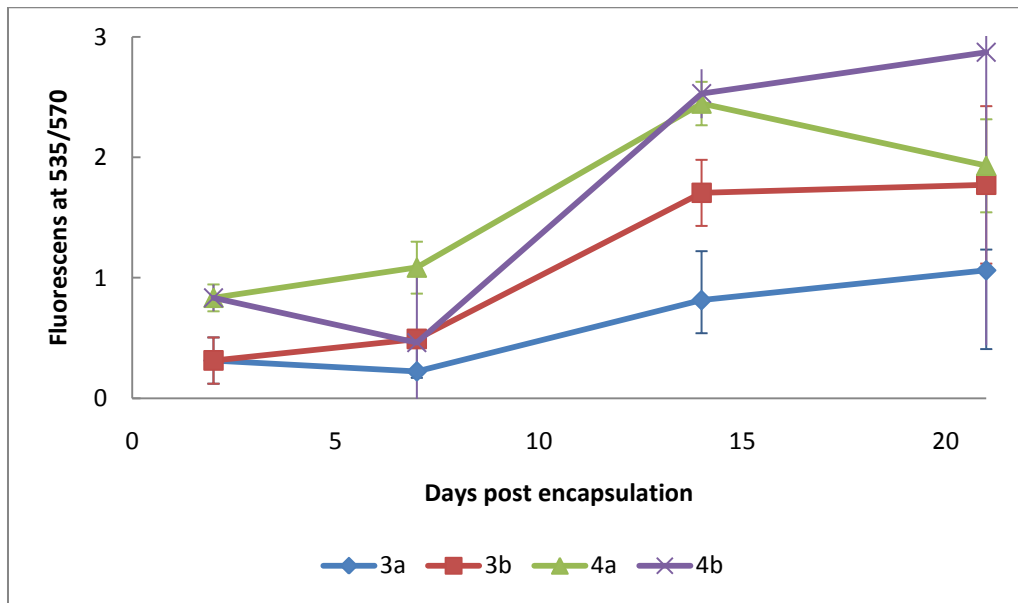


**Figure 3.19 Alamar Blue assay results for hMSCs in alginate beads. The errors bars represent the standard deviation for every reading based on three parallels. The absorbance values are based on 5000 cells. Sample 3 is not containing ALP and exposed to differentiation medium (3a) or to regular culture medium (3b); sample 4 is containing ALP and exposed to differentiation medium (4a) or to regular culture medium (4b).**

## 3.3.3 Morphology of cells inside beads

Morphology of the cells inside the alginate beads were investigated by staining their nucleus and cytoskeleton. Images from CLSM are shown in figure 3.20 and 3.21. At day 2 post encapsulation, the cells were round and no specific organization of the actin filament could be observed. The cells appeared to possess more elongated actin filaments already at day 7 in samples receiving differentiation medium. Cells without addition of differentiation medium seemed to obtain their original round shape throughout the time of the study. Thus, the samples given differentiation medium were the only ones establishing interaction with the alginate matrix.

Mineralization of the alginate beads seemed to have little effect on cell/matrix interactions, as no difference was observed between samples with, or without addition of ALP.

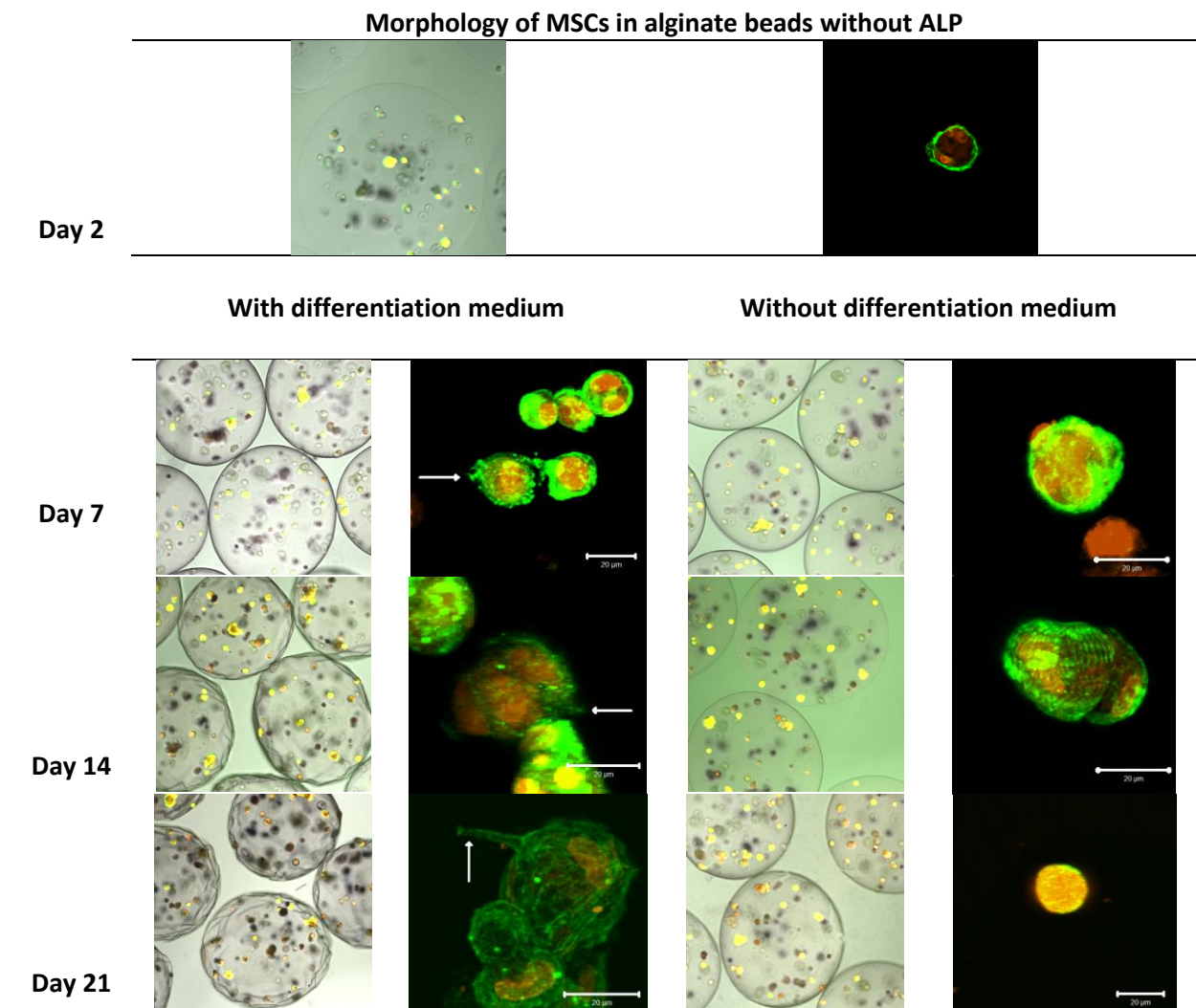**Morphology of MSCs in alginate beads without ALP**



Figure 3.20 CLSM images of cell morphology inside alginate beads without ALP stained with phalloidin (green) and DRAQ5 (red). Elongated filaments are marked with an arrow. The size bar is 20µm. Left pictures are magnified 100X.

**Morphology of MSCs in alginate beads containing 0.25mg/mL ALP**



**Day 2**

**With differentiation medium**          **Without differentiaton medium**

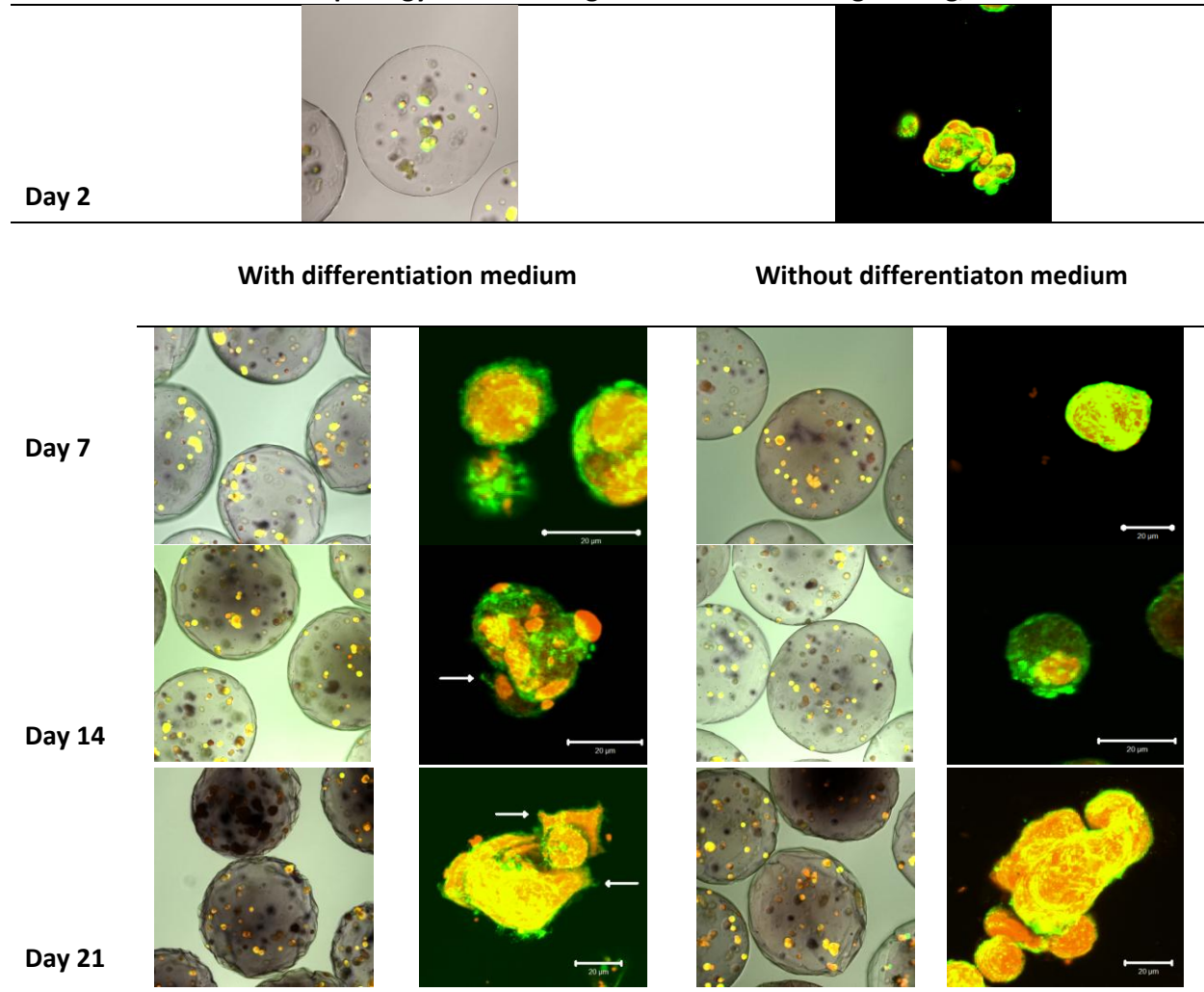

**Day 7**

**Day 14**

**Day 21**

Figure 3.21 CLSM images of cell morphology inside alginate beads stained with phalloidin (green) and DRAQ5 (red). Elongated filaments are marked with an arrow. The size bar is 20µm. Left pictures are magnified 100X.

### 3.3.4 ALP activity

ALP activity was measured on day 2 and day 9 post encapsulation. This means at day 0 and day 7 after initializing differentiation by addition of differentiation medium. The results are given in figure 3.22 and 3.23 for day 2 and day 9, respectively. At day 9 post encapsulation samples 3a and 4a were the two samples showing the greatest increase in ALP activity from t=0 to t=20. The differences between activity at t=20 for samples with and without differentiation medium are statistically significant ($p < 0.01$ and $p < 0.002$ for samples 3a/b and 4a/b, respectively). From the figures below it seems to be an increase in ALP activity from t=0 to t=20 in both sample 3 and 4 at day 2. This is surprising as differentiation medium had not yet been introduced, and sample 4 is the only sample with added enzyme. No statistically significant difference was observed between these samples.
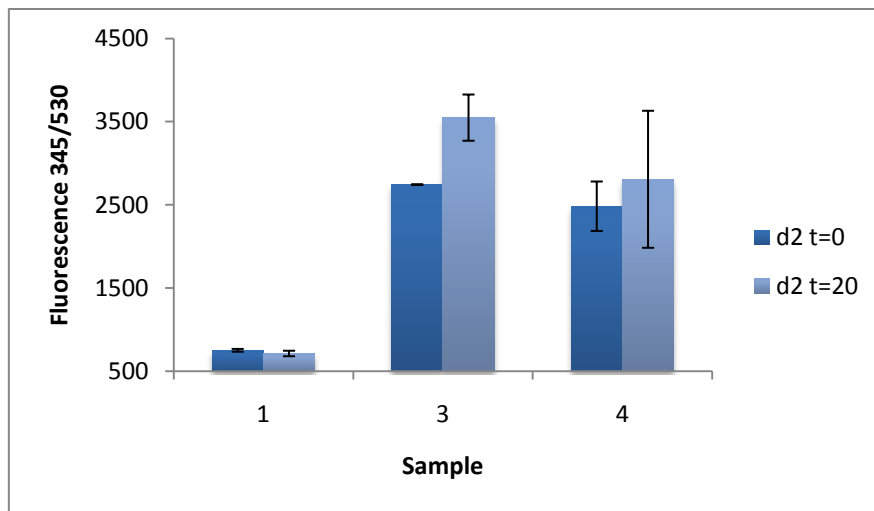


**Figure 3.22 ALP acitivity at day 2 post encapsulation. Fluorescense intensity was measured every minute for 20 minutes, The first (t=0) and the last (t=20) measurement are given in the histogram (n=3 ± 1 SD). Sample 3 did not contain external ALP, whereas sample 4 contained ALP from the day of encapsulation. Sample 1 was neither given ALP nor containing cells, and was used as a control.**
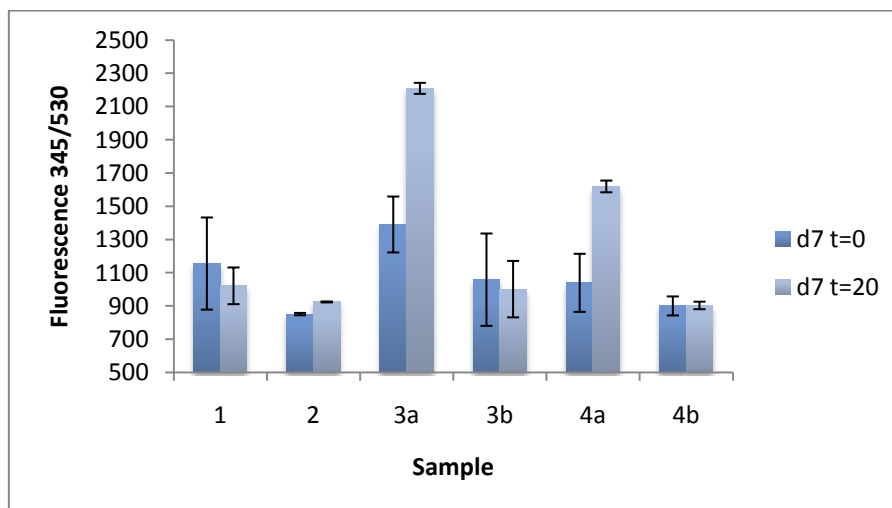


**Figure 3.23 ALP acitivity at day 9 post encapsulation/day 7 post differentiation. Fluorescense intensity was measured every minute for 20 minutes, The first and the last measurement are given in the histogram (n=3 ± 1 SD). Sample 3a was without external ALP, but given differentiation medium; sample 3b was without ALP and without differentiation medium; sample 4 was given ALP and differentiation medium; sample 4b was given ALP but not differentiation medium. Sample 1 contained neither ALP or cells; sample 2 contained ALP but not cells. The two latter were used as controls.**

### 3.3.5 PCR analysis of runx2 and osterix

RNA was isolated at day-1 (one day before encapsulation start), day 2, 7, 14 and 21 post encapsulation. At day -1 cells that had never been encapsulated were used. For the remaining days beads corresponding to approximately 1 million cells were isolated using citrate treatment to recover cells from beads. Table 3.4 gives an overview over total amount of isolated RNA and its purity from all samples.

Nearly all samples were considered to consist of pure RNA, as their $OD_{260/280}$ ratios were > 2. All calculations were based on the mean of three parallels. Next, PCR analysis was performed using probes (runx2 and osx).

**Table 3.4 RNA isolation results. Samples of pure RNA (no contamination) will obtain an $OD_{260/280}$ ration above 2. Sample 0 is unencapsulated hMSCs; sample 3 was not given enzyme nor differentiaion medium, sample 4 was given enzyme without differentiation medium; sample 3a was not given external ALP, but given differentiation medium; sample 3b was without ALP and without differentiation medium; sample 4 was given ALP and differentiation medium; sample 4b was given ALP but not differentiation medium. n=3.**

| Sample | Day (Post encapsulation) | Concentration of RNA (ng/µl) | Amount of RNA (µg) | $OD_{260/280}$ |
|--------|--------------------------|------------------------------|--------------------|----------------|
| 0 | -1 | 822.6 | 44 | 2.06 |
| 3 | 2 | 283.0 | 15 | 2.01 |
| 4 | 2 | 222.4 | 12 | 2.03 |
| 3a | 7 | 140.2 | 7.6 | 2.10 |
| 3b | 7 | 114.1 | 6.2 | 2.09 |
| 4a | 7 | 106.5 | 5.8 | 2.08 |
| 4b | 7 | 45.7 | 2.5 | 1.95 |
| 3a | 14 | 74.0 | 4.0 | 1.98 |
| 3b | 14 | 112.2 | 6.1 | 2.03 |
| 4a | 14 | 50.7 | 2.7 | 2.02 |
| 4b | 14 | 175.6 | 9.5 | 2.04 |
| 3a | 21 | 16.4 | 0.9 | 1.49 |
| 3b | 21 | 131.9 | 7.1 | 2.04 |
| 4a | 21 | 64.6 | 3.5 | 2.05 |
| 4b | 21 | 119.2 | 6.4 | 2.06 |

Amplification plot and relative expression of runx2 in all samples are given in figure 3.24 and 3.25.The amplification plot reveals a strong positive reaction for runx2 in all samples, as the $C_t$ values are all below 29.

runx2 was expressed by hMSCs pre encapsulation. This was not surprising as MSCs are known to express runx2 at low levels. At day 2 post encapsulation both samples with and without enzyme had comparable expression as the MSCs from day -1. At day 2 the samples were split in two and given differentiation or regular medium. All of these samples showed an increase in expression at day 7 compared with day 2. The samples given differentiation medium (3a/4a) showed a stronger expression at day 7 and day 14 compared with samples given regular medium (3b/4b). The former samples continued to hold a high runx2 expression throughout the time of the study. Sample 4b shows a gradually increasing expression, whereas sample 3b showed a decrease from day 7 until day 21 when the study was ended.
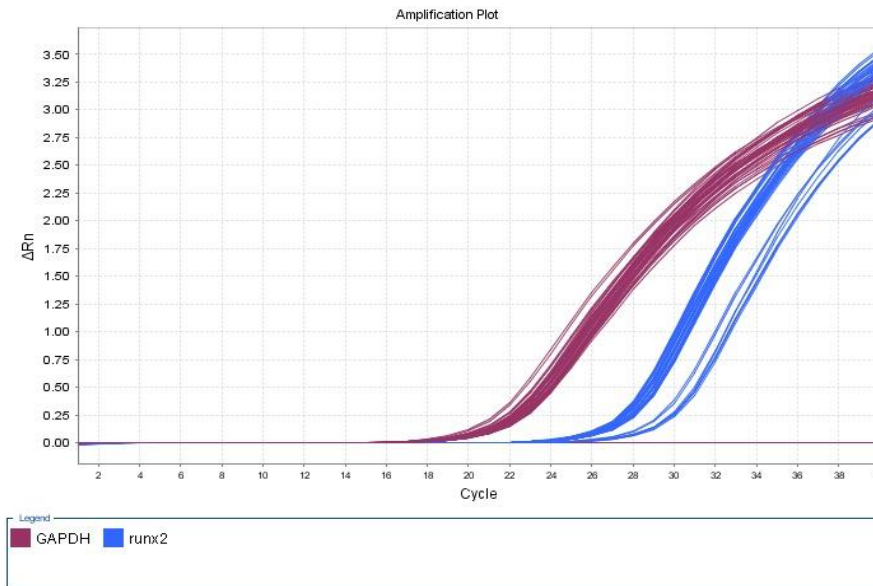
Figure 3.24 Amplification plot of runx2. The curve gives as impression of the $C_t$ values for all gapdh (purple) and runx2 (blue), at the point where the curves cross the threshold at y=1. $C_t$ values ≤ 29 indicates a strong positive reaction of the target gene. Values from 30-37 indicates a positive reaction. Values above 38 indicate a negative reaction that can be explained by contamination or other factors. Gapdh was used as an endogenous control.
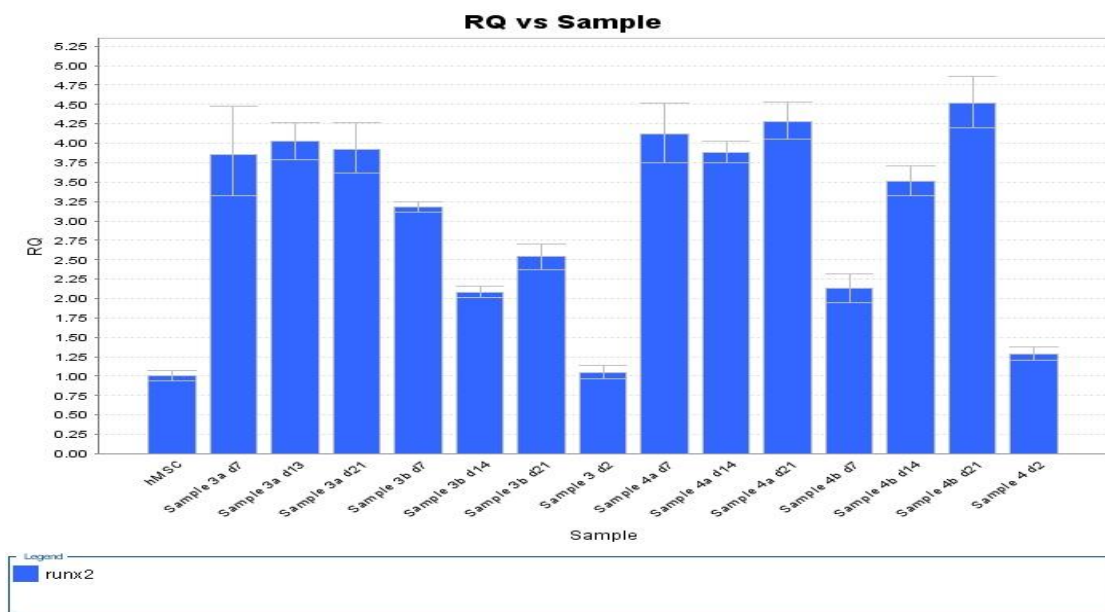


Figure 3.25 Relative expression of runx2 in unencapsulated hMScs and samples at day -1, 2, 7, 14 and 21 post encapsulation. The concentrations are normalized against unencapsulated hMSCs. Sample 3a was without external ALP, but given differentiation medium; sample 3b was without ALP and without differentiation medium; sample 4 was given ALP and differentiation medium; sample 4b was given ALP but not differentiation medium. Sample 1 contained neither ALP or cells; sample 2 contained ALP but not cells. The two latter were used as controls.

Amplification plot and relative expression of osterix are given in figure 3.26 and 3.27. The amplification plot reveals a positive or strong positive reaction for osterix in all samples, as the $C_t$ values are all below 37. MSCs did not show any expression of osterix.

osterix expression varied greatly between samples given differentiation medium and regular medium. Mineralization seemed to not affect differentiation as no difference was observed between samples that contained ALP and samples without ALP. Detection of osterix in all samples started at

day 2 post encapsulation, which was unexpected as osterix is considered a late marker for osteoblast differentiation. Expression of osterix seemed to increase in all samples throughout the study (from day 7 to day 21 post encapsulation), with the exception of sample 3a, where a subtle decrease in observed between day 14 and day 21.
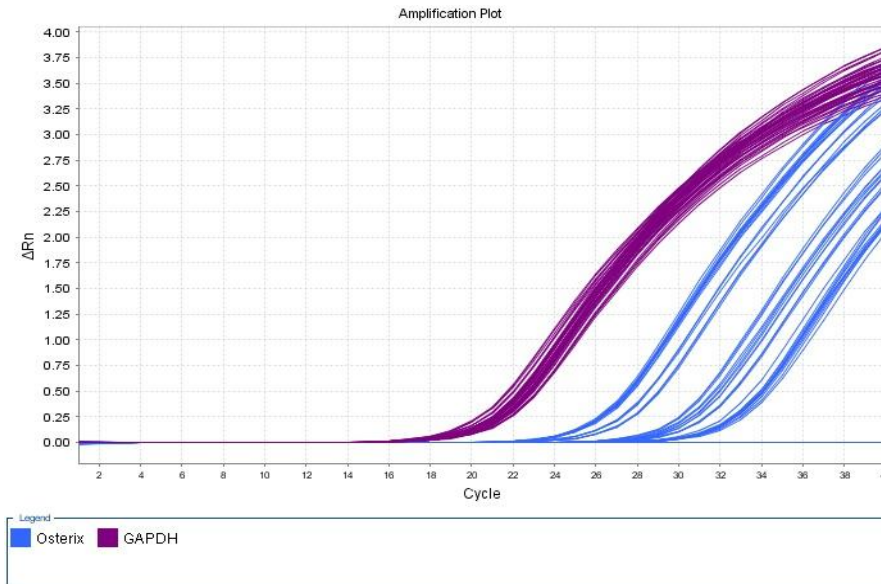


**Figure 3.26 Amplification plot of osterix. The curve gives as impression of the $C_t$ values for all gapdh (purple) and osterix (blue), at the point where the curves cross the threshold at y=1. $C_t$ values ≤ 29 indicates a strong positive reaction of the target gene. Values from 30-37 indicates a positive reaction. Values above 38 indicate a negative reaction that can be explained by contamination or other factors. Gapdh was used as an endogenous control.**
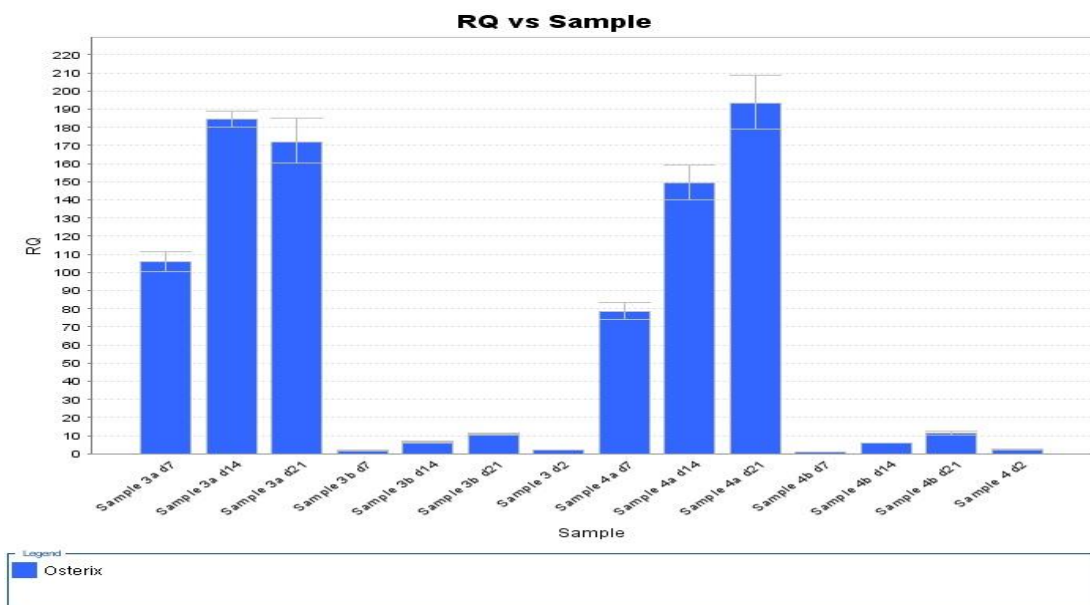


**Figure 3.27 Relative expression of osterix in unencapsulated MScs and samples at day -1, 2, 7, 14 and 21 post encapsulation. The concentrations are normalized against unencapsulated hMSCs. Sample 3a was without external ALP, but given differentiation medium; sample 3b was without ALP and without differentiation medium; sample 4 was given ALP and differentiation medium; sample 4b was given ALP but not differentiation medium. Sample 1 contained neither ALP or cells; sample 2 contained ALP but not cells. The two latter were used as controls.**

### 3.3.6 SEM images

At day 21 post encapsulation the remaining beads were prepared for SEM analysis. The results are given in figure 3.28. The alginate matrix seemed to be more porous in sample 3b compared to the rest of the samples. Sample 4a appeared mineralized as mineral composites were observed. Sample 4b seemed to be more mineralized compared with samples not given ALP (sample 3a/3b). Nevertheless, no obvious granules were observed in these three samples. The cells within beads given differentiation medium (3a/4a) appeared to have elongated actin filaments, confirming the observations seen on the CLSM. However, sample 3a seemed to be far more stretched compared to sample 4a. Additionally, sample 4b (given ALP, but not differentiation medium) seemed to interact with the matrix as well. Furthermore, there seemed to be a void between the cells and alginate matrix. This might be explained by shrinkage of the alginate during the preparations for SEM analysis.
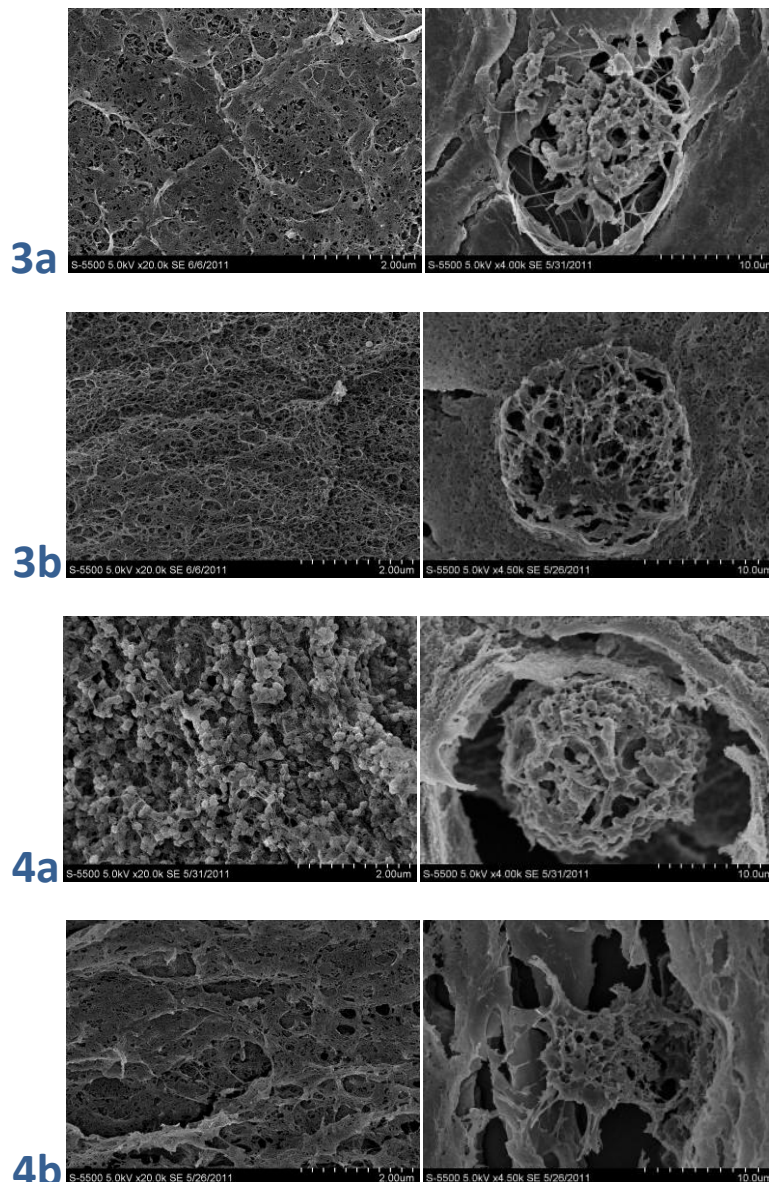


**Figure 3.28 SEM images of the alginate matrix (left), and cells within (right). Sample 3a is without enzyme but with added differentiation medium; sample 3b is with enzyme, but without differentiation medium; sample 4a is given both enzyme and differentiation medium, whereas sample 4b is without enzyme and differentiation medium. Left magnification: 20 k, right magnification: 4.5 k.**

In samples with added differentiation medium, collagen fibers were observed. Magnifications of the collagen are given in figure 3.29. The image to the right clearly shows a lot of fibers around what seems to be a MSC. To the left a magnification of these fibers are given.

In the mineralized samples the collagen seemed to be penetrating the matrix, compared with the unmineralized samples where the cells seemed to deposit collagen in a capsular way. In figure 3.30 the collagen fibers were observed interacting with both the mineral composites, and the alginate matrix.
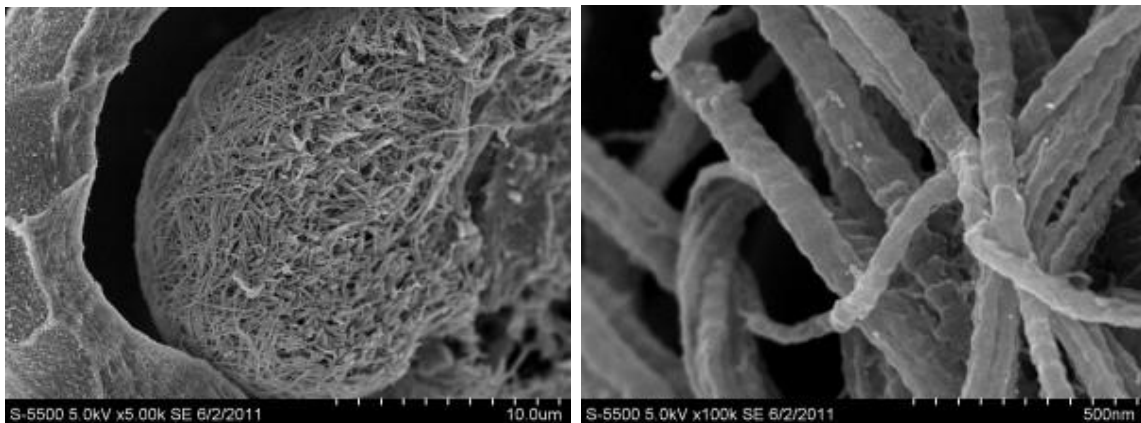


**Figure 3.29 SEM images of collagen around a cell (left), and magnification of the collagen fibers (right). The samples were taken out of the culture flask at the end of the study (day 21). Images are from sample 3a (unmineralized, differentiated). Left image: 5.0 k magnification, right image: 100 k magnification.**



**Figure 3.30 Collagen fibers interacting with both mineral composites, and the alginate matrix. The collagen was observed in sample 4a, which is given ALP and differentiation medium. Magnification: 20 k.**

# 4. Discussion

## 4.1 Bead stability

In initial experiments with osteosarcoma cells beads were mineralized using 0.5mg/mL ALP. The beads were rapidly and heavily mineralized appearing very dark in the light microscope at day 2 post encapsulation. After the first 48hours of continuous changing mineralization medium, the beads were cultured in regular medium. At this point the beads cracked open, and the majority were completely dissolved at day 5, post encapsulation (figure 3.1). The observation of decreasing bead stability subsequent to changing the mineralization medium into growth medium needed to be further study. For that reason addition of $CaCl_2$ to the regular growth medium was attempted, using different concentrations.

A possible explanation for the destabilization could be that the beads became brittle after the fast mineralization process, and thereby become ruptured by handling. However, as the medium changes in the mineralization process are far more frequent, this is not likely. Furthermore, compression measurements by Minli et al (2010) show that ALP mineralized alginate beads are elastic, but with a high resistance towards compression, confirming these observations.

As the beads remained intact after addition of $CaCl_2$ to the growth medium, it seemed that the low stability was due to other reasons. A probable cause could be that $CaCl_2$ was the limiting reagent in a continuing mineralization of the beads, whereby Ca-alginate crosslinks were broken as Ca-ions were used to generate calcium phosphate by reacting with the phosphate in the culture medium. Also, the medium contains calcium chelators (phosphate and carbonate) that may explain the reduced mechanical strength of the beads. Taken together, both of these postulations ought to be solved by adding more calcium to the medium, which was also the case.

Additionally, bead stability decreased more quickly as the ALP concentrations utilized for mineralization increased. This supports the presumption that $CaCl_2$ was the limiting reagent as the more mineralized the beads became; the more $CaCl_2$ was required for stabilization purposes.

Moreover, rapidly proliferating cells such as osteosarcoma cells may further decrease bead stability. Indeed, it was observed that bead stability was poorer in the experiments with osteosarcoma cells compared with experiments with MSCs. As osteosarcoma cells are rapidly proliferating they might be more potent in inducing mineralization, thus consuming Ca-ions more rapidly compared with MSCs. Again, this would cause loss of Ca-alginate cross-links, thus destabilization of the beads. It seems that the different growth patterns in different cell lines affect the destabilization process.

Furthermore, in experiments running over a longer period of time (over 14 days) cells were frequently observed growing outside the beads. Cells escaping from alginate/poly-L-lysine/alginate beads have been previously reported for osteosarcoma cells, and was suspected of being the cause of bead rupture (Rokstad, 2002). In the present study the penetrations of cells did not cause bead rupture, as long as Ca-ions were present in excess in the culture medium. MSCs seemed to penetrate the beads to a lesser extent compared with the osteosarcoma cells. An explanation could be that the MSCs were observed to cluster inside the beads, thus being less likely to tear away from the matrix.

Major drawbacks caused by the low stability were the difficulties in running certain experiments. For CLSM imaging the beads seemed to crack open if left too long in PBS/live/dead solution. Alizarin Red-

S was also affected as all beads cracked open during the experiment, as described in appendix B. Bead instability could possibly be overcome by the addition of CaCl$_2$ to all handling solutions. Nevertheless, precipitation of CP in phosphate buffers limits this, and other buffers might have been selected. Furthermore, when it comes to Alizarin Red-S addition of Ca-ions would affect results, as calcium is the component to be quantified.

Compared with the in situ mineralization method described in the introduction it seems that stability is poorer when using the enzymatic method. It was reported that the beads remained intact throughout the time of the studies (up to 30 days), without stabilizing them with Ca. However, the beads were observed to crack open if left too long in PBS (Sundrønning, 2010). This is explained by the phosphate ions, which acted as calcium chelators.

Nevertheless, bead stability may offer some advantages. The poor stability might give alginate the possibility to be degraded in the body. Today, alginate is not known to be degraded *in vivo*, without modifications, such as gamma-irradiation (Simmons, 2004). Thus, the beads in the present study could be directly implanted into a bone fracture side, to be gradually degraded revealing the cells within. Alginate would be degraded in the body as the concentration of calcium in the human body is much lower than the concentrations needed for stabilization purposes.

## 4.2 Cell survival

Viability of osteosarcoma cells inside alginate beads mineralized using 0.5 and 0.25mg/mL ALP was studied. The viability was found to be dependent on enzyme concentration. Viability of MSCs in mineralized beads was high throughout the time of the studies.

Viability of osteosarcoma cells inside mineralized alginate beads by the enzymatic method was hard to interpret. In all experimental samples, viability was estimated between 50-90%. However, as the alginate beads became greatly mineralized, image acquisition on CLSM was difficult. Nonetheless, there seemed to be a tendency for greater survival when a lower concentration of enzyme (0.25mg/mL) was used compared with a higher one (0.5mg/mL) (figure 3.6 and 3.7). In addition, because the lower concentration facilitated image acquisition and increased bead stability, the same concentration was introduced when using MSCs.

For MSCs the viability was >90% for all samples in initial experiments using 0.25mg/mL ALP (experiment M1, figure 3.9). However, the beads repeatedly appeared to be much less mineralized than with the osteosarcoma samples (figure 3.8). This might be due to a higher proliferation, and activity, of the osteosarcoma cells causing mineralization of the beads. To increase mineral content in beads with MSCs, increasing the ALP concentration to 0.5mg/mL was attempted. In this experiment cells showed good viability until reaching day 8 post encapsulation, when the study was ended (experiment M3, figure 3.13). Increasing the enzyme concentration prepared heavily mineralized beads (figure 3.11). At this point, image acquisition on CLSM was again a problem. Whether cells are all dead in the core of the bead was impossible to determine. On the other hand, the viability of the cells that were visible in the microscope appeared to be good (>90%).

Before encapsulation cells continuously expressed viability >95% when studied in the light microscope. Nevertheless, at day 2 post encapsulation the viability seemed to have decreased slightly, from >95% to 90% (experiments M1-4). The osteosarcoma cells showed a grater decrease, particularly in beads with addition of 0.5mg/mL ALP (from >95% to 50%, figure 3.6). This might be

explained by the shear forces needed to mix the cell suspension in the syringe pre encapsulation due to the high viscosity of the alginate solution. The drop in viability in the present study is nevertheless better than previously reported in studies regarding the particular problem (Kong, 2003).

Earlier studies have experienced high viability of MSCs when incorporating RGD peptides into the alginate beads. Weir et al reported viabilities of up to 80% during 21 days of culture when encapsulating MSCs in alginate beads. Weir et al also tested viability in alginate beads modified with calcium phosphate cement (CPC) resulting in 75% survival the same time period (Weir, 2010). Bidarra et al compared encapsulated MSCs that were given MSCGM and MSCDM respectively. Both samples maintained high viability (80-90%) throughout the time of the study (Bidarra, 2010). Evangelista et al also included samples without RGD peptides as controls. In these beads mouse mesenchymal stem cells (mMSCs) were encapsulated. No statistical significance was found between survival in RGD-samples and controls (Evangelista, 2007). In the two latter studies they used a cell concentration 10 fold as high as in the present study. This may contribute to higher survival as higher cell concentrations promotes cell interactions. However, cell survival in the present study indicates that cell survival is good regardless of initial cell concentration.

## 4.3 Metabolic activity

The metabolic activity of encapsulated MSCs in alginate beads was studied in experiment M4. Samples were tested at day 2, 7, 14 and 21 post encapsulation (figure 3.19). The metabolic activity was found to increase over the time of the study for all samples. From day 2 to day 7 post encapsulation the activity differed modestly. All samples showed an increase in activity between day 7 and day 14. From day 14 to day 21 samples showed no or little increase.

The minute change in metabolic activity for all samples from day 2 to day 7 could potentially be caused by the need for the cells to adapt to the new environment. The live/dead assay (figure 3.17 and 3.18) revealed an increase in cell clusters from day 7 to day 14 post encapsulation. As cells were continuously observed growing outside the beads from day 14 the increase in metabolic activity could point to cell proliferation. A smaller, relative increase in samples receiving differentiation medium (3a/4a) could point to an end in proliferation, in favor of differentiation.

Comparing metabolic activity between cell lines is hard, as different cell lines will behave differently inside alginate beads (Rokstad, 2006). However, earlier studies report an increase in metabolic activity, even if no proliferation is observed. This is especially evident in samples were RGD peptides are utilized (Bidarra, 2010). The reason for the increased activity is thought to be caused by different cellular functions such as cell differentiation, cytoskeleton rearrangement and synthesis of proteins. As actin filaments were observed in morphology studies, the increase in metabolic activity could be due to cytoskeleton rearrangements in the cells.

In another study where mMSCs[3] were utilized the findings suggest that alginate modified with RGD peptides result in higher metabolic activity. This is explained by the fact that peptides interacts with cells, triggering cellular actions (Evangelista, 2007).

---

[3] Mouse MSCs and human MSCs have been shown to differ somewhat in the expression of runx2 during the differentiation process towards osteoblast. When comparing mouse- and human MSCs the fact that they show different patterns in gene expression, and differences in surface receptor patters should be taken into account (Therese Standal, personal communication).

## 4.4 ALP assay

ALP activity was measured at day 2 and 9 post encapsulation in MSCs encapsulated in alginate beads. The activity of ALP gives an indication of whether cells are starting to differentiate.

At day 9 post encapsulation (figure 3.23) there was a statistical significant higher ALP activity in the two samples receiving differentiation medium (samples 3a and 4a) compared to the ones not receiving differentiation medium. This suggested that differentiation had indeed started in these samples.

Results from day 2 post encapsulation (figure 3.22) were unexpected as the sample without added ALP (sample 3) showed similar results as the sample with ALP (sample 4). However, as no difference between the samples initially containing ALP and not containing ALP was found, suggested that the encapsulated ALP from the beginning of the experiment no longer was active and did not influence the results.

Earlier studies have reported a maximum activity at day 7 (Matsuno, 2008), day 14 (Zhao, 2010, Weir, 2010) and day 21 (Bidarra, 2010) post encapsulation when encapsulating MSCs into alginate beads, which is surprising as ALP should only be expressed early in the differentiation (Matsuno, 2008). Both Bidarra et al and Weir et al also tested the activity of MSCs in beads receiving basal medium. These showed low and constant activity. This is in accordance with the findings in the present study, as ALP activity of undifferentiated samples was comparable to the controls at day 9.

## 4.5 Morphology

Morphology was studied by staining the nucleus and actin filaments of MSCs inside alginate beads. In initial experiments with MSCs (experiment M3) cells seemed to interact with each other by elongation of their actin filaments (figure 3.12). In the extended experiment (experiment M4) cells seemed to both interact with each other, and the matrix (figure 3.20 and 3.21).

In initial experiments (M3) cells were observed to interact with each other (figure 3.12). It seemed that they reach out towards each other rather than interacting with the matrix. The image in the figure is cross section only, so it is hard to make a conclusion.

In the extended experiment (M4) the mesenchymal stem cells appeared to have different morphology in the different beads. In samples given differentiation medium, cells appeared to possess an elongated cytoskeleton (figure 3.20 and 3.21). Some of the elongated actin filaments could be explained by cells trying to interact with each other, as especially evident in figure 3.20 day 7. However, elongations of the actin filaments were also apparent where there were no adjacent cells, as evident in figure 3.20, day 21 and figure 3.21 day 14. It seems that cells are indeed interacting with the matrix. However, not all cells in each bead had the described morphology. Indeed, some appeared in a round shape, interacting neither with neighboring cell nor with the alginate matrix.

In samples not given differentiation medium cells appeared to exist in a round shape throughout the duration of the study.

Evangelista et al (2007) showed that immobilization of mMSCs in alginate without modification with RGD lacked the assemblage of actin filaments, preventing interactions between cell and matrix. mMSCs in alginate beads modified with RGD was observed to possess elongated actin filaments, thus

creating a means of interacting with each other, and the matrix. This was explained by the RGD peptide interacting with integrins on cell membranes, directing the cell to assemble actin filaments. Morphology was also studied by Bidarra et al (2010). They reported that hMSCs interacted to a certain extent with the alginate matrix when modifying the alginate with RGD peptides. Bidarra et al also included control samples without RGD, and these remained in a round shape without interactions with the matrix. These observations lead to the conclusion that RGD peptides are essential for cell-matrix interactions. The findings in these articles were not confirmed in the present study, as cells interacted with the matrix when using alginate and CP, or alginate alone.

## 4.6 Citrate treatment

Initial problems regarding RNA isolation was found to be due to cell death caused by the citrate treatment used to isolate cells from the alginate beads. The more mineralized the beads were, the harder it was to dissolve them upon citrate treatment. This may be explained by the fact that the minerals seem to dissolve prior to the beads themselves. This was repeatedly observed in the light microscope during citrate treatments. As a consequence cells within mineralized alginate beads were often recovered in a lower percentage than the ones inside lesser mineralized beads.

In the literature little is described concerning cell recovery in alginate beads. However, citrate treatment is the method that seems to be most frequently utilized. Some describe dissolving the beads in citrate for 10-40 minutes (Häuselmann, 1994, Mok, 1994, Patel, 2004), but no data exist is on the topic of cell survival post treatment (Cohen, 2011). For that reason, Cohen et al. (2011) focused on MSC recovery from alginate beads, and cell survival in different suspensions commonly used when working with alginate beads. Cohen et al. report observing merely 12% survival of swine MSCs (sMSCs) when dissolving alginate beads in citrate for 20 minutes. This coincides with the observations found during the present study. Furthermore, Cohen et al. tested how EDTA influenced cell survival if used to dissolve beads, but these results were unsatisfactory as well. These results indicate that novel methods for recovering cells inside alginate beads need to be uncovered.

MSCs encapsulated in beads mineralized by the one-step method have been recovered using the citrate treatment at NTNU earlier. In this study the RNA quality, following the one step method, was repeatedly very poor (OD$_{260/280}$<<2), indicating DNA contamination (Sundrønning, 2010).

Ultimately, in the present study, recovering of cells using the sequential citrate treatment was accomplished with satisfactory result. The isolated RNA were observed to be of good quality (260/280 > 2) (table 3.4), and PCR results proved good and reliable. Using a sequential citrate treatment gives RNA of good quality as cell viability is kept as high as possible (up to 30%). RNA and alginate is hard to separate as they are both negatively charged polymers. By avoiding extensive exposure of cells to citrate, cell viability is maintained at a tolerable level (i.e no RNA is free in the medium, which would make it hard to separate RNA from alginate in the RNA isolation procedure).

## 4.7 PCR

PCR analyses were performed after recovering RNA by a sequential citrate treatment (appendix A), and subsequent synthesis of cDNA. RNA was of good quality. PCR results showed that runx2 was expressed in MSCs encapsulated in beads heavily mineralized (experiment M3, figure 3.14). Both runx2 and osterix were expressed in MSCs encapsulated in mineralized/unmineralized beads, with and without induced differentiation (experiment M4, figure 3.25 and 3.27).

Runx2 expression for unencapsulated MSCs and sample 3 (not given ALP) at day 2 post encapsulation were similar (figure 3.25). At day 2, expression in sample 4 (given ALP) was slightly higher. This suggests that ALP accelerated differentiation. However, none of the samples were at this point given differentiation medium, so the slight difference could be explained by the cell population retrieved from beads. After culturing samples 3a and 4a (not given ALP and given ALP, respectively) runx2 expression increased significantly from day 2 to day 7 post encapsulation, compared to samples 3b and 4b (not given differentiation medium). This suggests that the components in the differentiation medium indeed could penetrate the alginate beads, and thus exert their effect on the cells. Runx2 expression remained higher in samples with differentiation medium compared with samples in regular medium throughout the study. One exception was sample 4b (given ALP, cultured in regular medium). This sample showed a continuous increase in activity reaching day 21, when the expression was similar to the former. This suggested that mineralization might play a role in differentiation. The relatively high expression of runx2 in sample 3b on day 7 could not be explained.

Osterix expression showed greater differences between samples given differentiation medium compared with samples given regular medium (figure 3.27). The samples given differentiation medium (3a/4a) increased roughly 100- and 60-fold, respectively from day 2 to day 7 post encapsulation, suggesting that the MSCs were differentiating into mature osteoblasts. The expression continued to increase for both samples reaching day 14. At this point, osterix expression in sample 3a decreased slightly, whereas expression in sample 4a continued to increase until day 21 when the study was ended.

Samples cultured in regular medium (3b/4b) showed a comparable osterix expression profile. They increased 5-fold until day 14, and 10-fold until day 21 compared with the expression at day 21. This was surprising as they were not given differentiation medium. No apparent differences between mineralized and unmineralized beads were observed, suggesting that mineralization did not affect differentiation. On the contrary, alginate by itself, seemed to exert an effect on differentiation, but this was difficult to confirm.

Osterix expression has been analyzed in a study where human umbilical cord mesenchymal stem cells (hUCMSCs) were encapsulated in alginate beads cultured in differentiation medium. The results showed that hUCMSCs had a 12-fold increase in osterix expression from day 1 to day 7 post differentiation culturing start. A 3-fold reduction was observed between day 7 and day 14 (Zhao, 2010). These results differ somewhat from the results obtained in the present study. A reason for the difference was not found.

## 4.8 SEM

In the extended experiment (M4) beads were studied by SEM after the 21 days of culture. Both matrix and cells were studied (figure 3.28). Furthermore, collagen fibers were observed in pictures from samples receiving differentiation medium confirming results indicating that the stem cells had in fact differentiated into mature osteoblasts (figure 3.29 and 3.30).

In images of alginate beads in samples without ALP (3a/3b) there were no apparent mineralization (figure 3.28). However, some of the beads in sample 3a appeared mineralized, as they were dark in the light microscope. The lack of obvious minerals observed in SEM images may be due to the inhomogeneously distribution of mineralization between beads. The structure of the matrix in sample 3a (cultured in differentiation medium) seemed less porous compared with samples 3b

(cultured in regular medium). This has been observed earlier in similar beads mineralized by the in situ method (Sundrønning, 2010). Observations of cells in the same beads revealed that only cells in beads from sample 3a appeared to be interacting with the matrix (figure 3.28). This supports the observations made in the morphology studies described above.

In images of alginate beads in samples <u>with ALP</u> (4a/4b) minerals were observed to a larger extent in sample 4a (figure 3.28). This might yet again be explained by the small bead population studied in SEM. The density of minerals seemed to be higher compared with beads mineralized with the in situ method (Sundrønning, 2010). The cytoskeleton of cells seemed to be more expanded in cells in sample 4b (cultured in regular medium), compared with sample 4a (cultured in differentiation medium). This is also surprising as cells from sample 4b did not seem to interact with the matrix in morphology studies previously described.

Bidarra et al (2010) reported cells interacting to certain extent with alginate modified with RGD peptides when studying them in SEM. Cell-matrix interactions in the present study appear different, as the filaments appeared more extended.

Evangelista et al (2007) cultured an osteoblast cell line into alginate modified with RGD, and into unmodified alginate. The cell morphology was studied in transmission electron microscope (TEM). Osteoblasts within RGD modified alginate showed fibrils suspected of being collagen at day 3 post encapsulation. These fibers were never observed in unmodified beads. Additionally, osteoblast in modified beads had a larger number of mitochondria, probably due to increased metabolic activity, and had a more round nucleus, compared with cells in unmodified alginate.

The morphology of the cells in the present study was comparable to the osteoblasts in RGD-modified alginate as described above, suggesting first and foremost, that they are in fact mature osteoblast. Secondly, it suggests that modification with RGD could be substituted with modification with calcium phosphate minerals. This might be a good thing as coupling of RGD to alginate have been problematic in the past in reproducing coupling efficiency (Westhrin, 2010).

During preparation of the samples for SEM analysis a lot of the samples material disappeared during CPC. Only three or four sections of the bead were left. The pictures were, nevertheless, regarded as representative.

## 4.9 Differentiation of MSCs in alginate beads
Mesenchymal stem cells seemed to have differentiated into mature osteoblasts in both samples receiving differentiation medium, regardless of mineralization.

This is especially apparent in the PCR results, where cells cultured in differentiation medium were found to express osterix, a specific marker for mature osteoblasts. Runx2 was showed a continuous and high expression. Runx2 expression and ALP activity is usually connected. The reason for the disagreement between these analyses could be due to differences in bead population, and sensitivity of the analysis. For ALP analysis only an estimate of 4000 cells were used, compared with a million in PCR. Furthermore, PCR is far more sensitive, suggesting that the PCR results are the most reliable.

The metabolic activity increased over time in culture in all samples, although less increase over time was observed for samples cultured in differentiation medium. As osterix expression was high in samples cultured in differentiation medium, the increase in activity is probably not caused by proliferation, as osterix is a known proliferation inhibitor (Zhang, 2008). The increase in activity could consequently point to differentiation.

Morphology of the cells given differentiation medium appeared more osteoblast-like, as they contained actin filaments interacting with the matrix. Moreover, SEM images showed that collagen fibers were present in both samples. This further confirms the presence of mature osteoblasts. Minerals were observed in both samples, but in a slighter degree in beads without ALP, compared to samples with ALP. This suggests that ALP is not essential for mineralization, all though it speeds up the mineralization process significantly. Light microscopy pictures confirmed these observations, as samples appeared dark.

Cell viability remained > 90 % up to day 21 when the study was ended.

## 4.10 Future perspectives

**Bead stability**

Increasing bead stability would be advantageous, as methods such as mineral quantification by Alizarin Red-S could be accomplished. Increasing bead stability has previously been solved by addition of $CaCl_2$ to the culture medium, by modification of the beads, such as addition of poly-L-lysine or chitosan, or by adding a small amount of acrylamide to the alginate. Any of these latter methods could offer a potential mean of stabilizing the alginate beads.

**ALP activity**

ALP activity was measured only on day 2 and day 9 post encapsulation in the present study. ALP activity has previously been demonstrated to be as its maximum at day 14 and 21 post encapsulation as described in section *4.3 ALP activity.* As ALP activity is often used together with runx2 to evaluate differentiation of MSCs, it could be interesting to continue to measure the activity throughout the period of a study.

**Cell recovery**

In order to yield sufficient cell numbers for RNA analysis the cell recovery method should be studied in more detail. In the present study, at best, 30 % of the cells were recovered after a sequential citrate treatment. Increasing the yield would decrease the work-load and -time significantly. This is due to the fact that a lower cell number would be much more easily up-cultured *in vitro*. Furthermore, smaller amounts of cells would be cost effective because smaller amounts of reagents (such as MSC medium) would be needed. As of now, citrate and EDTA seem to be the standard reagents for cell recovery purposes. As the beads in the present study are of poor stability, reagents with phosphate ions could be an interesting alternative. In addition, such reagents, for cell recovery, should not be harmful to the cells.

**Cell adhesion**

To promote both adhesion and bone formation, including RGD peptides in the immobilization matrix seem to be a good alternative. They have been shown to promote both adhesion and direct differentiation of myoblasts into skeletal muscle cells by varying M:G ratio in the alginate and density and sequence of the peptides (Rowley, 2001). For bone cell adhesion RGD seem to be a good candidate. This peptide has been shown to enhance adhesion of bone marrow stromal cells to HA composites (Durrieu, 2004). Furthermore, RGD is shown to drastically increase bone formation *in vivo* in alginate beads (Augst, 2006). As a bonus, coupling of RGD peptides might be beneficial, as the binding could increase bead stability.

**Confirm differentiation**

Occurrence of mature functioning osteoblasts should be further confirmed by testing gene expression of marker genes specific for mature osteoblasts, such as OCN and BSP (Zhang, 2010). OCN levels can also be measured by ELISA by measuring OCN concentration in the culture medium. This is due to the fact that osteoblasts excrete the protein. In addition collagen gene markers should be analyzed to support the observations of collagen in beads by SEM analysis.

# 5. Conclusion

Enzymatic mineralization of alginate beads was found to be a cell friendly way of mineralizing alginate beads. Mineralization of the beads was observed in the light microscope, by visual inspection, as well as by SEM. Cell viability remained high when using a concentration of 0.25mg/ml ALP. Osteosarcoma cells were used as model cells in initial experiments. They proved to be good for optimizing the enzymatic mineralization method, but behaved differently compared with mesenchymal stem cells in terms of viability, and activity. Alginate beads were unstable and needed addition of $CaCl_2$ for stabilization purposes. An improved method for cell recovery was prepared. This *sequential* citrate treatment led to successful isolation of RNA with good quality.

Mesenchymal stem cells receiving differentiation medium were observed to differentiate into mature osteoblasts within the beads. This was confirmed by gene expression analysis, cell morphology, ALP activity and the presence of collagen. Proliferation of MSCs in beads was additionally observed, although only to a small degree. Metabolic activity measurements confirmed little cell proliferation, nor cell death. Cell morphology in differentiated samples was recognized by showing elongated actin filaments, compared with the ones cultured in regular medium. This suggested that the cells were able to interact with the matrix. The occurrence of collagen fibers in SEM images further confirmed the presence of mature osteoblasts.

Samples cultured in regular medium with or without added ALP showed an increase of osterix expression until day 21 when the study was ended. This was surprising, as it inferred that the alginate matrix itself might influence differentiation of MSCs into osteoblasts, and that mineralization has little effect.

Encapsulating mesenchymal stem cells into alginate beads mineralized by the enzymatic method is cell friendly, and allows the cells to differentiate into mature osteoblast when cultured in differentiation medium. Alginate without minerals seemed to influence differentiation to a certain extent, suggesting that minerals are not needed for differentiation to occur. The minerals do, however, speed up following mineralization of the beads.

# References

ABBAH, S. A., LU, W. W., CHAN, D., CHEUNG, K. M. C., LIU, W. G., ZHAO, F., LI, Z. Y,, LEONG, J. C. Y., LUK, K. D. K. 2008. Osteogenic behavior of alginate encapsulated bone marrow stromal cells: an in vitro study. *J mater Sci: Mater Med,* 19**,** 2113-2119.

AL-NASIRY, S., GEUSENS, N., HANSSENS, M., LUYTEN, C., PIJNENBORG, R. 2007. The use of Alamar Blue assay for quantitative analysis of viability, migration and invasion of choriocarcinoma cells. *Human Reproduction,* 22**,** 1304-1309.

AUGST, A. D., KONG, H. J., MOONEY D. J. 2006. Alginate hydrogels as biomaterials. *Macromolecular Bioscience,* 6**,** 623-633.

BERGER, R., RÜHLEMANN, I. 1988. Stable ionotropic gel for cell immobilization using high molecular weight pectic acid. *Acta Biotechnologica,* 8**,** 401-405.

BEVAN, D. L., GILSON, C. D., THOMAS, A. 1995. An improved method for preparing micro-organism laden alginate bead specimens for accurate scanning electron microscope examination *Biotechnology Techniques,* 9**,** 913-916.

BIDARRA, S., BARRIAS, C. C., BARBOSA, M. A., SOARES, R., GRANJA, P. L. 2010. Immobilization of human mesenchymal stem cells within RGD-grafted alginate microspheres and assessment of their aniogenic potential. *Biomacromolecules,* 11**,** 1956-1964.

BOSKEY, A. L. 1998. Biomineralization: conflicts, challenges, and opportunities. *J Cell Biochem,* 30**,** 83-91.

CAPLAN, A. I. 1991. Mesenchymal Stem Cells. *Journal of Orthopaedic Research,* 9**,** 641-650.

CAPLAN, A. I. 2007. Adult mesenchymal stem cells for tissue engineering versus regenerative medicine. *J. Cellular Physiology,* 213**,** 341-347.

CAPLAN, A. I., DENNIS, J. E. 2006. Mesenchymal stem cells as trophic mediators. *J Cell Biochem,* 98**,** 1076-1084.

CHAPLIN, M. 2010. *Alginate* [Online]. London. Available: http://www.btinternet.com/~martin.chaplin/hyalg.html [Accessed 20. october 2010].

CHRISTENSON, R. H. 1997. Biochemical markers of bone metabolism: an overview. *Clin Biochem* 30**,** 573-593.

COHEN, J., ZALESKI, K. L., NOURISSAT,G., JULIEN, T. P., RANDOLPH, M. A., YAREMCHUK, M. J. 2011. Survival of porcine mesenchymal stem cells over the alginate recovered cellular method. *Journal of Biomedical Materials Research,* 96A**,** 93-99.

COLFEN, H. 2010. Biomineralization: A crystal-clear view. *Nature Materials,* 9**,** 960-961.

COX, W. G., SINGER, V. L. 1999. A high-resolution, fluorescence-based method for localization of endogenous alkaline phosphatase. *J Histochem Cytochem,* 47**,** 1443-1455.

DOCHEVA, D., HAASTERS, F., SCHIEKER, M. 2008. Mesenchymal Stem Cells and Their Cell Surface Receptors. *Current Rheumatology Review,* 4.

DONATI, I., HOLTAN, S., MØRCH, Y.A., BORGOGNA, M., DENTINI, M., SKJÅK-BRÆK, G. 2005. New hypothesis on the role of alternating sequences in calcium-alginate gels. *Biomacromolecules,* 6**,** 1031-1040.

DURRIEU, M. C., PALLU, S., GUILLEMOT, F., BAREILLE, R., AMÉDÉE, J., BAQUEY, C. H. 2004. Grafting RGD containing peptides onto hydroxyapatite to promote osteoblastic cells adhesion. *Journal of Materials Science: Materials in medicine,* 15**,** 779-786.

ENDRES, M., WENDA, N., WOEHLECKE, H., NEUMANN, K., RINGE, J., ERGGELET, C., LERCHE, D., KAPS, C. 2010. Microencapsultation and chondrogenic differentiation of human mesenchymal progenitor cells from subchondral bone marrow in Ca-alginate for cell injection. *Acta Biomaterialia,* 6**,** 436-444.

EVANGELISTA, M. B., HSIONG, S. X., FERNANDES, R., SAMPAIO, P., KONG, H.-J., BARRIAS, C. C., SALEMA, R., BARBOSA, M. A., MOONEY, D. J., GRANJA, P. L. 2007. Upregulation of bone cell differentiation through immobilization within a synthetic extracellular matrix. *Biomaterials,* 28**,** 3644-3655.

GARGIONI, R., NETO, F. F., BUCHI, D. F., RANDI, M. A. F., FRANCO, C. R. C., PALUDO, K. S., PELLETIER, E., FERRARO, M. V. M., CESTARI, M. M., BUSSOLARO, D., RIBEIRO, C. A. O. 2006. Cell death and DNA damage in peritoneal macrophages of mice (Mus musculus) exposed to inorganic lead. *Cell Biology International,* 30**,** 615-623.

GHIDONI, I., CHLAPANIDAS, T., BUCCO, M., CROVATO, F., MARAZZI, M., VIGO, D., TORRE M. L., FAUSTINI, M. 2008. Alginate cell encpasulation: new advances in reproduction and cartilage regenerative medicine. *Cytotechnology,* 58**,** 49-56.

GKIONI, K., LEEUWENBURGH, S. C. G., DOUGLAS, T. E. L., MIKOS, A. G., JANSEN, J. A. 2010. Mineralization of Hydrogels for Bone Regeneration. *Tissue Engineering; Part B,* 16.

GOLUB., E. E. 2009. Role of Matrix Vesicles in Biomineralization. *Biochem Biophys Acta.,* 1709**,** 1592-1598.

GREGORY, C. A., GUNN, G., PEISTER, A., PROCKOP, D J. 2004. An Alizarin red-based assay of mineralization bt adherent cells in culture: comparison with cetylpyridinium chloride extraction. *Analytical Biochemistry,* 329**,** 77-84.

GRELLIER, M., GRANJA, P. L., FRICAIN J-C., BIDARRA, S. J., RENARD, M., BAREILLE, R., BOURGET, C., AMÉDÉE, J., BARBOSA, M. A. 2009. The effect of the co-immobilization of human osteoprogenitors and

endothelial cells within alginate microspheres on mineralization in a bone defect. *Biomaterials,* 30**,** 3271-3278.

HAMID, R., ROTSHTEYN, Y., RABADI, L., PARIKH, R., BULLOCK, P. 2004. Comparison of alamar blue and MTT assays for high thorough-put screening. *Toxicology In Vitro,* 5**,** 703-710.

HAUG, A. 1961. The affnity of some divalent metals to different types of alginate. *Acta Chem Scand,* 15**,** 1794-1795.

HUANG, Z., REN, P-G., MA, T., SMITH, L., GOODMAN, S. B. 2010. Modulating osteogenesis of mesenchymal stem cells by modifying growth factor availability. *Cytokine,* 51**,** 305-310.

HWANG, S. N., ZHANG, C., HWANG, S-Y., VARGHESE, S., 2009a. Mesenchymal stem cell differentiation and roles in regenerative medicine. *Syst Biol Med,* 1**,** 97-106.

HWANG, Y.-S., CHO, J., TAY, F., HENG, J. Y. Y., HO, R., KAZARIAN, S. G., WILLIAMS, D. R., BOCCACCINI, A. R., POLAK, J. M., MANTALARIS, A. 2009b. The use of murine embryonic stem cells, alginate encapsulation, and rotary microgravity bioreactor in bone tissue engineering. *Biomaterials,* 30**,** 499-507.

HÄUSELMANN, H. J., FERNANDES, R. J., MOK, S. S., SCHMID, T. M., BLOCK, J. A., AYDELOTTE, M. B., KUETTNER, K. E., THONAR, E. J-M. A. 1994. Phenotypic stability of bovine articular chondrocytes after long-term culture in alginate beads. *Journal of Cell Science,* 107**,** 17-27.

IBSEN, C. J. S., BIRKEDAL, H. 2010. Modification of bone-like apatite nanoparticle size and growth kinetics by alizarin red S *Nanoscale,* 2**,** 2478-2486.

INVITROGEN 2005. LIVE/DEAD Viability/Cytotoxicity Kit *for mammalian cells*. *In:* TECHNOLOGIES, I. D. (ed.) *Product information.* Eugene, Oregon: Invitrogen.

JETHVA, R., OTSURU, S., DOMINICI, M., HORWITZ, E. M. 2009. Cell therapy for disorder of bone. *Cytotherapy,* 11**,** 3-17.

JUHÁSOVÁ, J., JUHÁS, S., KLÍMA, J., STRNÁDEL, J., HOLUBOVÁ, M., MOTLÍK, J. 2011. Mesenchymal stem cells in 2D and 3D environment. *Ahead of print*.

KASSEM, M., ABDALLAH, B. M., SAEED, H. 2008. Osteoblastic cells: Differentiation and trans-differentiation. *Archives of Biochemistry and Biophysics,* 473**,** 183-187.

KELLY, D. J., JACOBS, C. R. 2010. The Role of Mechanical Signals in Regulating Chondrogenesis and Osteogenesis of Mesenchymal Stem Cells. *Birth Defects Research,* 90**,** 75-85.

KONG, H. J., SMITH, M. K., MOONEY, D. J. 2003. Designing alginate hydrogels to maintain viability of immoblized cells. *Biomaterials,* 24**,** 4023-4029.

KUO, C. K., MA, P. X. 2008. Maintaining dimensions and mechanical properties of ionically crosslinked alginate scaffolds *in vitro*. *Inc. J Biomed Mater Res,* 84**,** 899-907.

KWEI, S. P., MOFFAT, K. L., DOTY, S., LU, H. H. 2010. Effect of Hydroxyapatite Particles on Stem Cell Response in Nanofiber Scaffolds. *Bioengineering Conference.* Proceedings of the 2010 IEEE 36th Annual Northeast: Dept. of Biomed. Eng., Columbia Univ., New York, NY, USA

LIAN, J. B., STEIN, G. S., JAVED, A., VAN WIJNEN, A. J., STEIN, J. L., MONTECINO, M., HASSAN, M. Q., GAUR, T., LENGNER, C. J., YOUNG, D. W. 2006. Networks and hubs for the transcriptional control of osteoblastogenesis. *Rev Endocr Metab Disord,* 7**,** 1-16.

LIU, X., MA, P. X. 2004. Polymeric scaffolds for bone tissue engineering. *Ann Biomed Eng,* 32**,** 477-486.

LIVAK, K. J., SCHMITTGEN, T. D. 2001. Analysis of Relative Gene Expression Data Using Real-Time Quantitative PCR and the. 2^-ΔΔCt Method. *Methods Cell Biol,* 25**,** 402-408.

MARKAKI, A. E. 2009. alamarBlue Assay for Assessment of Cell Proliferation using the FLUOstar OPTIMA. Available: http://www.bmglabtech.com/db_assets/applications/downloads/applications/195-alamarblue-cell-proliferation.pdf [Accessed 6. April].

MARTINSEN, A., SKJAK-BRAEK, G. & SMIDSROD, O. 1989. Alginate as immobilization material: I. Correlation between chemical and physical properties of alginate gel beads. *Biotechnol Bioeng,* 33**,** 79-89.

MATSUNO, T., HASHIMOTO, Y., ADACHI, S., OMATA, K., YOSHITAKA, Y., OZEKI, Y., UMEZU, Y., TABATA, Y., NAKAMURA, M., SATOH, T. 2008. Preparation of injectable 3D-formed β-tricalcium phosphate bead/alginate composite for bone tissue engineering. *Dental Materials Journal,* 27**,** 827-834.

MCBEATH, R., PIRONE, D. M., NELSON, C. M. 2004. Cell shape, cytoskeletal tension, and RhoA regulate stem cell lineage commitment. *Dev Cell,* 6**,** 483-495.

MCHUGH, D. J. 2003. A guide to the seaweed industry. *FAO Fisheries Technical Paper - T441* [Online]. Available: www.fao.org [Accessed 11.2.2010].

MOK, S. S., MASUDA, K., HAUSELMANN, H. J., AYDELOTTE, M. B., THONAR, E. J-M. A. 1994. Aggrecan Synthesized by Mature Bovine Chondrocytes Suspended in Alginate. *The Journal of Biological Chemistry,* 269**,** 33021-33027.

MORIGUCHI, T., YANO, K., NAKAGAWA, S., KAJI, F. 2003. Elucidation of adsorption mechanism of bone-staining agent alizarin red S on hydroxyapatite by FT-IR microspectroscopy. *Journal of Colloid and Interface Science,* 260**,** 19-25.

MØRCH, Y. A., DONATI, I., STRAND, B. L., SKJÅK-BRÆK, G. 2006. Effect of $Ca^{2+}$, $Ba^{2+}$, and $Sr^{2+}$ on Alginate Microbeads. *Biomacromolecules,* 7**,** 1471-1480.

MØRCH, Y. A., STRAND L. B., SKJÅK-BRÆK, G. 2009. Alginate structure function relationship relevant to their use for cell transplantation. *In:* HALLÉ, J. J., DE VOS, P., ROSENBERG, L. (ed.) *The Bioartificial Pancreas and Other Biohybrid Therapies.* Research Science Post.

NAKAMURA, H. 2007. Morphology, Function, and Differentiation of Bone Cells. *Journal of Hard Tissue Biology,* 16**,** 15-22.

NUDELMAN, F., PIETERSE, K., GEORGE, A., BOMANS, P. H. H., FRIEDRICH, H., BRYLKA, L. J., HILBERS, P. A. J., DE WITH, G., SOMMERDIJK, A. J. M. 2010. The role of collagen in bone apatite formation in the presence of hydroxyapatite nucleation inhibitors. *Nature Materials,* 9**,** 1004-1009.

OLDERØY, M. Ø., XIE, M., STRAND, B. L., DRAGET, K. I., SIKORSKI, P., ANDREASSEN, J-P. 2011. Polymorph switching in the calcium carbonate system by well-defined alginate oligomers. *Crystal Growth & Design,* Ahead of print.

OLDERØY, M. Ø., XIE, M., STRAND, B. L., FLATEN, E. M., SIKORSKI, P., ANDREASSEN, J-P. 2009. Growth and nucleation of calcium carbonate vaterite crystals in prescence of alginate. *Crystal Growth & Design,* 9**,** 5176-5183.

ORIMO, H. 2010. The Mechanism of Mineralization and the Role of Alkaline Phosphatase in Health and Disease. *J Nippon Med Sch,* 77**,** 4-12.

OSATHANON, T., GIACHELLI, C. M., SOMERMAN, M. J. 2009. Immobilization of alkaline phosphatase on microporous nanofibrous fibrin scaffolds for bone tissue engineering. *Biomaterials,* 30.

PANETTA, N. J., GUPTA, D. M., QUARTO, N., LONGAKER, M. T. 2009. Mesenchymal cells for skeletal tissue engineering. *Panminerva Med,* 51**,** 25-41.

PATEL, A., SLAATS, B., HALLMANN, J., TILCHER, R., BEITZEN-HEINEKE, W., VORLOP, K-D. Year. Encapsulation and application of bacterial antagonists and a nematophagous fungus for biological pest control. *In:* International Workshop on Bioencapsulation, 2004 Bilbao, Spain.

PETRENKO, Y. A., IVANOV, R. V., PETRENKO, A. Y., LOZINSKY, V. I. 2011. Coupling of gelatin to inner surfaces of pore walls in spongy alginate-based scaffolds facilitates the adhesion, growth and differentiation of human bone marrow mesenchymal stromal cells. *J Mater Sci,* Epub ahead of print.

PUCHTLER, H., MELOAN, S. N., TERRY, M. S. 1969. On the history and mechanism of Alizarin and Alizarin Red S stains for calcium. *Journal of Histochemistry & Cytochemistry,* 17**,** 110-124.

ROEDER, R. K., CONVERSE, G. L., KANE, R. J., YUE, W. M. 2008. Hydroxyapatite-reinforced polymer biocomposites for synthetic bone substitutes. *Journal of the Minerals, Metals and Materials Society*, 38-45.

ROKSTAD, A. M., DONATI, I., BORGOGNA, M., OBERHOLZER, J., STRAND, B. L., ESPEVIK, T., SKJÅK-BRÆK, G. 2006. Cell-compatible covalently reinforced beads obtained from a chemoenzymatically engineered alginate. *biomaterials,* 27, 4726-4737.

ROKSTAD, A. M., HOLTAN, S., STRAND, B. L., STEINKJER, B., RYAN, L., KULSENG, B., SKJÅK-BRÆK, G., ESPEVIK, T. 2002. Microencapsulation of Cells Producing Therapeutic Proteins: Optimizing Cell Growth and Secretion. *Cell Transplantation,* 11, 313-324.

ROWLEY, J. A., MOONEY, D.J. 2001. Alginate type and RGD density control myoblast phenotype. *Biomed. material,* 60, 217-223.

SHAFIEE, A., SEYEDJAFARI, E, SOLEIMANI, M., AHMADBEIGI, N., DINARVAND, P., GHAEMI, N. 2011. A comparison between osteogenic differentiation of human unrestricted stem cells and mesenchymal stem cells from bone marrow and adipose tissue. *Biotechnol Lett.,* Ahead of print.

SHIN, H., ZYGOURAKIS, K., FARACH-CARSON, M. C., YASZEMSKI, M. J., MIKOS, A. G. 2004. Modulation of differentiation and mineralization of marrow stromal cells cultured on biomimetic hydrogels modified with Arg-Gly-Asp containing peptides. *Journal of Biomedical Materials Research,* 69A, 535-543.

SIMMONS, C. A., ALSBERG, E., HSIONG, S., KIM, W. J., MOONEYA, D. J. 2004. Dual growth factor delivery and controlled scaffold degradation enhance in vivo bone formation by transplanted bone marrow stromal cells. *Bone,* 35, 562-569.

SINGER, N. G., CAPLAN, A. I. 2011. Mesenchymal stem cells: Mechanisms of inflammation. *Annu. Rev. Pathol. Mech. Dis.,* 6, 457-478.

SKJÅK-BRÆK, G., MARTINSEN, ANITA. 1991. Applications of some Algal Polysaccharides in Biotechnology. *In:* GUIRY, M. D., BLUNDEN, G. (ed.) *Seaweed Resources in Europa: Uses and Potential.* John Wiley & Sons Ltd.

SMIDSROD, O. 1974. Molecular basis of some physical properties of alginates in the gel state. *Faraday Discuss Chem Soc,* 57, 263-274.

SMIDSROD, O. & SKJAK-BRAEK, G. 1990. Alginate as immobilization matrix for cells. *Trends Biotechnol,* 8, 71-8.

SMIDSRØD, O. & ANDRESEN, I.-L. 1979. *Biopolymerkjemi,* Trondheim, Tapir.

SMITH, P. J., WILTSHIRE, M., ERRINGTON, R. J. 2004. DRAQ5 labeling of nuclear DNA in live and fixed cells. *In:* ROBINSON, P. J. (ed.) *Curr Protoc Cytom.* New York: Wiley

SPOERKE, E. D., ANTHONY, S. G., STUPP, S. I. 2009. Enzyme Directed Templating of Artificial Bone Material. *Adv. Mater. ,* 21**,** 425-430.

SUNDRØNNING, S. B. 2010. *Encapsulation of human mesenchymal stem cells in phosphate mineralized alginate beads.* Master, the Norwegian University of Science and Technology.

TELFORD, W. G., COX, W. G, STINER, D., SINGER, V. L., DOTY, S. B 1999. Detection of endogenous alkline phosphatase activity in intact cells by flow cytometry using the fluorogenic ELF-97 phosphatase substrate. *Cytometry,* 37**,** 314-319.

TELFORD, W. G., COX, W. G., SINGER, V. L. 2001. Detection of endogenous and antibody-conjugated alkaline phosphate with ELF-97 phosphate in multicolor flow cytometry applications. *Cytometry,* 43**,** 117-125.

TOMOMATSU, O., TACHIBANA, A., YAMAUCHI, K., TANABE, T. 2008. A film of collagen/calcium phosphate composite prepared by enzymatic mineralization in an aqueous phase. *Journal of the Ceramic Society of Japan,* 116**,** 10-13.

TSUCHIDA, H., HASHIMOTO, J., CRAWFORD, E., MANSKE, P., LOU, J. 2003. Engineered allogenic mesenchymal stem cells repair femoral segmental defect in rats. *J Orthop Res,* 21**,** 44-53.

UNUMA, H. 2007. Use of Enzymes for the Processing of Biomaterials. *Int. J. Appl. Ceram. Technol.,* 4**,** 14-21.

WANG, D. A., SHELTON, R. M., COOPER, P. R., LAWSON, M., TRIFFITT, J. T., BARRALET, J. E. 2003. Evaluation of sodium alginate for bone marrow cell tissue engineering. *Biomaterials,* 24**,** 3475-3481.

WANG, J., DE BOER, J., DE GROOT, K. 2008. Proliferation and differentiation of MC3T3-E1 cells on calcium phosphate/chitosan coatings. *J Dent Res,* 87**,** 650-654.

WEIR, M. D., XU, H. H. K. 2010. Human bone marrow stem cell-encapsulating calcium phosphate scaffolds for bone repair. *Acta Biomaterialia,* 6**,** 4118-4126.

WESTHRIN, M. 2010. Novel alginate matrix for tissue engineering. Trondheim: Department of biotechnology, Project work, NTNU.

WILDMAN, R. 2007. *Minerals - Calcium Recommendation, Bones, Muscle and More* [Online]. The nutrition doctor. Available: http://www.thenutritiondr.com/node/184 [Accessed 5. june 2011].

WULF, E., DEBOBEN, A., BAUTZ, F. A., HAULSTICH, H., WIELAND, T. 1979. Fluorescent phallotoxin, a tool for the visualization of cellular actin. *Proc Natl Acad Sci USA,* 76**,** 4498-4502.

XIE, M., OLDERØY, ANDREASSEN, J-P., SELBACH, S. M., STRAND, B. L., SIKORSKI, P. 2010. Alginate-controlled formation of nanoscale calcium carbonate and hydroxyapatite mineral phase within hydrogel networks. *Acta Biomaterialia,* 6**,** 3665-3675.

XIE, M., OLDERØY, M., ZHANG, Z., ANDREASSEN, J-P., STRAND, B. L., SIKORSKI, P. 2011. Biocomposites prepared by alkaline phosphatase mediated mineralization of alginate microbeads. Trondheim: NTNU, University of Birmingham.

YAMAUCHI, K., GODA, T., TAKEUCHI, N., EINAGA, H., TANABE, T. 2004. Preparation of collagen/calcium phosphate multilayer sheet using enzymatic mineralization. *Biomaterials,* 25**,** 5481-5489.

YAO, K. L., TODESCAN, R. J., SODEK, J. 1994. Temporal changes in matrix protein synthesis and mRNA expression during mineralized tissue formation by adult rat bone marrow cells in culture. *J Bone Miner Res,* 9**,** 231-240.

YILGOR, P., SOUSA, R. A., REIS, R. I., HASIRCI, N., HASIRCI, V. 2010. Effect of scaffold architecture and BMP-2/BMP-7 delivery on in vitro bone regeneration. *J Mater Sci,* 21**,** 2999-3008.

ZHANG, C. 2010. Transcriptional regulation of bone formation by the osteoblast-specific transcription factor Osx *Journal of Orthopaedic Surgery and Research,* 5.

ZHANG, C., CHO, K., HUANG, Y., LYONS, J. P., ZHOU, X., SINHA, K., MCCREA, P. D., DE CROMBRUGGHE, B. 2008. Inhibition of Wnt signaling by the osteoblast-specific transcription factor Osterix. . *Proc Natl Acad Sci USA,* 105**,** 6936-6941.

ZHAO, L., WEIR, M. D., XU, H. H. K. 2010. An injectable calcium phosphate-alginate hydrogel-umbilical cord mesenchymal stem cell paste for bone tissue engineering. *Biomaterials,* 31**,** 6502-6510.

# Appendix A                    Citrate treatment

No cells were left after the citrate treatment in the experiment described in section 3.1 Initial experiments. At first, it was hypothesized that the centrifugation was the major cause for the loss of cells. As it was discovered that this was not the case further steps had to be taken in order to optimize the treatment to increase the yield of recovered cells.

## A.1 Citrate treatment in 2D

Further studies on citrate treatment were conducted. U2OS cells in culture were added 10 mL citrate, and after 10 minutes 10mL trypan blue were added to give an impression on cell survival post treatment (figure A.1).
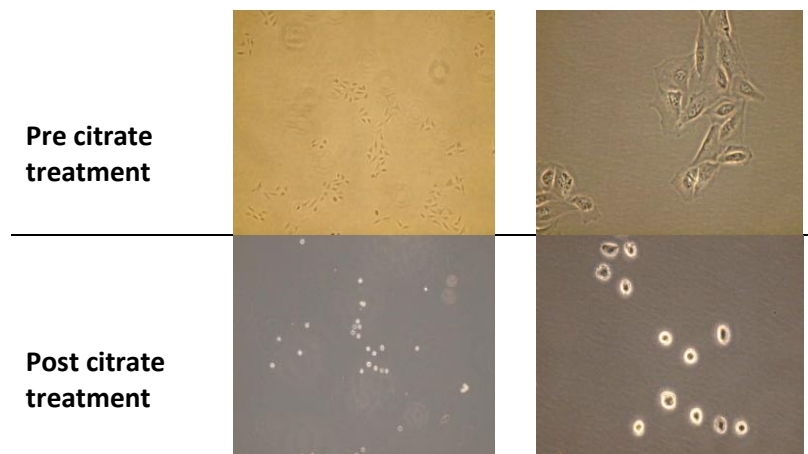


**Figure A.1. Osteosarcoma cells pre/post citrate treatment in 2D. The left picture was taken with a 10X objective, and the right with a 40X objective.**

As it was impossible to quantify cell survival both pre and post treatment, all that could be drawn from this experiment was that the morphology had changed. Pre citrate treatment the cells were stretched out, and afterwards they became more compressed.

## A.2 Citrate treatment of Osteosarcoma cells encapsulated in alginate beads

In another experiment mineralized beads with osteosarcoma cells were split in two and exposed to citrate in volumes of 5 and 20mL, respectively. In figure A.2 is an illustration as to how mineralized the beads were at the time of citrate exposure.



**Figure A.2. Osteosarcoma cells encapsulated in alginate beads at day 7 post encapsulation. The image is magnified 40X.**

Pictures during the citrate treatment were taken every 5 minutes and the results are given in figure A.3. Cells were counted before treatment and after 15 minutes of citrate exposure.
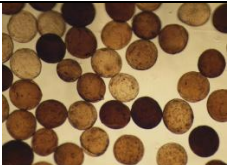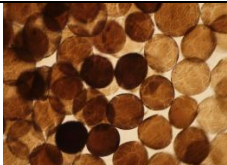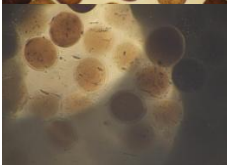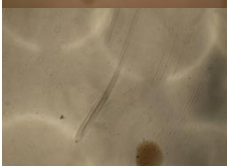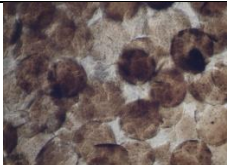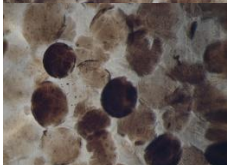
| Time | Cells added 20 mL of citrate | Cell survival | Cells added 5mL of citrate | Cell survival |
|---|---|---|---|---|
| 0 |  | Viability: 55% ~ 400.000 live cells |  | Viability: 55% ~ 400.000 live cells |
| 5 | | | | |
| 10 | | | | |
| 15 | | Viability: 30% ~70.000 live cells | | Viabillity: 45% ~180.000 live cells |
| | Addition of 20mL citrate (7min) | Viability: 5% ~10.000 live cells | Addition of another 5 mL citrate | |
| 15 | | |  | |
| 20 | | | | |
| 25 | | | | |
| 30 | | | | Viability: 10% ~30.000 live cells |

**Figure A.3 Pictures of beads with encapsulated osteosarcoma cells undergoing citrate treatment. The pictures were taken every 5 minutes. Magnification is 40X.**

Seeing that more cells were left after addition of 5mL of citrate compared with 20mL, this volume was selected for further studying. Additionally, as 180.000 live cells were present after 15 minutes of treatment a new method was set up with the goal of retrieving these cells before addition of more citrate to dissolve the remaining beads.

## A.3 Sequential citrate treatment of encapsulated osteosarcoma cells at d13

Osteosarcoma cells encapsulated in beads mineralized with 0.25 and 0.5 mg/mL ALP were prepared as described in table 2.1 experiment U3. A 50:50 relationship between beads with different ALP concentrations was prepared. The amount of beads should account for 550.000 live cells. Every 6 minutes after addition of 5mL citrate the beads/bead particles remaining were allowed to segregate and the suspension left was pipette off and centrifuged at 1000g for 3 min. This method will henceforth be referred to as the *sequential citrate treatment*. The cells were counted in an automated cell counter. Pictures taken during the citrate treatment, the survival of the cells and the total number of live cells are given in figure A.4.
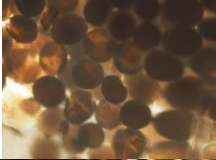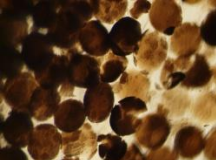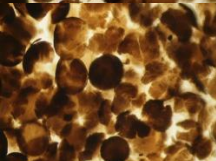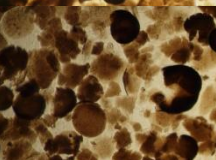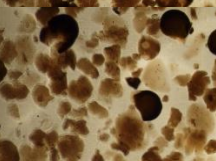
| Time after addition of citrate (min) | Image | Survival (%) | Live cells |
|:---:|:---:|:---:|:---:|
| 0 | | 80 | 550.000 |
| 6 | | 60 | 240.000 |
| 12 | | 73 | 580.000 |
| 18 | | 60 | 130.000 |
| 24 | | 77 | 720.000 |
| 30 | | 32 | 104.000 |
| 36 | | 15 | 300.000 |



**Figure A.4 Osteosarcoma cells encapsulated in alginate beads during citrate treatment to retrieve cells.**

Clearly this is wrong. Starting out with 550.000 cells, would by no means result in the recovery of about 2 millions. It was suspected that the cell counter could not tell the difference between bead fragments and living cells.

## A.4 Improving sequential citrate treatment experiment

For further assessment a new experiment was set up where 2 million osteosarcoma cells were encapsulated in alginate beads mineralized with 0.25mg/mL ALP. The main goal was to count the beads in both the automated cell counter and manually in Burker counting chambers. The survival of the cells inside the beads pre citrate treatment was assessed by live/dead assay and CLSM before starting the treatment. The live/dead images and light microscope pictures are given in figure A.5.
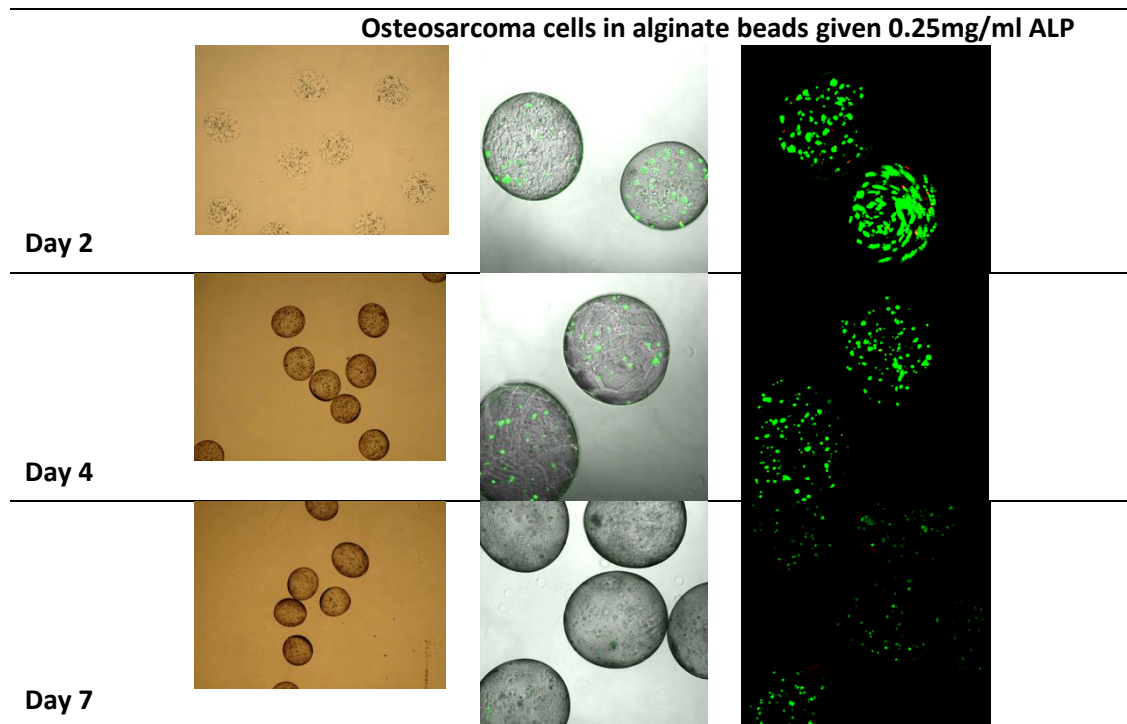


**Figure A.5 U20S encapsulated in alginate beads mineralized with 0.25mg/mL ALP at day 0, day 3 and day 7. The images to the left are taken with a light microscope to give an impression on the mineralization of the beads. The middle picture is a CLSM cross section, and the image to the right is a 3D projection of a z stack. Live cells appeared green, whilst dead cells appear red. The life image is magnified 40X, and the two right pictures are magnified 100X.**

Some of the beads appeared to crack open as they waited for CLSM assessment. This had been observed in earlier experiments and was thought to be due to the phosphate in the PBS.

The citrate treatment on these cells resulted in 0 % recovery when counted manually, thus verifying the hypothesis that the automated cell counter cannot distinguish live cells from bead fragments.

## A.5 Sequential citrate treatment of encapsulated mesenchymal stem cells

Following, the beads were treated with citrate to attain the cells within. An amount of beads that accounts for 2 million cells was prepared and 5mL of citrate was added. The suspension was gently mixed during the six first minutes, and at that point the beads which remained intact were allowed to descend. The rest of the suspension was pipetted off and centrifuged for 3 min at 1000rpm. The remaining beads was given another 5mL of citrate and further mixed. Results are given in figure A.6.
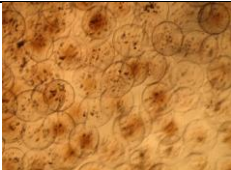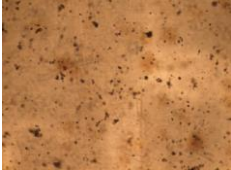
| Time (min) | Picture | Survival (%) | Number of live cells |
|:---:|:---:|:---:|:---:|
| 0 |  | 90 | 260.000 |
| 6 | | 90 | 215.000 |
| 8 | | 0 | 0 |
| | | | **Sum 475.000 (~25% recovery)** |

**Figure A.6 Pictures taken during the citrate treatment, the survival of the cells and the total number of live cells during citrate treatments on MSCs encapsulated in alginate beads mineralized with 0.25mg/mL ALP.**

As the beads were poorly mineralized the citrate treatment went fast. Probably more heavily mineralized beads will be harder to dissolve.

The recovered cells were subsequently incubated in a culture flask for 24 hours, and counted again the following day. At this point about 300.000 cells were left, and all were prepared for RNA analysis. The eluted RNA was quantified using NanoDrop. Unfortunately, only 180ng was recovered.

## A.6 Survival of mesenchymal stem cells in citrate

Recovering cells from alginate beads are usually accomplished using citrate or EDTA. However, cell yields in the present study proved to be unsatisfactory. Little is described in the literature on the subject. In 2011 Cohen et al. report observing merely 12% survival of swine MSCs (sMSCs) when dissolving alginate beads in citrate for 20 minutes. How cells were affected by citrate, EDTA and calcium chloride is given in figure A.7. PBS was initially used as a control. Surprisingly, PBS also seemed to decrease cell viability by roughly 20%. An explanation for this was not found.
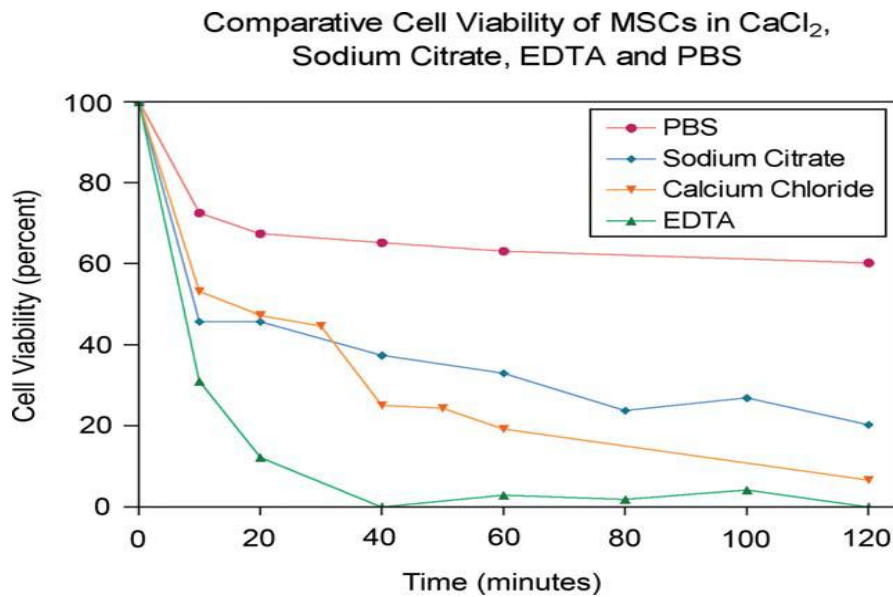


**Figure A.7 Survival of mesenchymal stem cells exposed to PBS, Sodium Citrate, calcium chloride and EDTA (Cohen, 2011).**

Summarized, it seems that osteosarcoma cells respond poorly to citrate treatments, whereas MSCs appear to possess a superior tolerance. Finally, the parameters for the sequential citrate treatment (volume of citrate, time of exposure, number of parallels) need to be tailored for each experiment depending, primarily, on how mineralized the beads are.

**References:**

*COHEN, J., ZALESKI, K. L., NOURISSAT,G., JULIEN, T. P., RANDOLPH, M. A., YAREMCHUK, M. J. 2011. Survival of porcine mesenchymal stem cells over the alginate recovered cellular method. Journal of Biomedical Materials Research, 96A, 93-99.*

# Appendix B          Alizarin Red-S

Alizarin Red can be used to study both the degree of mineralization, and the distribution of minerals throughout the beads (Puchtler, 1969). The method is based on dying the calcium levels compared to assaying inorganic phosphate. This is an advantage as a lot of phosphate is present without being part of the mineralization precipitates (Gregory, 2004). Two possible mechanisms for ARS staining are given in figure B.2. It seems that the salt form is the salt form is the one mostly observed (Ibsen, 2010). ARS is not specific for calcium ions, but will react with a range of ions, resulting in different colored precipitates (Puchtler, 1969).
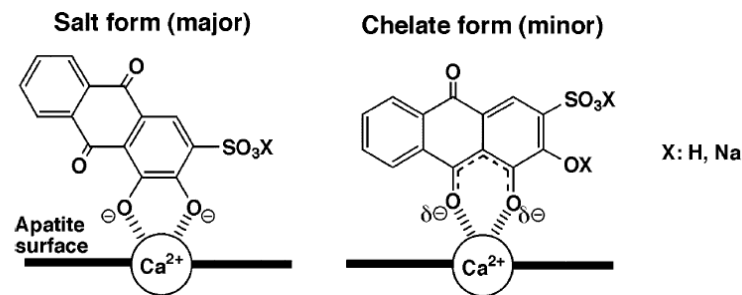


**Figure B.2 Two proposed mechanisms of Alizarin Red S absorbed onto hydroxyapatite. Neither of the two involves the sulphuric group, as has been believed previously (Moriguchi, 2003).**

Attempts were made in order to determine the mineral content in alginate beads. Firstly, a method used for beads mineralized by the in situ one step method was attempted.

*Method 1:* A few beads were transferred from the culturing flask to a sterile tube. Next, 10 beads were added to a 24 well plate, using three parallels. 250µl of medium was added to each well. Subsequently, formaldehyde (FAH, 4%) was added to fixate the beads, after which the plate was put on ice for ten minutes. The samples were washed once with 1mL PBS and once with saline solution. At this point 40mM Alizarin Red (500µl) was added and the plate was incubated for 30 min with gentle agitation at RT. Following, the beads were washed twice with sterile water, and incubated for 15 min with 500ul PBS. The PBS was subsequently removed and 10% CPC/10mM sodium phosphate buffer (250ul, pH=7) was added. The plate was incubated for one hour with gentle agitation. A dilution series was made consisting of duplicates of 800, 400, 200, 100, 50, 25, 12.5, and 0 µM ARS, and their absorbance at 570 nm was measured.

This method could not be completed as no beads were left in the wells after the ARS-S treatment. Initially, this was thought to be caused by the handler pipetting up beads whilst washing the samples or by the poor stability of the beads, making them crack open. Consequently, the method was attempted once again, this time with extremely careful pipetting. The samples were observed every 5 minutes in the microscope during ARS-S staining. Not surprisingly, no beads, or a lot of alginate particles were observed in the wells, thus confirming that bead stability was again an issue. Some beads remained intact and pictures were taken in the light microscope (figure B.3).
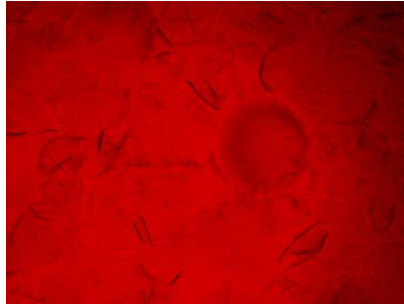
Figure B.3. Light microscope picture taken during initial experiments on ARS-S. The sample is sample 2, that is mineralized and without cells. For the samples containing cells, only MSCs remained in the wells and no alginate particles could be observed.

Clearly, the beads need to be stabilized during staining. This proved to be hard as ARS-S is not specific for calcium ions, but reacts with other cations as well. As a consequence, $Ba^{2+}$- ions were added to sterile water, and this solution was used as the sole washing agent in the next experiment. This means that PBS and saline solution were discarded. Again the samples were kept under close observations in the light microscope. Following pictures were taken after roughly 17 minutes, when the plate was taken off the agitation apparatus (figure B.4).
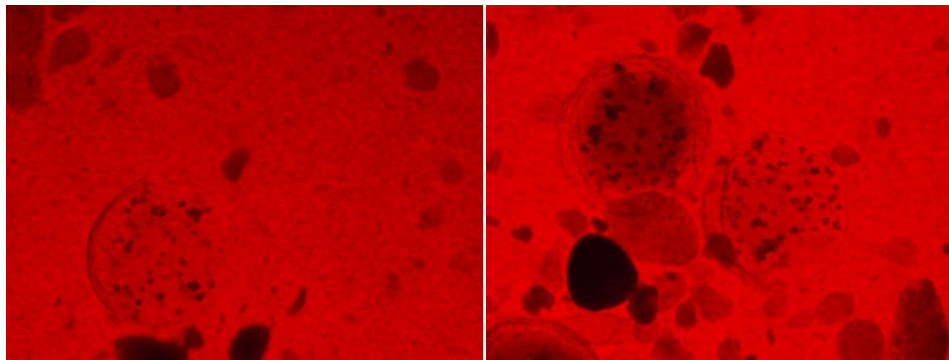


Figure B.4: Light microscope pictures taken at t=17 during ARS-S staining. The left picture shows sample 4b, mineralized, with cells and undifferentiated. The right picture shows sample 4a, mineralized, with cells and differentiated.

A lot of precipitates were observed in the wells. These were thought to be of ARS-S/$Ca^{2+}$ and ARS-S/$Ba^{2+}$. After trying to wash the cells, all were lost. To test whether the ARS-S precipitated with any other of the solution a small test was set up where ARS-S was added to wells with different solution and left on gentle agitation for 30 minutes. The results are given in table B.1.

Table B.1 Reaction of ARS-S with different solutions. ARS-S was added to wells containing the mentioned chemicals, and left under gentle agitation for 30 minutes.

| Solution | Precipitates observed |
|---|---|
| Sterile water | No |
| Tap water | No |
| Saline solution | Yes |
| Solely ARS-S | No |

After seeing that ARS-S did not react with tap water, a new experiment was set up, based on another method used for beads mineralized by the in situ method. Additionally, the beads were kept in eppendorf tubes until ARS-S staining and washing was completed, that is prior to adding CPC.

*Method 2:* Approximately 50 beads were transferred to eppendorf tubes, fixated with FAH in the fridge for four days. Beads for consequently washed three times with tap water before ARS-S (500µl) were added to each tube. Samples were left on gentle agitation for 20 minutes before they were extremely carefully washed three times with tap water.  Next, samples were added to a 24 well plate in three parallels and light microscope pictures were taken after washing (figure B.5). Subsequently, 10% CPC/10mM sodium phosphate buffer (250ul, pH=7) was added, and the plate was left on gentle agitation for one hour. At this point, the solution without beads was transferred to a 96 well plate for absorbance measurements.  A dilution series was made consisting of duplicates of 800, 400, 200, 100, 50, 25, 12.5, and 0 µM ARS. All samples were tested in duplicates.
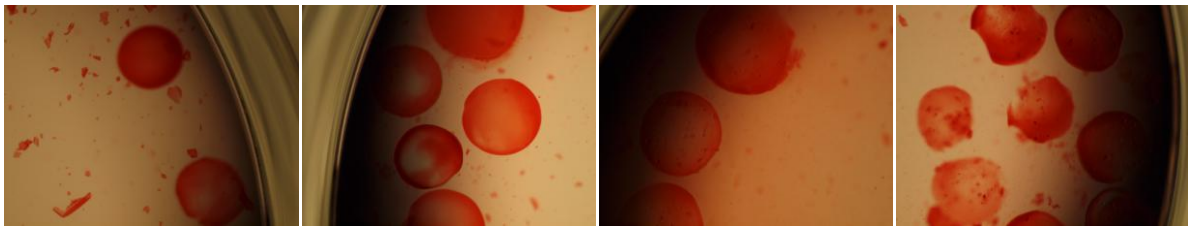


**Figure B.5 Images from ARS-S. From the left; Sample 1 (unmineralized and without cells); sample 2 (mineralized without cells); Sample 3a (unmineralized with cells); sample 4a (mineralized with cells). Images are taken after staining with ARS-S and careful washing in tap water.**

It was apparent that the beads were not washed as thoroughly as they should have been. This was again due to the poor stability of the beads. Consequently results obtained from this experiment are not as viable as they need to be to make a definite conclusion on mineral content. Nevertheless, results and the standard curve are given in figure B.6 and B.7.

Linear regression of the standard curve yielded the formula y= 0.0012X + 0.0375 ($R^2$=0.9997). This formula was used to calculate ARS-S concentration in the samples.

The calculated concentration reveal that the samples with cells given mineralization medium were higher compared with the samples not given mineralization medium. Conversely, this difference is not observed in controls, as sample 1 (unmineralized without cells) is calculated to having higher ARS-S concentration compared with sample 2 (mineralized without cells). No statistical significant differences were observed.
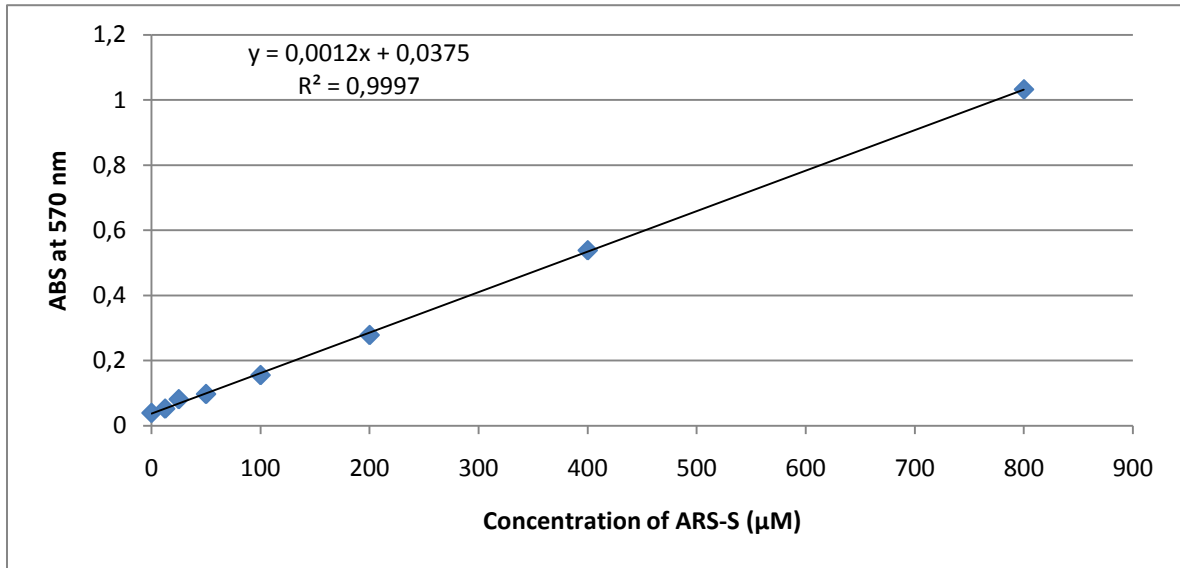
**Figure B.6. Standard curve based on readings from the dilution series of ARS-S.**
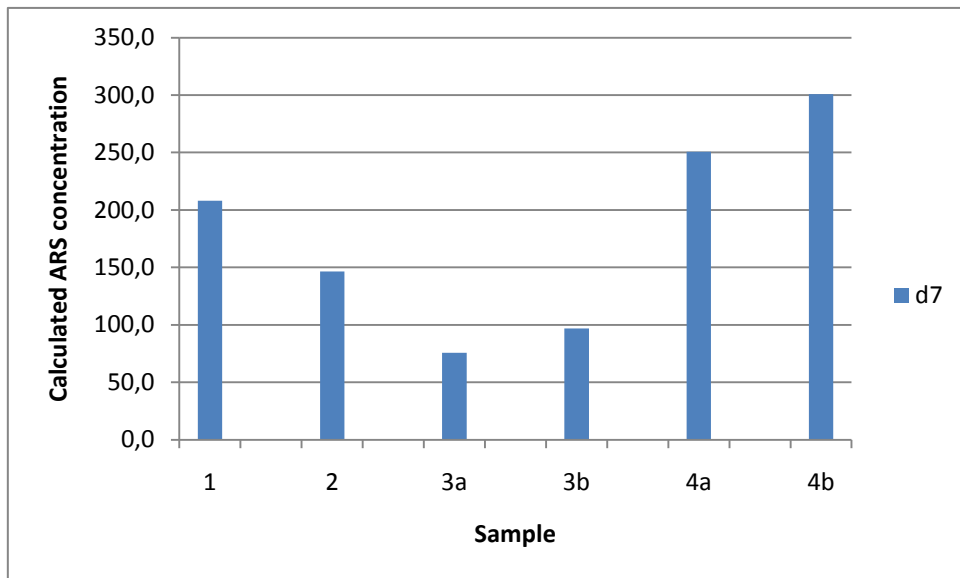


**Figure B.7 Mineral content of alginate beads. Samples include; unmineralized beads without cells (Samples 1); mineralized beads without cells (sample 2); unmineralized differentiated beads with cells (sample 3a); unmineralized undifferentiated beads with cells (Sample 3b); mineralized, differentiated beads with cells (Sample 4a) and mineralized, undifferentiated beads with cells (Sample 4b).**

**References;**

GREGORY, C. A., GUNN, G., PEISTER, A., PROCKOP, D J. 2004. An Alizarin red-based assay of mineralization bt adherent cells in culture: comparison with cetylpyridinium chloride extraction. *Analytical Biochemistry,* 329**,** 77-84.

IBSEN, C. J. S., BIRKEDAL, H. 2010. Modification of bone-like apatite nanoparticle size and growth kinetics by alizarin red S Nanoscale, 2**,** 2478-2486.

MORIGUCHI, T., YANO, K., NAKAGAWA, S., KAJI, F. 2003. Elucidation of adsorption mechanism of bone-staining agent alizarin red S on hydroxyapatite by FT-IR microspectroscopy. *Journal of Colloid and Interface Science,* 260**,** 19-25.

PUCHTLER, H., MELOAN, S. N., TERRY, M. S. 1969. On the history and mechanism of Alizarin and Alizarin Red S stains for calcium. *Journal of Histochemistry & Cytochemistry,* 17**,** 110-124.